University of Alberta

Comparison of Action Spectra of Microorganisms and DNA Absorbance Spectra for UV Disinfection of Water

by

Ren Zhuo Chen

A thesis submitted to the Faculty of Graduate Studies and Research
in partial fulfillment of the requirements for the degree of

Master of Science

in

Environmental Engineering

Department of Civil and Environmental Engineering

Edmonton, Alberta

Spring, 2007

Library and Archives Canada

Published Heritage Branch

395 Wellington Street
Ottawa ON K1A 0N4
Canada

Bibliothèque et Archives Canada

Direction du Patrimoine de l'édition

395, rue Wellington
Ottawa ON K1A 0N4
Canada

Your file Votre référence
ISBN: 978-0-494-29945-6
Our file Notre référence
ISBN: 978-0-494-29945-6

NOTICE:
The author has granted a non-exclusive license allowing Library and Archives Canada to reproduce, publish, archive, preserve, conserve, communicate to the public by telecommunication or on the Internet, loan, distribute and sell theses worldwide, for commercial or non-commercial purposes, in microform, paper, electronic and/or any other formats.

The author retains copyright ownership and moral rights in this thesis. Neither the thesis nor substantial extracts from it may be printed or otherwise reproduced without the author's permission.

AVIS:
L'auteur a accordé une licence non exclusive permettant à la Bibliothèque et Archives Canada de reproduire, publier, archiver, sauvegarder, conserver, transmettre au public par télécommunication ou par l'Internet, prêter, distribuer et vendre des thèses partout dans le monde, à des fins commerciales ou autres, sur support microforme, papier, électronique et/ou autres formats.

L'auteur conserve la propriété du droit d'auteur et des droits moraux qui protège cette thèse. Ni la thèse ni des extraits substantiels de celle-ci ne doivent être imprimés ou autrement reproduits sans son autorisation.

In compliance with the Canadian Privacy Act some supporting forms may have been removed from this thesis.

While these forms may be included in the document page count, their removal does not represent any loss of content from the thesis.

Conformément à la loi canadienne sur la protection de la vie privée, quelques formulaires secondaires ont été enlevés de cette thèse.

Bien que ces formulaires aient inclus dans la pagination, il n'y aura aucun contenu manquant.

Canada

DEDICATION

To my dearest family for their continuously encouraging and supporting to have this degree and in memorial of my father and my brother.

ABSTRACT

Evaluation of the disinfection efficiency of Medium-Pressure lamp ultraviolet (UV) reactors for water and wastewater treatment is potentially affected by the germicidal action spectra of the target pathogen and the surrogate microorganisms used in bioassays. The action spectra of *Bacillus subtilis* spores and *Salmonella typhimurium* LT2 were determined and their respective DNA absorbance spectra were measured. The absorbance spectra of the purified chromosomal nucleic acids from both species were similar and were consistent with that reported for other species in the literature. In addition, the action spectra of *S. typhimurium* LT2 matched its DNA absorbance spectrum closely. In contrast, the action spectrum of *B. subtilis* spores, a microorganism with a much higher resistance to UV, was different from its measured DNA absorbance spectrum. The results suggest that the water industry should consider use of a correction factor when using *B. subtilis* spores for evaluating the performance of MP UV reactors.

ACKNOWLEDGEMENTS

To the people who participated in both a large and small manner to make this thesis possible, I am very appreciative. I would like to extend my sincere gratitude to my supervisors, Dr. Stephen A. Craik and Dr. James R. Bolton, who created an environment that has been educational and enjoyable throughout the course of this study and the completion of the thesis. I would like to extend my appreciation to our technicians Maria Demeter and Garry Solonynko for helping with countless facets. I would also like to thank my graduate student fellows for their help. I would like to acknowledge the Natural Sciences and Engineering Research Council of Canada (NSERC) and the Canadian Foundation for Innovation (CFI) for providing the necessary funding this research for funding this research project.

TABLE OF CONTENTS

1 INTRODUCTION 1

1.1 Background 1

1.2 Scientific Hypothesis 3

1.3 Thesis Overview 3

1.3.1 Research Objectives 3

1.3.2 Organization of this Thesis 4

2 LITERATURE REVIEW 5

2.1 Definitions and Units 5

2.2 UV Inactivation or Disinfection 9

2.2.1 History of the UV Disinfection of Water 9

2.2.2 Mechanisms of UV Inactivation 10

2.2.3 Sources of UV light 14

2.3 UV Inactivation Action Spectrum and DNA Absorbance Spectrum 16

2.3.1 Inactivation Action Spectra for Bacteria 17

2.3.2 Inactivation Action Spectra for Viruses and Phages 17

2.3.3 Inactivation Action Spectra for *Bacillus subtilis* Spores 18

2.3.4 Nucleic Acids and Protein Absorbance Spectra 20

2.3.5 Comparison of Inactivation Action Spectra and a 'Standard' DNA Absorbance Spectrum 23

2.4 *Bacillus subtilis* Spores 24

2.4.1 Nature of *B. subtilis* Spores 24

2.4.2 Environment of Spore DNA 25

2.4.3 Photochemistry of Spore DNA and the Repair of Damaged Spore DNA 27

2.4.4 An Important Surrogate Organism 29

2.4.5 UV Inactivation of *B. subtilis* Spores 31

2.5 Salmonella 32

2.5.1 Nature of *Salmonella* spp. 32

2.5.2 Description of the Diseases 32

2.5.3 Environmental Significance 33
2.5.4 UV Inactivation of *Salmonella* spp. 35
2.6 Problem Statement and Needs for this Research 37
3 COMPARISON OF THE ACTION SPECTRUM AND THE DNA ABSORBANCE SPECTRUM OF *BACILLUS SUBTILIS* SPORES 41
3.1 Introduction 41
3.2 Materials and Methods 43
3.2.1 *Bacillus subtilis* Spores Production, Preparation of Test Suspensions, and Enumeration 43
3.2.2 UV Exposure 45
3.2.3 Fluence (UV Dose) Determination 47
3.2.4 Data Analysis and Modeling 49
3.2.5 Measurement of Absorbance Spectra of *B. subtilis* DNA and Decoated Spores 50
3.3 Results and Discussion 52
3.3.1 UV Fluence-Inactivation Response Curves 52
3.3.2 Wavelength Dependence of Inactivation Rate Constant, Number of Critical Targets and Threshold Fluence 53
3.3.3 Comparison of the Inactivation Action Spectra of *B. subtilis* Spores 56
3.3.4 Comparison of Wavelength Dependence of the Shoulder Effects 59
3.3.5 Absorbance Spectra of *Bacillus subtilis* DNA and Decoated Spores 61
3.3.6 Comparison of the Action Spectrum of *B. subtilis* Spores and the DNA Absorbance Spectra of *Bacillus subtilis* 63
3.3.7 Effect of Inactivation Spectra on Germicidal Fluence Determination 65
3.4 Conclusions 68
4 COMPARISON OF THE ACTION SPECTRUM AND THE DNA ABSORBANCE SPECTRUM OF *SALMONELLA TYPHIMURIUM* LT2 69
4.1 Introduction 69
4.2 Materials and Methods 71
4.2.1 *S. typhimurium* LT2 Production, Preparation of Test Suspensions, and Enumeration 71

4.2.2 UV Exposures 72
4.2.3 Fluence (UV dose) Determination 73
4.2.4 Data Analysis and the Statistical Method 74
4.2.5 Measurement of the Absorbance Spectrum of *Salmonella typhimurium* LT2 DNA 74
4.3 Results and Discussion 75
4.3.1 UV Fluence-Inactivation Response Curves 75
4.3.2 Wavelength Dependent of Inactivation Rate Constant, Number of Critical Targets and the Threshold Fluence 77
4.3.3 Comparison of the Inactivation Action Spectra of *S. typhimurium* LT2 with that of *E. coli* 79
4.3.4 Comparison of the Action Spectrum and the DNA Absorbance Spectrum of *S. typhimurium* LT2 80
4.3.5 Effect of Action Spectra on Germicidal Fluence Determination 81
4.4 Conclusions 82

5 GENERAL DISCUSSION, CONCLUSIONS AND RECOMMENDATIONS .. 84
5.1 General Discussion 84
5.1.1 DNA and RNA Absorbance Spectra 84
5.1.2 Inactivation Action Spectra of Surrogate or Challenge Microorganisms 85
5.1.3 Action Spectra of Waterborne Pathogens 87
5.1.4 Differences between the Action Spectra of UV-Sensitive Microorganisms and UV-Resistant Microorganisms 90
5.1.5 Effect of Action Spectra on Polychromatic UV Reactor Validation Using Bioassay 91
5.2 Conclusions and Recommendations 94

REFERENCES 97
APPENDIX-A: DETAILED EXPERIEMENTAL METHODS 105
Appendix A-1: Preparation of Nutrient Agar for *B. subtilis* Spores Enumeration 105

Appendix A-2: Protocol for the Measurement of Irradiance Using the Ferrioxalate Actinometer 106
Appendix A-3 Method for preparation of MacConkey agar plate for *Salmonella typhimurium* LT2 114

APPENDIX-B RAW DATA AND SUPPORTIVE INFORMATION 115
Appendix B-1: CFU Enumeration of *Bacillus subtilis* Spores 115
Appendix B-2: 95% JCR of Inactivation Rate Constant k and Number of Critical Targets n_c from the Multiple-Target Model for *B. subtilis* Spores 126
Appendix B-3 CFU Enumeration of *Salmonella typhimurium* LT2 137
Appendix B-4: 95% JCR of Inactivation Rate Constant k and Number of Critical Targets n_c from the Multiple-target Model for *S. typhimurium* LT2 148
Appendix B-5: Original Results for Absorbance Measurement of DNA and decoated spores solution 159
Appendix B-6: Paired t-Test for Comparison of the Difference of Action Spectra 161

LIST OF TABLES

Table 3.1 Characteristics of the narrow band UV light produced by the MP lamp and the band-pass filters 46
Table 3.2 Wavelength dependence of the inactivation rate vonstant (*k*), number of critical targets (n_c) and threshold fluence (H_f) of *B. subtilis* spores (ATCC 6633) 56
Table 4.1 Wavelength dependence of inactivation rate constant (k), number of critical targets (n_c) and threshold fluence of *S. typhimurium* LT2 (SGSC SL 3770) 78
Table 5.1 Weighted germicidal fluence delivered to microorganisms by a MP lamp 94
Table A-1 Sensor factor for the International Light Radiometer 113
Table B-1 CFU enumeration of *B. subtilis* spores for the 222 nm band 115
Table B-2 CFU enumeration of *B. subtilis* spores for the 225 nm band 116
Table B-3 CFU enumeration of *B. subtilis spores* for the 231 nm band 117
Table B-4 CFU enumeration of *B. subtilis* spores for the 243 nm band 118
Table B-5 CFU enumeration of *B. subtilis* spores for the 251 nm band 119
Table B-6 CFU enumeration of *B. subtilis* spores for the LP lamp..... 120
Table B-7 CFU enumeration of *B. subtilis* spores for the 262 nm band 121
Table B-8 CFU enumeration of *B. subtilis* spores for the 269 nm band 122
Table B-9 CFU Enumeration of *B. subtilis* spores for the 279 nm band..... 123
Table B-10 CFU enumeration of *B. subtilis* spores for the 291 nm band 124
Table B-11 CFU enumeration of *B. subtilis* spores for the 302 nm band 125
Table B-12 CFU enumeration of *S. typhimurium* LT2 for the the 222 nm band 137
Table B-13 CFU enumeration of *S. typhimurium* LT2 for the 225 nm band 138
Table B-14 CFU enumeration of *S. typhimurium* LT2 for the the 231 nm band 139
Table B-15 CFU enumeration of *S. typhimurium* LT2 for 243 nm band 140
Table B-16 CFU Enumeration of *S. typhimurium* LT2 for 251 nm band..... 141
Table B-17 CFU enumeration of *S. typhimurium* LT2 for LP lamp 142
Table B-18 CFU enumeration of *S. typhimurium* LT2 for 262 nm band 143
Table B-19 CFU enumeration of *S. typhimurium* LT2 for 269 nm band 144
Table B-20 CFU enumeration of *S. typhimurium* LT2 for 279 nm band 145
Table B-21 CFU enumeration of *S. typhimurium* LT2 for 291 nm band 146

Table B-22 CFU enumeration of *S. typhimurium* LT2 for 302 nm band 147
Table B-23 Comparison of the difference of action spectra of *B. subtilis* spores using paired t-Test (95% confidence) 161
Table B-24 Comparison of the difference of action spectrum of *E. coli* and the action spectrum of *Salmonella* using paired t-Test (95% confidence)..... 162

LIST OF FIGURES

Figure 2.1: UV bands in the electromagnetic spectrum 8
Figure 2.2: Schematic of a UV collimated beam apparatus 9
Figure 2.3: Photochemical dimerization of two thymine bases 12
Figure 2.4: Spectral emittance of UV light by a MP lamp (This study) 16
Figure 2.5: Action spectra of bacteria, protozoan, virus and bacteriophage; DNA and protein absorbance spectrum. All spectra have been 'normalized' so that the values at 254 nm are 1.00. 20
Figure 2.6: Absorbance spectra of nucleic acids 22
Figure 2.7: Schematic structure of a spore (Adapted from Setlow 1995) 25
Figure 2.8: UV fluence response of *Bacillus subtilis* spores 30
Figure 2.9: Fluence response of *Salmonella* spp. 37
Figure 3.1: UV fluence-inactivation response of *B. subtilis* spores (ATCC 6633) in 0.05 M phosphate buffered de-ionized water at different wavelengths 54
Figure 3.2: Approximation of the shouldered inactivation curves by linear functions 55
Figure 3.3: Comparison of action spectra of *B. subtilis* spores (ATCC 6633) 59
Figure 3.4: Relative shoulder coefficients for inactivation of *B. subtilis* spores (ATCC 6633) as a function of wavelength as determined in this and previous studies 61
Figure 3.5 Comparison of the absorbance spectra of DNA extracted and purified from *B. subtilis* spores and vegetative cells, the absorbance spectrum of decoated *B. subtilis* spore and the spore action spectrum 63
Figure 4.1: UV fluence-inactivation responses of *Salmonella typhimurium* LT2 (SGSC SL 3770) in 0.05 M phosphate buffered de-ionized water at different wavelengths 76
Figure 4.2: Action spectra of *S. typhimurium* LT2 (SGSC SL 3770), its DNA absorbance spectrum, and *E. coli* action spectrum, and the 'standard' DNA absorbance spectrum 80
Figure 5.1: Absorbance spectra of nucleic acids (DNA or RNA) from different organisms 85
Figure 5.2: Comparison of action spectra of MS2 bacteriophage 88
Figure 5.3: Comparison of action spectra of some waterborne pathogens 89

Figure B-1: 95% JCR of k and n_c of 222 nm band for *B. subtilis* spores 126
Figure B-2: 95% JCR of k and n_c of 225 nm band for *B. subtilis* spores 127
Figure B-3: 95% JCR of k and n_c of 231 nm band for *B. subtilis* spores 128
Figure B-4: 95% JCR of k and n_c of 243 nm band for *B. subtilis* spores..... 129
Figure B-5: 95% JCR of k and n_c of 251 nm band for *B. subtilis* spores 130
Figure B-6: 95% JCR of k and n_c of LP lamp 254 nm band for *B. subtilis* spores..... 131
Figure B-7: 95% JCR of k and n_c of 262 nm band for *B. subtilis* spores 132
Figure B-8: 95% JCR of k and n_c of 269 nm band for *B. subtilis* spores 133
Figure B-9: 95% JCR of k and n_c of 279 nm band for *B. subtilis* spores 134
Figure B-10: 95% JCR of k and n_c of 291 nm band for *B. subtilis* spores 135
Figure B-11: 95% JCR of k and n_c of 302 nm band for *B. subtilis* spores 136
Figure B-12: 95% JCR of k and n_c of 222 nm band for *S. typhimurium* LT2..... 148
Figure B-13: 95% JCR of k and n_c of 225 nm band for *S. typhimurium* LT2 149
Figure B-14: 95% JCR of k and n_c of 231 nm band for *S. typhimurium* LT2 150
Figure B-15: 95% JCR of k and n_c of 243 nm band for *S. typhimurium* LT2 151
Figure B-16: 95% JCR of k and n_c of 251 nm band for *S. typhimurium* LT2 152
Figure B-17: 95% JCR of k and n_c of LP lamp 254 nm band for *S. typhimurium* LT2.. 153
Figure B-18: 95% JCR of k and n_c of 262 nm band for *S. typhimurium* LT2 154
Figure B-19: 95% JCR of k and n_c of 269 nm band for *S. typhimurium* LT2 155
Figure B-20: 95% JCR of k and n_c of 279 nm band for *S. typhimurium* LT2 156
Figure B-21: 95% JCR of k and n_c of 291 nm band for *S. typhimurium* LT2 157
Figure B-22: 95% JCR of k and n_c of 302 nm band for *S. typhimurium* LT2 158
Figure B-23: Absorbance spectra of *Bacillus subtilis* measured using 1 cm-pathlength quartz cuvettes 159
Figure B-24: DNA absorbance spectrum of *S. typhimurium* LT2 measured using 1 cm-pathlength quartz cuvettes 160

LIST OF ABBREVIATIONS

ATCC	American Type Culture Collection
CFU	Colony Forming Units
DBP	Disinfection by Products
DNA	Deoxyribonucleic acid
DPA	Dipicolinic Acid
JCR	Joint Confidence Region
LT2ESWTR	Long Term 2 Enhanced Surface Water Treatment Rule
Log	Logarithm (10 base)
LP	Low Pressure mercury discharge lamp
MP	Medium Pressure mercury discharge lamp
NER	Nucleotide Excision Repair
PBDI	Phosphate-Buffered Deionized Water
REF	Reduction Equivalent Fluence
RNA	Ribonucleic Acid
SASP	Small Acid Soluble Proteins
SGSC	*Salmonella* Genetic Stock Center
SP	Spore Photoproduct
USEPA	United States Environmental Protection Agency
UV	Ultraviolet

LIST OF SYMBOLS

A	Absorption coefficient
A_{rel}	Absorbance relative to 254 nm
$E_{o\lambda}$	Incident spectral irradiance
E_λ	Transmitted spectral irradiance
H'	UV fluence
H_t'	Threshold UV fluence
k	Inactivation rate constant
k_{rel}	Inactivation rate constant relative to 254 nm
n	Number of parameters estimated
n_c	Number of critical targets in the multiple-target model
N	Concentration of viable microorganisms after UV exposure
N_0	Concentration of viable microorganisms before UV exposure
p	Number of parameters
S_c	Size of critical confidence region
S_R	Sum of residual squares
T_λ	Spectral transmittance
λ	Wavelength

1 INTRODUCTION

1.1 Background

Ultraviolet (UV) treatment has been used for wastewater disinfection for many years. This technology is becoming popular as an alternative disinfection technology to chlorination in drinking water treatment processes. Unlike chemical disinfection, some advantages of the UV treatment of water and wastewater include: (1) minimal concern about formation of disinfection by-products compared to conventional chlorine-based disinfection, (2) insignificant effect of water pH and temperature, (3) effective inactivation of some chlorine-resistant protozoan parasites, such as *Giardia* and *Cryptosporidium* (Craik et al. 2001; Bukhari et al. 1999). Also, this technology was proposed by the Long Term 2 Enhanced Surface Water Treatment Rule (LT2ESWTR) to give additional inactivation credits for *Giardia* and *Cryptosporidium* (USEPA 2006). As well, UV treatment can induce the inactivation of a wide range of pathogenic microorganisms including bacteria, fungi, protozoa and viruses (Chang et al. 1985; Wilson et al. 1992; Shin et al. 2005).

The most common UV light sources for water disinfection are mercury discharge lamps. Both low pressure (LP) mercury lamps and medium pressure (MP) lamps have been applied for both water and wastewater disinfection. LP mercury vapour lamps, which generate primarily monochromatic (single wavelength) UV light at 253.7 nm, have been used to inactive pathogens in water and wastewater. However, MP lamps, which produce polychromatic (multiple wavelength) UV light, have been introduced more recently. Although the germicidal UV efficiency of MP lamps is much lower than that of LP lamps, fewer lamps are required in an operating reactor due to the higher output

intensity of MP lamps. This then allows a significant reduction in maintenance costs for MP reactor systems. Therefore, MP lamps are commonly used in large scale water disinfection systems. As well, researchers have employed MP lamps to conduct UV disinfection studies (Bukhari et al. 1999; Craik et al. 2000; Linden et al. 2005). The method for calculating the effective fluence (also called UV dose) of MP lamps is more complex than that of LP lamps. The germicidal effectiveness of a MP UV light depends on both the UV wavelength distribution and the wavelength sensitivity of the target microorganisms. It is important to quantify the relative germicidal effectiveness of each wavelength for a microorganism to determine accurately a germicidal fluence. This involves the determination of the *action spectrum* (defined as the relative inactivation response to a given fluence versus wavelength) for a given microorganism.

The wavelength range of UV light between 200 and 300 nm is considered to be the most effective in inactivating microorganisms. Studies have demonstrated that the sensitivity of a microorganism's inactivation is highly dependent on wavelength (Gates 1929; Rauth 1965; Linden et al. 2001). The inactivation mechanism of microorganisms by UV light is believed to be due primarily to damage to their DNA or RNA. The absorbance spectrum of DNA has often been used as a surrogate for the action spectrum of a microorganism, when an action spectrum is not available. This is based on the assumption that the quantum yield for inactivation is independent of wavelength. However, the quantum yield can be dependent on wavelength, and in addition biological changes other than DNA damage can be induced by UV treatment (Setlow 1960). Some recent studies have shown that the action spectrum of some UV-resistant microorganisms, such as adenovirus, MS2 coliphage and *Bacillus subtilis* spores, can

vary significantly from the 'standard' DNA absorbance spectrum (Linden et al. 2005; Mamane-Gravetz et al. 2005). Some microbes likely have their own unique action spectrum. To determine accurately the germicidal fluence for a pathogen, or pathogen surrogate and to validate a UV reactor using a polychromatic UV source, it is necessary to measure the action spectrum of target microorganisms rigorously and then compare them to their own DNA absorbance spectrum.

1.2 Scientific Hypothesis

The scientific hypothesis for this study was that if the inactivation of a microorganism by UV light is induced primarily by damage to the DNA or RNA causing an inhibition of its ability to reproduce, then the action spectrum of a given microorganism should be consistent with its own DNA or RNA absorbance spectrum, under the assumption that the quantum yield for inactivation is not wavelength dependent. However, if UV induces other bioactivity inhibitions, such as a loss of the enzymatic activity of critical proteins, and/or photon energy absorbed by other components in a microorganism that can be transferred to DNA or RNA, then the action spectrum could be different from its DNA or RNA absorbance spectrum. This may be why some other microorganisms have demonstrated action spectra different from the DNA absorbance spectra.

1.3 Thesis Overview

1.3.1 Research Objectives

The objectives of this study were to:

- Determine the fluence responses vs. wavelength of *B. subtilis* spores and *Salmonella typhimurium* LT2 using a set of narrow band UV light filters, and characterize the inactivation action spectra of *B. subtilis* spores and *S. typhimurium* LT2;
- Measure the DNA absorbance spectra of these two microorganisms and compare them to their own action spectra;
- Evaluate a potential effect of different action spectra on the germicidal fluence and polychromatic UV reactor validation using bioassays.

1.3.2 Organization of this Thesis

This thesis is presented in five chapters and one appendix. Chapter 1 gives a general background and briefly describes the research problems and study objectives. A detailed literature review is given in Chapter 2. Chapter 3 describes the experimental determination of the *B. subtilis* spore inactivation action spectrum and its DNA absorbance spectrum. This chapter includes a brief introduction, description of methods and materials, results and discussion, and conclusions. Chapter 4 provides a similar description for studies on *S. typhimurium*. General conclusions and recommendations arising from the study and other literature for surrogate microorganisms and pathogens are addressed in Chapter 5. A full set of references is provided after Chapter 5. The Appendix contains supportive data and information for this study.

2 LITERATURE REVIEW

2.1 Definitions and Units

Before reading through this thesis, the definitions of some terms will help to understand some terms/concepts used herein.

Disinfection refers to the inactivation of disease-causing organisms, such as pathogenic bacteria, viruses, protozoa and helminthes.

Inactivation is the reduction in the ability of microorganisms to reproduce and/or cause disease as result of a chemical or physical treatment (such as UV). It is often expressed on a log scale and is defined as $-\log[N/N_0]$ where N and N_0 are the concentrations of live microorganisms in the water before and after a UV exposure, respectively. The *survival ratio* N/N_0 is a related term and is also used in this thesis.

Different terms for describing the conditions of UV exposure have been used throughout the literature. The terminology reported herein was adopted from Bolton (1999), and Bolton and Linden (2003).

Irradiance (mW/cm^2) is defined as the total power incident from all upward directions on an infinitesimal element of surface of area dA containing the point under consideration divided by dA (Bolton and Linden 2003). The unit of *irradiance* or *fluence rate* (defined later) in the International System is W/m^2; however, mW/cm^2, which is very common in North America, will be used in this thesis. *Irradiance* is appropriately used when a flat surface is being irradiated. The term *irradiance* will be used in this thesis to

describe UV exposures carried out with collimated beam apparatus and related measurements made by a radiometer or by chemical actinometry.

Fluence rate is defined as the total radiant power incident from all directions onto an infinitesimally small sphere of cross sectional area *dA* divided by *dA*. When using a collimated beam, the irradiance and the fluence rate are essentially the same if the beam is almost parallel. However, *fluence rate* is herein used for the term describing the average radiant power density across a test suspension or in a UV reactor.

Spectral irradiance (mW cm^{-2} nm^{-1}) herein refers to a relative irradiance in a narrow wavelength range measured by a spectroradiometer.

Although "UV dose" is commonly used in most of the UV disinfection literature, the term *fluence* is more appropriate (Bolton and Linden 2003). *Fluence* is defined as the total radiant energy of all wavelengths passing from all directions through an infinitesimally small sphere of cross sectional area d*A*, divided by d*A*. In this study, *fluence* was obtained by the multiplication of average *fluence rate* within a suspension by the exposure time (in seconds). Rather than following the International system, the unit mJ/cm^2 will be used in this research, since it is more commonly used in the water and wastewater treatment industry.

Fluence-inactivation response is the quantitative relation between the fluence (UV Dose) of UV light delivered to a test suspension and the level of inactivation of organisms induced in that suspension.

Action spectrum is defined as the relative response to a given fluence versus wavelength. It is relative to the response of 254 nm herein.

Spore is a small reproductive body capable of reproducing the organism under suitable conditions.

Quantum yield is a measure of the photon efficiency of a photochemical reaction. It is defined as the number of moles of product formed or reactant removed per einstein of photons absorbed. One einstein is one mole (6.023×10^{23}) of photons.

Germicidal efficiency refers to the microorganism inactivation that occurs at a given fluence. It can be interpreted by the inactivation rate constant of a wavelength band and is relative to that of 254 nm.

Bandpass filter is designed to transmit a specific waveband. An optical bandpass filter is composed of many thin layers of dielectric materials, which have differing refractive indices to produce constructive and destructive interference in the transmitted light. The *bandpass filters* used in this study are designed to transmit narrow wavebands centred from 200 to 320 nm.

Absorbance (A) is the logarithm to the base 10 of the ratio of the incident spectral irradiance ($E_{o\lambda}$), essentially monochromatic, to the spectral irradiance of transmitted radiation (E_λ):

$$A = \log (E_{o\lambda} / E_\lambda) \qquad \text{Eqn (2.1)}$$

Absorbance and *transmittance* (T_λ) are related by

$$A_\lambda = -\log T_\lambda \qquad \text{Eqn (2.2)}$$

In practice, the absorbance is determined as the ratio of the spectral irradiance of light that passes through a reference [e.g., deionized (DI) water] to that of light passing through a sample solution of the same path length.

In the electromagnetic spectrum, *UV light* lies between the edges of the visible region and the x-ray region. As shown in Figure 2.2, its wavelength range is from 100 nm to 400 nm. Light photons within this wavelength range can cause chemical changes when absorbed. The spectrum of UV light is divided into four bands: Vacuum UV (100 nm to 200 nm), UVC (200 nm to 280 nm), UVB (280 nm to 315 nm), and UVA (315 nm to 400 nm) (Meulemans, 1986). The wavelength region between 200 nm and 320 nm has been studied herein.

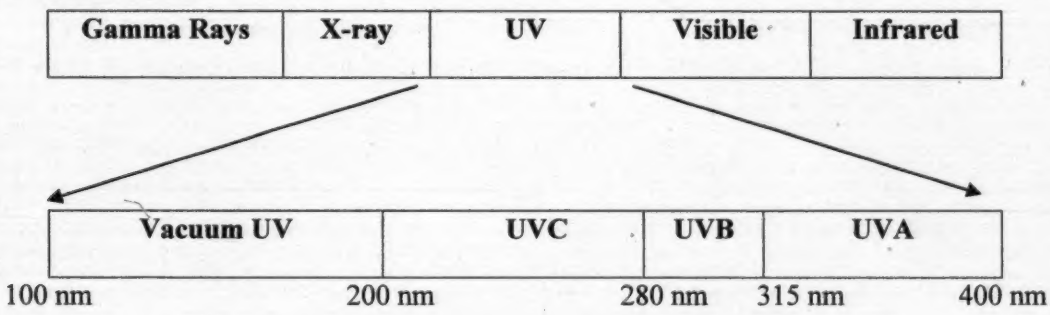

Figure 2.1: UV bands in the electromagnetic spectrum

A *collimated beam apparatus* is a device used to expose a microorganism suspension or a photochemical reaction to a well defined UV fluence rate under controlled laboratory conditions. Figure 2.2 shows a configuration of a collimated beam apparatus. It is typically comprised of a UV lamp, a UV transparent window with a shutter, a collimating tube, a sample container, and supporting components, such as a fan, a stirring system and a power supply for the UV lamp (Bolton and Linden 2003). The UV lamp is housed in an upper cabinet and is separated from a long collimating tube by the shutter. A collimating tube provides a homogeneous and quasi-parallel beam on a given

surface. As illustrated in Figure 2.2, a bandpass filter was placed above the collimator tube to isolate a wavelength band from a medium pressure (MP) lamp used for this study.

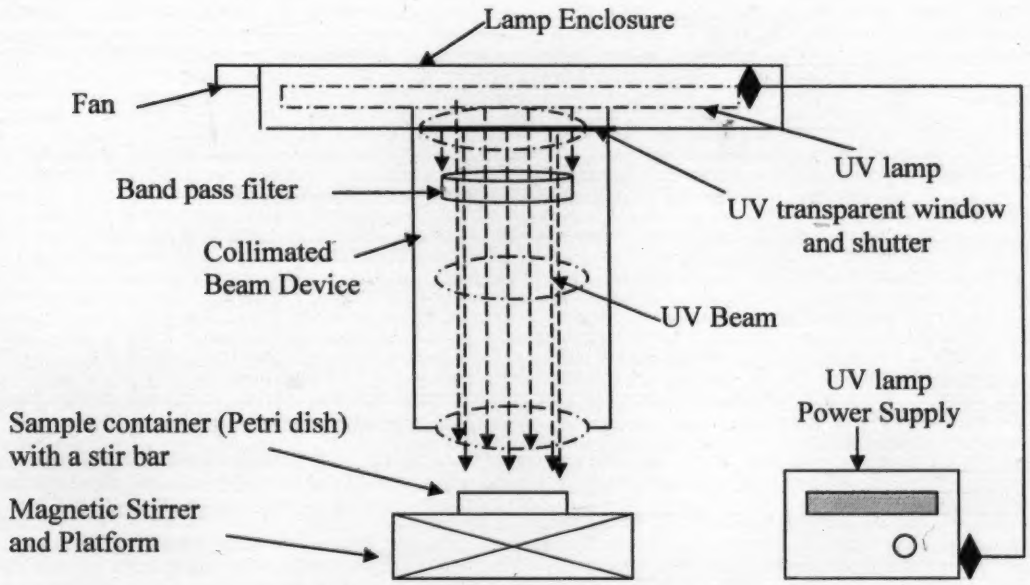

Figure 2.2: Schematic of a UV collimated beam apparatus

2.2 UV Inactivation or Disinfection

2.2.1 History of the UV Disinfection of Water

UV light was recognized to have lethal effects on microorganisms by exposure to sunlight in the late 19th century. The first application of UV to the disinfection of drinking water took place in France in 1910. Several water utilities in Europe and the North American used UV disinfection to inactivate pathogens in drinking water and wastewater in subsequent years (Linden 1998). At that time, this technology was expensive, not very reliable and had maintenance difficulties (Wolfe 1990). However, interest in UV disinfection of water declined in the 1920s because of the emergence of chlorination, a

reliable, low-cost technology at that time. Despite the decline, many researchers still studied the UV induced biological effects on microorganisms for other applications such as genetic mutation.

In the 1970s, new research raised concerns about the toxicity of chlorine to life in receiving waters. Furthermore, Disinfection By-Products (DBP) formed by chlorination of drinking water were reported to be potentially carcinogenic and genotoxic (NCI 1976). Alternative disinfection approaches, including ozone, chlorine dioxide and UV treatment, have been more intensively investigated since then. The advance of UV lamp ballast and electronics technology has made this technology reliable and economical. Since the mid-1980s, UV disinfection of wastewater in North America has become more and more popular due to its many advantages over chlorination. In Europe, UV treatment has been widely employed to disinfect drinking water from vulnerable groundwater sources. The application of UV disinfection of drinking water advanced greatly after the finding of its effective inactivation of *Cryptosporidium* oocysts expounded by Bolton et al. (1998) and Clancy et al. (1999). Since then, many studies have now demonstrated that *Cryptosporidium* oocysts and *Giardia* cysts (Bukhari et al. 1999;Craik et al. 2000; Craik et al. 2001) are inactivated by relatively low UV fluences. As well, many water utilities have employed UV disinfection reactors in their facilities or are in the planning or design stages. Intense studies of UV disinfection in water and wastewater are still going on.

2.2.2 Mechanisms of UV Inactivation

According to Jagger (1967), the biological effects of UV on microorganisms are the partial result of photochemistry. The occurrence of a photochemical reaction involves:

1) absorption of photons by a molecule that possess a vulnerable (i.e., weak) bond(s);

2) alteration of the vulnerable bond(s) by an absorbed photon with sufficient excitation energy; and

3) formation of a new relatively stable configuration or dissociation into two fragments.

In a given microorganism, germicidal UV light is absorbed mainly by nucleic acids (RNA, DNA) and by proteins. Nucleic acids are the most important targets in terms of the inactivation of microorganisms. They are composed of purines, pyrimidines, carbohydrates, and phosphoric acid. The phosphates and carbohydrates are not expected to be affected by UV light because of their poor absorption of UV and linking to the bases by single bonds. The important absorbers within nucleic acids are the nucleotide bases, adenine (A), guanine (G), thymine (T) and cytosine (C) in DNA, and A, G, uracil (U) and C usually in RNA (Harm 1980). These bases are the critical components affected by germicidal UV light. The pyrimidines are approximately 10 times more sensitive to UV than the purines (Jagger 1967). Therefore, the most important targets for inactivation effects on nucleic acid are thymine and cytosine in DNA and uracil and cytosine in RNA.

The photoproducts of pyrimidines are usually dimers. In DNA, thymine dimers, cytosine dimers and thymine-cytosine dimers are formed. For example, if two thymine bases are located adjacent to each other, the thymine bases are covalently linked to form a dimer by an absorbed photon. The 5,6 double bonds of the thymine bases become saturated to form a four-number ring structure as shown in Figure 2.3. Indeed, for most microorganisms, thymine dimers are more readily produced by the action of germicidal

UV light on DNA than any other types of dimers. Furthermore, thymine dimers are fairly stable in DNA (Jagger, 1967). The photoproducts of *Bacillus subtilis* spore DNA have been identified as being different from those of DNA in vegetative cells. This will be described later. The UV induced damage of a section of a DNA or RNA molecular chain is called a *lesion*. Multiple lesions can be produced by UV light in a single DNA or RNA strand.

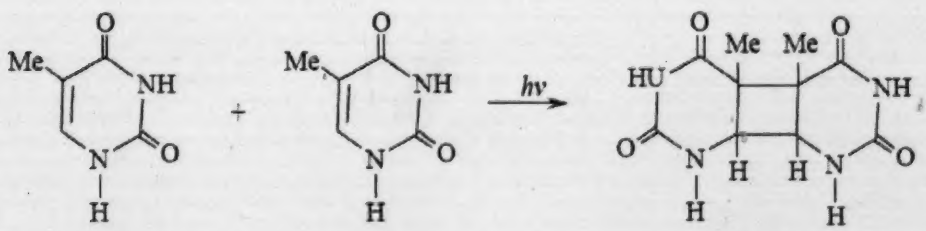

Figure 2.3: Photochemical dimerization of two thymine bases
(Adapted from Bolton, 2001)

The replication of DNA can be inhibited by the presence of lesions. In double-stranded DNA, a purine or pyrimidine base on a DNA strand is hydrogen-bonded to a complementary base in the other strand. For a double-strand DNA to replicate, the DNA first splits into two separate strands. Complementary pyrimidine or purine bases are then attached onto the two separate strands by phosphodiester linkages. This reaction is catalyzed by DNA polymerase enzymes (Friedberg et al. 1995). Thus, two identical copies of DNA are formed. In case of lesions, the enzymes responsible for DNA replication cannot recognize the bases and the complementary pyrimidine or purine are not attached. Enough lesions will prevent the replication of DNA during cell mitosis and

will thus prevent cell replication and infection within a host. This is the primary mechanism of UV inactivation.

It is abundantly clear that absorption of germicidal UV photons by nucleic acids contributes to the main inactivation effects for many microorganisms. This does not mean that absorption by other molecules is without effect. In particular, it has been suggested that proteins may often be involved in the lethal effect, because of their high cell concentration, their role in nucleic synthesis, their involvement in chromosome structure, and other effects on bioactivity (Jagger 1967). Setlow (1960) studied the inactivation effect of UV on DNase, an enzyme that catalyzes DNA hydrolysis. It was found that the quantum yield for protein inactivation by UV light was approximately 0.07, and that the inactivation action spectrum was similar to the absorption spectrum of cystine. One study demonstrated that the crosslinking of DNA and protein induced by UV from a LP lamp may play a significant role in the inactivation of *E. coli* cells (Smith et al. 1966). However, only limited studies have investigated the protein-nucleic acid interactive mechanism of inactivation by germicidal UV and the degree of involvement of protein is difficult to be quantified.

As discussed above, absorbed photon energy can be directly utilized to cause a photochemical reaction. On the other hand, the electronic excitation energy can be transferred. As pointed out by Jagger (1967), excitation energy transfer is of considerable importance in biology. It is likely that excitation energy can be transferred from one molecule to another unattached molecule (Jagger 1967). One of important energy transfer mechanisms is called *triplet energy transfer* (Lamola et al. 1970). If a molecule is in a triplet excited state, excitation energy transfer can occur with distances over 10 nm.

Within the wavelength range of a germicidal UV light, the most important absorbers are usually nucleic acids and proteins in a microorganism. Thus, photon energy absorbed by proteins can be transferred to nucleic acids. It is possible that proteins can act as photosensitizers to contribute to DNA damage.

Some microorganisms have the ability to repair the lesions of their DNA. Repair is usually by light or dark reactivation. According to Harm (1980), there are three or more types of repair mechanisms: 1) reversal of the UV-induced alteration, 2) Replacement of UV-damaged nucleotides, and 3) combination of undamaged regions in replicating DNA molecules. UV-induced dimerization can be reversed by the action of specific enzymes called DNA photolyases that are catalyzed by near UV/visible light (320–500 nm) in a process known as *photoreactivation*. All three mechanisms may also occur as a result of a separate group of enzymes that do not require light to function. These recovery processes may explain the apparent resistance of certain microorganisms, such as *B. subtilis* spores, to UV light (Setlow 2001). However, these repair mechanisms can be overcome by exposure to higher UV fluence (Bolton 2001). Thus, occurrence of one or two of these processes in an irradiated microorganism may partially contribute to its UV resistance, especially at low UV fluence.

2.2.3 Sources of UV light

Mercury lamps are made with a quartz envelop and are charged with a certain amount of mercury. Both LP mercury vapour lamps and MP mercury lamps have been utilized in this research work.

LP UV lamps are charged with a very small (i.e., a few mg) amount of mercury. The mercury vapour pressure is only 1 Pa; in this condition, the lamp emits primarily two

resonance lines at 184.9 nm and 253.7 nm. When LP lamps are used for water disinfection, the portion of UV light at wavelength of 184.9 nm is usually absorbed by the quartz envelop. One requires an envelop with very pure quartz to allow the 184.9 nm emission to escape. The 184.9 nm UV light is absorbed by O_2 in the air to generate ozone (O_3). Any 184.9 nm UV light that enters the water is absorbed by water to form OH radicals and may contribute a small amount to disinfection. However, the quartz sleeve usually used in most UV reactors absorbs the 184.9 nm UV light, so very little reaches the water. Under certain conditions, the UV light efficiency, that is, the ratio of the radiant power emitted by the source to the electrical power input, can be up to 60% at 254 nm. However, this efficiency can only be achieved at very low power levels (Heering 2004). Most LP lamps used in water disinfection have an efficiency of 30–40% at 253.7 nm. The LP lamps used in disinfection studies are designed to yield nearly monochromatic emission at 253.7 nm.

A MP mercury lamp is made with a bulb of quartz that is charged with a much larger amount of mercury than that found in LP lamps. MP lamps produce polychromatic light continuously between 185 and 850 nm. As shown in Figure 4, this spectral range includes the germicidal UV wavelengths from 200 to 300 nm. Much higher UV intensities can be achieved with MP lamps. Because large portions of the lamp power yield light at wavelengths outside of the germicidal range, most MP lamps have a germicidal UV efficiency of less than 20%. In spite of this lower efficiency, fewer lamps are required in an operating reactor due to their high output intensity. Hence, this reduces the maintenance costs significantly. One study indicated that the MP lamp emission was more effective in inhibiting subsequent photoreactivation of *E. coli* than narrow band

germicidal UV light at 230 nm, 254 nm, and 300 nm (Oguma et al. 2003). Due to their high output, MP lamps are most advantageous in large water and wastewater treatment plants where the number of lamps required and the associated cost of maintenance and replacement become significant economic variables.

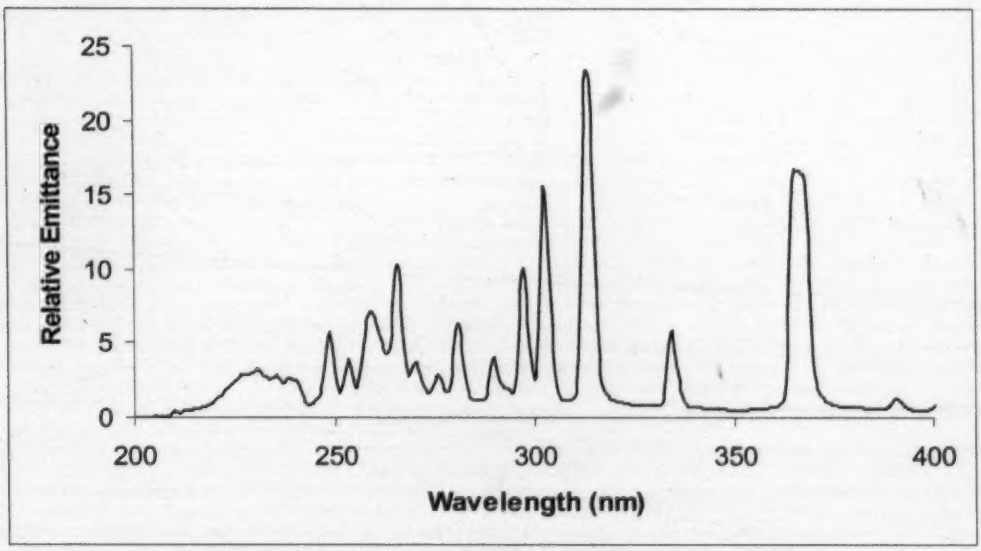

Figure 2.4: Spectral emittance of UV light by a MP lamp (This study)

2.3 UV Inactivation Action Spectrum and DNA Absorbance Spectrum

As described previously, DNA or RNA are the primarily targets in terms of UV inactivation of a microorganism. In theory, if the quantum yield is independent of wavelength for germicidal UV and other factors are negligible, the DNA absorbance spectrum can be used as a surrogate for the action spectrum. Researchers have measured the action spectra of many microorganisms using different methods. These microorganisms included bacteria, spores, virus, phages and protozoan parasites.

2.3.1 Inactivation Action Spectra for Bacteria

One of the earliest studies of action spectra by UV light was conducted by Gates (1930). Gates built a quartz prism monochromator apparatus to investigate the germicidal efficiency of a set of narrow band germicidal UV wavelengths with nominal wavelengths ranging from 230 to 302 nm. Both *Escherichia coli* and *Staphylococcus aureus* were studied, and the germicidal efficiency for both bacteria exhibited a significant dependence on wavelength. These spectra showed the highest efficiency in terms of inactivation around 265 nm. Jagger (1967) further compared the action spectra of these two bacteria to the relative absorbance spectrum of mouse liver DNA by Tsuboi (1950). Both relative action spectra showed fair consistency with the DNA absorbance spectrum in the region 240 to 280 nm.

2.3.2 Inactivation Action Spectra for Viruses and Phages

Later studies of inactivation action spectra were determined for viruses or phages. An action spectrum of T1 bacteriophage was characterized at ten narrow wavelength bands generated using a monochromator (Fluke and Pollard 1949). The inactivation rate constants were determined at fluence levels for less than 2-log inactivation. The results were found to be similar to those obtained by Gates (1930), except for a rather high inactivation rate at 280 nm. A comparison of the UV spectra of the vaccinia virus with that of the T2 bacteriophage showed a difference (Sime and Bedson 1973), in that the action spectrum was characterized by a broad peak from 255 to 275 nm, a low sensitivity region at wavelengths longer than 275 nm and a sharply increased sensitivity at wavelengths below 235 nm. In contrast, the action spectrum for T2 bacteriophage had two peaks, one at around 265 nm and another at 280 nm. The action spectra of both

microorganisms diverged in shape from a typical DNA absorbance spectrum, particularly at wavelengths from 270 to 280 nm and below 240 nm. A comparison of these two relative action spectra with published works (Zelle and Hollaender 1954; Rauth 1965) for these and similar viruses showed mutual consistency within similar viruses. The action spectrum of the herpes simplex virus also exhibited a secondary peak at 280 nm (Cameron 1973; Sime and Bedson 1973). These researchers suspected that the secondary peak at 280 nm was due to the involvement of protein absorption.

2.3.3 Inactivation Action Spectra for *Bacillus subtilis* Spores

The reported action spectrum of a species may vary between published studies. An investigation of the inactivation spectra of five strains of dry *Bacillus subtilis* spores in a vacuum condition was conducted using a monochromator (Munakata et al. 1991). The inactivation rate constants were determined at narrow wavelength bands centred at 220, 235, 255 and 270 nm. The fluence rate was measured by a spectroradiometer. In four of the five strains tested, the lowest inactivation rate constant, and, therefore the lowest sensitivity to UV was determined to be 255 nm. This did not match the DNA absorbance spectrum. In another study, however, the action spectrum of *B. subtilis* spores, either in a vacuum condition or in a liquid suspension, matched the DNA absorbance spectrum fairly well at wavelengths longer than 230 nm where there is a peak around 265 nm (Lindberg and Horneck 1991). In comparison, the later study used filters to isolate a wavelength band, and the fluence rate was measured by ferrioxalate actinometry. Furthermore, it was not clear how the averaged fluence rate was calculated for both studies.

More recent studies characterizing the action spectra of *B. subtilis* spores were conducted by Cabaj et al. (2002) for liquid-cultivated spores and Mamane-Gravetz et al. (2005) for surface-cultivated spores. Both studies used monochromators to isolate wavelength bands and used spectroradiometers to measure fluence rate in simulated drinking water. The action spectra were determined from the inactivation rate constants, using non-linear regression and linear regression, respectively, from semi-log fluence response curves. The lowest sensitivity of *B. subtilis* spores to germicidal UV light in the water matrix was determined to be around 240 nm as shown in Figure 2.5. These two action spectra agree well with each other (Mamane-Gravetz et al. 2005). However, the relative spectra of another parameter, the shoulder coefficient, were found to be significantly wavelength dependent and was quite different between these two studies. In fact, the shoulder coefficient is directly related to the number of critical targets (n_c) in the multiple-targets model. Theoretically, n_c should be independent of wavelength for the same batch of microorganisms in an identical medium. Therefore, it is necessary to characterize the action spectrum of *B. subtilis* spores using different techniques, such as wavelength bands isolated by bandpass filters, fluence rate measurement using chemical actinometry, and sophisticated data processing.

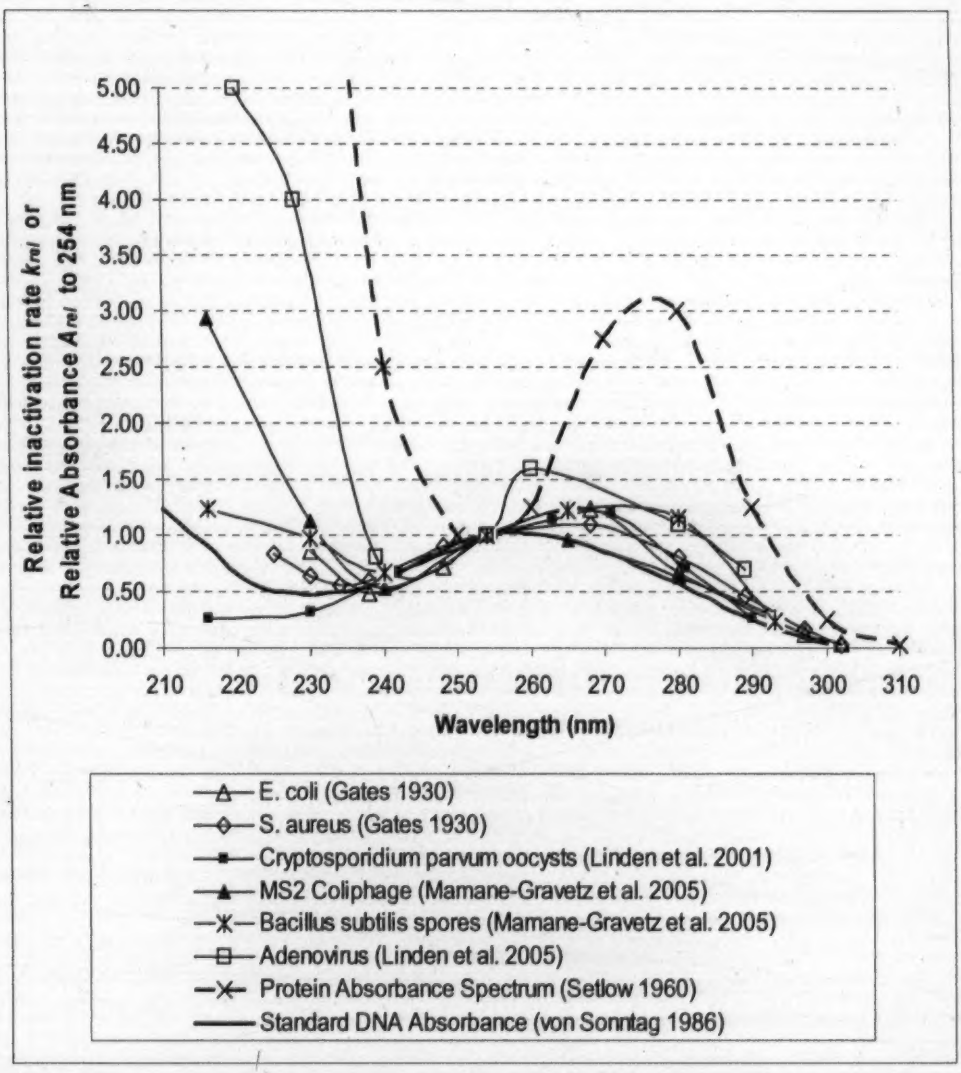

Figure 2.5: Action spectra of bacteria, protozoan, virus and bacteriophage; DNA and protein absorbance spectrum. All spectra have been 'normalized' so that the values at 254 nm are 1.00.

2.3.4 Nucleic Acids and Protein Absorbance Spectra

The main UV absorbers within nucleic acids are the nucleotide bases. In DNA, the pyrimidine derivatives are adenine and guanine and the pyrimidine derivatives are

cytosine and thymine. In RNA, the counterpart of thymine is usually uracil. It was reported that the absorption spectra of the component bases differ to some extent (Davidson 1965). The UV absorbance spectrum of nucleic acids from different organisms, therefore, can be expected to differ to some degree as the relative composition of the bases differ. Three reported DNA or RNA absorbance spectra, generated from material derived from the organs of animals, have been used to interpret the results of UV inactivation studies. These are: the DNA spectrum by Harm (1980) from calf thymus, that by Tsuboi (1950) from mouse liver, and that by Wilfinger 1997) from calf thymus. As shown in Figure 2.6, the absorption spectra of nucleic acids (DNA or RNA) from large animals do not differ very much. However, little published literature is available for the absorption spectra of the DNA or RNA from microorganisms (i.e., bacteria, viruses or protozoa). It is thus necessary to characterize these absorbance spectra for microorganisms in order to calculate accurately the fluence delivered from polychromatic UV lamps in water disinfection systems

In proteins, the structural components that absorb UV light most strongly are the aromatic amino acids and peptide bonds (Jagger 1967). Amongst the amino acids, tryptophan, phenylalanine and tyrosine are the strongest absorbers at wavelengths below 240 nm. The absorbance spectra for tryptophan and tyrosine also show a secondary peak around 280 nm, and that for phenylalanine had a secondary peak around 260 nm. The peptide bond is a strong absorber only at wavelengths less than 240 nm and does not absorb significantly above 240 nm. In terms of UV absorbance, the interaction among the amino acids in a protein is negligible (Wetlaufer 1962). The total absorbance of a protein solution is expected to be the sum of the absorbance of the component amino acids.

Proteins usually exhibit a weak peak absorbance about 280 nm, and higher absorbance in the region below 240 nm, which is attributed primarily to the amino acids tryptophan and tyrosine. In nucleic acids, on the other hand, all the nucleotide bases show high absorbance in the germicidal UV region. In comparison, nucleic acids absorb 10-20 times as much as an equal concentration of proteins in the region 240-290 nm (Harm 1980; Jagger, 1967). The higher absorbance of proteins below 230 nm, compared to that of nucleic acids, is primarily due to the absorption of the peptide bonds and aromatic amino acids. Although proteins function critically in cells, their UV absorbance compared with that of nucleic acids is of minor consequence in most of the germicidal wavelength ranges.

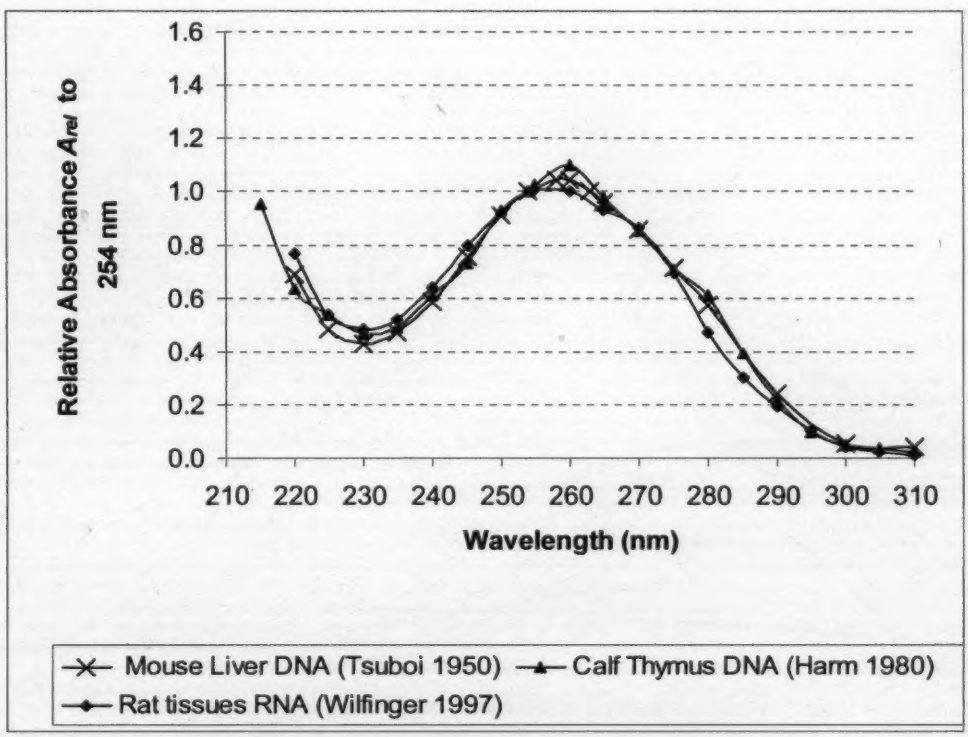

Figure 2.6: Absorbance spectra of nucleic acids

2.3.5 Comparison of Inactivation Action Spectra and a 'Standard' DNA Absorbance Spectrum

The action spectra for microorganisms are compared with the 'standard' DNA and protein absorbance spectra in Figure 2.7. *Cryptosporidium parvum* oocysts, the most UV sensitive microorganism studied so far, has an action spectrum (Linden et al. 2001) that matches well with the DNA absorbance spectrum above 230 nm, but is less sensitive for lower wavelengths. The action spectra of the fairly sensitive vegetative bacteria, such as *E. coli* and *S. aureus* studied by Gates (1930) are similar to the DNA absorbance spectrum, but show slightly higher sensitivities below 240 nm and at around 280 nm, as is demonstrated in Figure 2.5. The action spectrum of *B. subtilis* spores is consistent with those of vegetative bacteria below 265 nm, but has a significantly higher sensitivity around 280 nm, compared to those of other microorganisms. This is probably due to the unique DNA conformation and binding of DNA by small acid soluble proteins, a point that will be discussed later. The action spectrum of MS2 coliphage (Mamane-Gravetz et al. 2005), the second most germicidally UV resistant microorganism known, shows similar consistency with the 'standard' DNA absorbance spectrum above 240 nm, but diverges significantly below 240 nm. The most UV resistant microorganism that has been identified is adenovirus. Its action spectrum, measured by Linden at al. (2005), shows a significant difference from the 'standard' DNA absorbance spectrum. A germicidal factor of >5 from 229 nm to 254 nm was determined. From the peak around 260 nm to 289 nm, the relative sensitivity is much larger than that of the DNA absorbance spectrum. The inactivation spectra of all microorganisms described in Figure 2.5 seem to lie between the 'standard' absorbance spectrum of DNA and that of proteins. Therefore, the inactivation

of UV sensitive microorganisms is likely primarily due to the damage to nucleic acids (DNA or RNA). Thus, the inactivation action spectra of UV sensitive microorganisms should be close to that for the DNA absorbance spectrum. It is postulated that the inactivation of UV resistant microorganisms may involve more complex biological damage induced from photons absorbed by DNA and other absorbers, such as proteins. Hence, the action spectra of UV resistant microorganisms may be different from the DNA absorbance spectrum.

2.4 *Bacillus subtilis* Spores

2.4.1 Nature of *B. subtilis* Spores

Bacillus spores are derived from their vegetative cells, which are mostly aerobic and facultative bacteria. When grown in the absence of certain nutrients, these cells initiate the process of sporulation. This process includes: 1) the formation of two nucleoids in a cell; 2) the formation of an asymmetric septum that separates the cell into large and small forespores; 3) engulfment of the forespore by the large cell. 4) the formation of several external layers to the forespore and other biochemical events; 5) the lysis of the large cell and the release of a free spore (Setlow 1995). The average size of a spore is approximately 1.5 μm in length and 0.7 μm in diameter with an ellipsoidal shape. The structure of the spore is significantly different from that of a vegetative cell (Figure 2.7). From the outside in, the layers include the exosporium, the proteinaceous spore coat, the cortex composed of peptidoglycan, the inner core, containing most of the spore enzymes, ribosomes, and spore DNA.

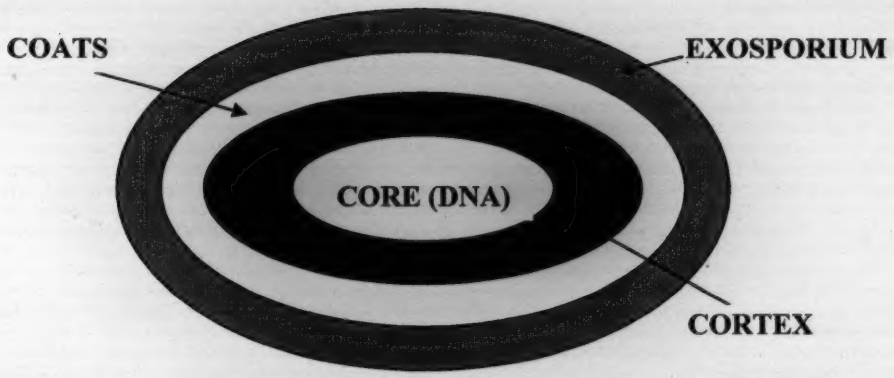

Figure 2.7: Schematic structure of a spore (Adapted from Setlow 1995)

Dormant *B. subtilis* spores can survive in the absence of exogenous nutrients or in harsh environments for a long period of time, due to significant changes during sporulation. The metabolic dormancy of spores is one important adaptation involved in long-term survival. There are two possible approaches for minimizing the deleterious effects of DNA damage: 1) protect dormant spore DNA from damage; and/or 2) repair of any DNA damage when spores germinate, resume metabolism, and activate macromolecular biosynthesis. In addition to long-term survival, spores are fairly resistant to chemical and physical treatments including oxidizing agents, heat, desiccation, UV and γ radiation (Setlow 1995). To safeguard the survival of a spore, the most important step is to ensure that its DNA is undamaged, or that any damage to the DNA is repaired during germination.

2.4.2 Environment of Spore DNA

The principal environmental features involved in preventing DNA damage in dormant spore are: 1) an internal pH of 6.5-7.0, which is one pH unit lower than the value

in vegetative cells, 2) low water content, and 3) the presence of small molecules unique to dormant spores (Setlow 1995). Setlow (1988) concluded that the pH and low water content do not contribute to the prevention of the DNA lesions arising from UV exposure However, he found that a group of small acid-soluble proteins (SASP) of the α/β-type that bind to the DNA of spores may play a significant role in the resistance of these spores to UV light and hydrogen peroxide (Setlow 1992a; Setlow and Setlow 1993a).

The α/β-type SASP are synthesized during sporulation and are rapidly degraded to amino acids at the beginning of spore germination. Studies have shown that these proteins are associated with DNA in spores and are nonspecific double-strained DNA binding proteins (Setlow 1995). Binding the SASP of DNA to vegetative cells *in vitro* has been found to have significant effects on DNA topology (Nicholson et al. 1990). A protein/DNA ratio of 4:1 to 5:1 has been measured in this binding (Setlow et al. 1992). With this binding stoichiometry, there is enough protein in spores to saturate the spore chromosome and to change DNA into an A-like conformation (Setlow 1992b). Also, the plasmid DNA from spores has approximately 50% more negative supertwists than that from vegetative cells (Nicholson and Setlow 1990). The binding of α/β-type SASP results stiffening and straightening of the DNA. Binding of these proteins to the exterior of the DNA helix protects the DNA backbone from attack from both enzymes and oxidative chemicals. Another major conformational change arising from this binding is that the protein changes from a random coil to the highly helical structure of DNA. This conformational change protects the protein against damage, such as methionine oxidation or asparagines deamidation (Setlow 2001). Indeed, removal of the majority of these proteins results in UV-sensitive spores (Mason and Setlow 1986), whose DNA

photochemistry and plasmid superhelicity are similar to those of vegetative cells. It is clear that the saturation of spore DNA with a group of SASPs is extremely important for *B. subtilis* spores to resist many physical and chemical treatments including UV light.

Another significant component in spore core is pyridine-2,6-dicarboxylic acid or dipicolinic acid (DPA), which accounts for approximately 10% of spore dry weight. DPA is unique in spores and is not found in vegetative cells. DPA release is one of the earliest events in spore germination. It was postulated that the presence of DPA also alters the structure of the α/β-type SASP/DNA complex (Setlow 2001). However, this postulation has not been confirmed yet.

2.4.3 Photochemistry of Spore DNA and the Repair of Damaged Spore DNA

Many studies of the UV resistance and DNA photochemistry of *B. subtilis spores* have employed 254 nm UV light. These spores are significantly (5 to 50 times) more UV resistant than their vegetative cell counterparts (Setlow 1988). Donnellan and Setlow (Donnellan and Setlow 1965) reported that DNA in spores has a unique UV photochemistry. They found that levels of cyclobutane thymine dimers in the DNA of irradiated spores were undetectable but were readily detected in the DNA of vegetative cells. The inhibition of the formation of these thymine dimers is primarily due to the α/β-type SASPs around the DNA. While more recent work has suggested that a small amount of these dimers is produced in spores, this photoproduct does not contribute appreciably to spore inactivation. However, a novel photoproduct, termed spore photoproduct (SP), has been detected in the DNA of UV irradiated spores. SP is also generated between two adjacent thymines on the same DNA strand. The structure of SP was determined to be 5-thyminyl-5, 6-dihydrothymine (Varghese 1970). However, a good molecular explanation

of this novel photochemistry is not available because the precise structure of the *α/β*-type SASP/DNA complex is not known (Setlow, 2001).

As noted above, one effect of *α/β*-type SASP binding is to alter the UV photochemistry of DNA, where the SP photoproduct is formed rather than cyclobutane dimers. SP is potentially a lethal lesion to a *B. subtilis* spores. There are two repair systems for SP. One repair system is nucleotide excision repair (NER), which can also repair cyclobutane dimers and is generally found in vegetative cells and other living organisms (Britt 2004;Munakata and Rupert 1972). It is possible that SP may be repaired to some small degree by recombinational repairs (Munakata and Rupert 1975). In the NER system, the gene products, whose synthesis is induced by UV damage, are similar to those found in *E. coli.* Another repair system is SP-specific repair. This repair is a monomerization of the SP by SP-lyase encoded in a two-gene operon. SP-lyase is a [4Fe-4S] enzyme, which requires SP binding to a double-stranded DNA substrate (Setlow 2001). In addition, the SP-lyase also requires S-adenosylmethiomine and a reductant for cleavage of SP into two thymines without DNA backbone cleavage (Slieman et al. 2000). Unlike DNA monomerzation in many microorganisms, this repair does not require light. The results of experiments conducted with *B. subtillis* spores indicated that SP-lyase plays a more important role in spore resistance to germicidal UV light than does NER (Xue and Nicholson 1996). A review by (Setlow 2001), however, indicated that both repair systems are very important for spores resistant to 254 nm UV light.

Furthermore, presence of DPA in the spore core has an effect on the DNA photochemistry. The decrease of DPA levels *in vitro* caused the increased resistance to UV light at 254 nm, and the fact that DPA increases the yield of SP as function of 254

nm (Setlow and Setlow 1993b). DPA appears to act as a photosensitizer (Ross and Setlow 2000) and the action mechanism can be explained by triplet energy transfer (Douki et al. 2005a). In this mechanism, excitation energy resulting from the absorption of photons by DPA can be transferred to the DNA of *B. subtilis* spores.

It is obvious that proteins such as α/β-type SASP and SP-lyase, in *B. subtillis* spore DNA play critical roles in determining the resistance of spores to UV light. The inactivation of these proteins might contribute to the lethal action of UV on spores, although no published literature is available that proves this mechanism. However, there is possible evidence of this mechanism in previously published works by Cabaj et al. (2002) and Mamane-Gravetz et al. 2005).

2.4.4 An Important Surrogate Organism

Most pathogens in water are usually present in very low concentrations, and are difficult to isolate, identify and enumerate. Therefore, it is necessary to use surrogate microorganisms in water disinfection studies in order to assess the performance of UV reactor equipment. An ideal surrogate microorganism should have the following characteristics:

1. The surrogate should equally or less sensitive to UV light than the challenge pathogens,
2. The surrogate should be inexpensive, non-pathogenic and easily cultured and enumerated in a laboratory, and
3. The UV fluence response of the surrogate should be reproducible and reliable.

B. subtilis spores exist in a variety of environments including in municipal wastewater or untreated drinking water. Spores can survive in harsh conditions and can be easily stored in a laboratory for a long time. Furthermore, spores are resistant to many physical and chemical treatments including UV light. The resistance characteristics of spores reduce the potential for effects of variation in test water matrix composition on the outcome of a UV disinfection or UV reactor validation study. *B. subtilis* spores have commonly been used in UV disinfection studies (Chang et al. 1985; Sommer and Cabaj 1993; Cabaj et al. 2001;Sommer and Cabaj 1993; Cabaj et al. 2002; Mamane-Gravetz and Linden 2005;Uvbiama and Craik 2005). Regulatory agencies have proposed that *B. subtilis* spores be used a surrogate microorganism for UV reactor validation (DVGW 1997; USEPA 2003).

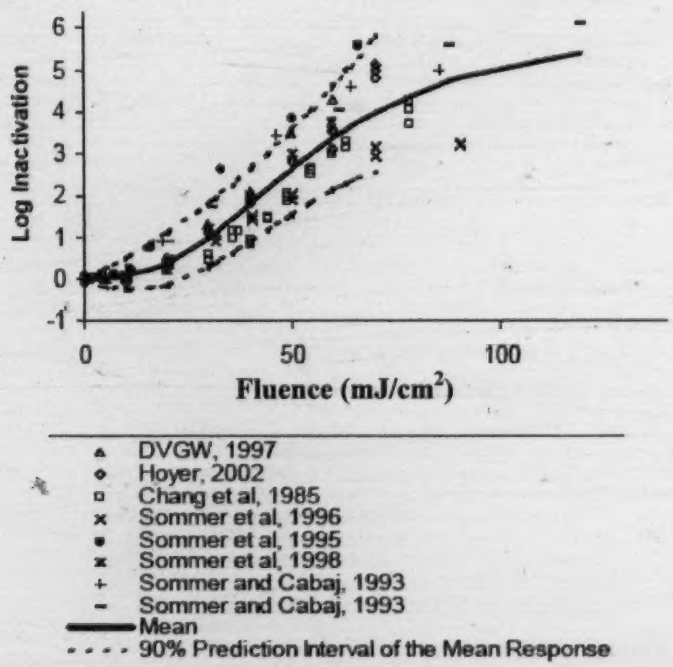

Figure 2.8: UV fluence response of *Bacillus subtilis* spores
(Adapted from USEPA 2003)

2.4.5 UV Inactivation of *B. subtilis* Spores

UV inactivation of *B. subtilis* spores has been studied and the UV fluence inactivation response has been characterized by several researchers. Figure 2.8 summarizes fluence-inactivation responses from the published literature. These researchers have all used a collimated beam apparatus to carry out the UV exposures; however, the spore production methods were different. *B. subtilis* spores exhibit a minor shoulder in the UV fluence response on a semilog plot possibly due to the self-repaired ability of their double-stranded DNA (Harm 1980). As shown, the mean response shows a significant tailing-off when the log inactivation level is greater than 4. In addition, the fluence-inactivation response of spores is affected by the age, density, lysozyme sensitivity, DNA heterogeneity and cultivation medium used for sporulation (Cerf 1977). In terms of the sporulation medium effect, Sommer and Cabaj (1993) reported that spores cultivated in a surface solid medium were significantly more sensitive to UV than those cultivated in a liquid medium. Cabaj et al. (2002) used Schaeffer's broth as the sporulation medium to study the inactivation spectrum of *B. subtilis* spores (ATCC 6633), while Mamane-Gravetz et al. (2005) used Columbia solid agar. The first-order inactivation rate constants for LP UV light (254 nm) for these studies were 0.0612 and 0.0127 cm^2/mJ, respectively. Although the inactivation rate constants determined in the two studies are considerably different, the inactivation spectra are similar (Mamane-Gravetz et al. 2005). The inactivation rate constant reported by Uvbiama (Uvbiama 2006) at University of Alberta for this same spore strain was approximately 0.09 cm^2/mJ. He used a modified Schaeffer broth method to produce the spores. This strain of spores and the modified Schaeffer broth method will be used in this study.

2.5 Salmonella

2.5.1 Nature of *Salmonella* spp.

Salmonella is a Gram-negative facultative rod-shaped bacterium in the family *Enterobacteriaceae*, the same proteobacterial family as *Escherichia coli*, and is generally considered to be an enteric bacterium. More than 2000 serovars of *Salmonella* spp. have been identified. All these serovars are potentially pathogenic to humans and can cause illness (Maier et al. 2000). *Salmonella* spp. nomenclature has been controversial. The original taxonomy of the genus was based on clinical relatedness, e.g., *Salmonella typhi*, *Salmonella cholerae-suis, Salmonella abortus-ovis*, etc. Subsequently, the newly discovered serovars were named from the geographical origin of the first isolated strain. In medical practice, the serovars names are kept for the vernacular terminology, such as *Salmonella ser. typhimurium* or shorter *S. typhimurium*.

2.5.2 Description of the Diseases

A variety of both cold- and warm- blooded animals can be infected by *Salmonella* spp. *S. typhi*, which causes typhoid, and *S. paratyphi*, which causes paratyphoid fever, are usually found only in humans. The pathogenicity may differ from strain to strain. An oral dose for 50% human typhoid infections (D_{50}) is more than 10^5 *S. typhi* cells, whereas the D_{50} for humans is at least 10^9 *S. typhimurium* cells. The symptoms of typhoid and paratyphoid fever are more severe in the elderly, infants and infirm.

In the pathogenesis of intestinal disease, *Salmonella* spp. organisms enter the human digestive tract, penetrate the intestinal mucosa and enter into the mesenteric lymph nodes. There, replication of the bacteria occurs, and an enterotoxin is produced

and some of the bacteria lyse. From the mesenteric lymph nodes, viable bacteria and the enterotoxin may be released into the bloodstream. The symptoms of salmonellosis may include nausea, vomiting, abdominal cramps, diarrhea, fever, and headache and septicemia (Maier et al. 2000).

2.5.3 Environmental Significance

Salmonellosis is primarily due to food-borne transmission and is the second leading cause of food-borne disease in the United States (Maier et al. 2000). *Salmonella* spp. can be associated with all kinds of food. Meat (cattle, pigs, chickens, etc.) contaminated by these bacteria can support their growth and multiplication. Other foods, such as eggs, cream, mayonnaise etc., also allow multiplication of *Salmonella* spp. Vegetables and fruits may carry *Salmonella* spp. when fertilized or irrigated with water of fecal origin, or washed with contaminated water. In a typical cycle of typhoid by food ingestion, a wastewater treatment facility for a community discharges poorly-treated effluent into a waterbody. *Salmonella* spp. bacterium present in the effluent passes into edible shellfish living in the waters. Shellfish can concentrate *Salmonella* spp. but the bacteria do not grow inside the larger organisms. Ingestion by human of these uncooked seafoods may cause typhoid or other salmonellosis. It is necessary to disinfect these bacteria during wastewater treatment processes to disrupt the pathway of transmission.

Surface waters may be contaminated with *Salmonella* spp. when receiving domestic sewage effluents, meat processing wastes, or stockyard wastes. In addition, *Salmonella* spp. can survive municipal wastewater treatments if disinfection is not sufficient in these processes, after which sub-treated effluents are released into the surface water. One study reported that *Salmonella* spp. was detected in 8 out of 128

samples from surface waters in Greece including river water and lake waters (Arvanitidou et al. 1997). Furthermore, surface waters may serve as the source water of drinking water.

Water-borne salmonellosis has been documented for more than one hundred years. In the United States, during the Civil War, typhoid fever of encamped soldiers was widespread because they drew drinking water at a point downriver from an upriver point contaminated by their disposal of waste. In 1890, it was reported that more than 30 people out of every 100,000 died of typhoid fever in the United States. This situation improved significantly because of the emergence and popularization of filtration and chlorination treatments of drinking water in the early 20th century. These new practices led to a dramatic decrease of the death rate from 36 to 5 cases per 100,000 people between 1900 and 1928 in the United States (Maier et al. 2000). In Israel, the documented cases of water-borne salmonellosis and typhoid decreased from more than one thousand to zero from 1976 to 1997 (Tulchinsky et al. 2000). However, *Salmonella* spp. contamination of drinking water and outbreaks of salmonellosis are still reported in some communities without proper disinfection of drinking water. In 1993, a large water-borne outbreak of *S. typhimurium* was reported in Gideon, Missouri, a city with an unchlorinated community water supply. In this event, more than 650 persons were sick; 15 were hospitalized, and 7 died (Angulo et al. 1997). In Mysore, India, it was reported that 8 out of 37 samples of bore well water use for drinking purposes were with positive for *Salmonella* spp. (Nagaraju and Sastri 1999). Sufficient disinfection of both wastewater and drinking water can significantly mitigate the risk of *Salmonella* spp. infections and protect public health.

2.5.4 UV Inactivation of *Salmonella* spp.

As an important pathogen in water, the UV inactivation of *Salmonella* spp. has been studied using LP lamps. The fluence-inactivation responses of *Salmonella* spp. from different studies are summarized below. As demonstrated in Figure 2.9, the UV sensitivity of *Salmonella* spp. can differ among serovars even, within the same study (Tosa and Hirata 1998). The most resistant serovar in these studies is *S. anatum*, which requires 15 mJ/cm^2 to achieve 3-log inactivation. Nonetheless, all the *Salmonella* spp. serovars are fairly sensitive to UV light, and they can be effectively inactivated by drinking water UV reactors, in which the design germicidal fluence is usually at least 40 mJ/cm^2. The fluence-inactivation responses of the same serovar reported in different studies tends to be the same. For example, the fluence-inactivation of *S. typhi.* (Chang et al. 1985; Wilson et al. 1992) and of *S. enteritidis* (Tosa and Hirata 1998; Koivunen and Heinonen-Tanski 2005) do not exhibit much difference among the studies. The difference between the fluence-inactivation characteristics of the two strains is greater than the variation among the fluence-inactivation characteristics of same strain between studies.

No published work has reported the UV action spectrum of these bacteria. The only available approach for estimating the effectiveness of a polychromatic UV light source for an organism, for which the action spectrum is unknown, is to use the 'standard' DNA absorbance spectrum as a surrogate to calculate a germicidal weighting factor. The chromosomal nucleic acid of *Salmonella* spp. is double-stranded DNA, and the photochemistry of *Salmonella* spp. can be assumed to be the same as many other vegetative cells, as described previously. For example, much like *E. coli.*, it can be assumed that the inactivation action spectrum of *Salmonella* spp. should be similar to that

of its DNA absorbance spectrum because it is relatively sensitive to UV light. It can be further assumed that the 'standard' DNA absorbance spectrum derived from absorbance measurements of the DNA of entirely different organisms is a reasonable model for the DNA absorbance spectrum of *Salmonella* spp. This approach is, therefore, based the critical assumption that the 'standard' DNA absorbance spectrum reported in the literature is an appropriate surrogate for the actual action spectrum of these pathogens. However, this assumption needs to be tested, and the inactivation action spectrum needs to be well characterized to estimate accurately the weighted germicidal fluence from a polychromatic source. As well, no published literature is available for the DNA absorbance spectrum of *Salmonella* spp.

Some strains of *Salmonella* with artificial mutations are avirulent. The strain of *Salmonella typhimurium* LT2 has a highly attenuated of virulence and has been commonly used as a surrogate for virulent *Salmonella* spp. in laboratory studies. The chromosomal nucleic acids of *S. typhimurium* LT2 are not significantly different from those of virulent stains. The sensitivity of this strain to UV light is not expected to be very different from virulent strains. Therefore, *S. typhimurium* LT2 was selected as a surrogate for this study.

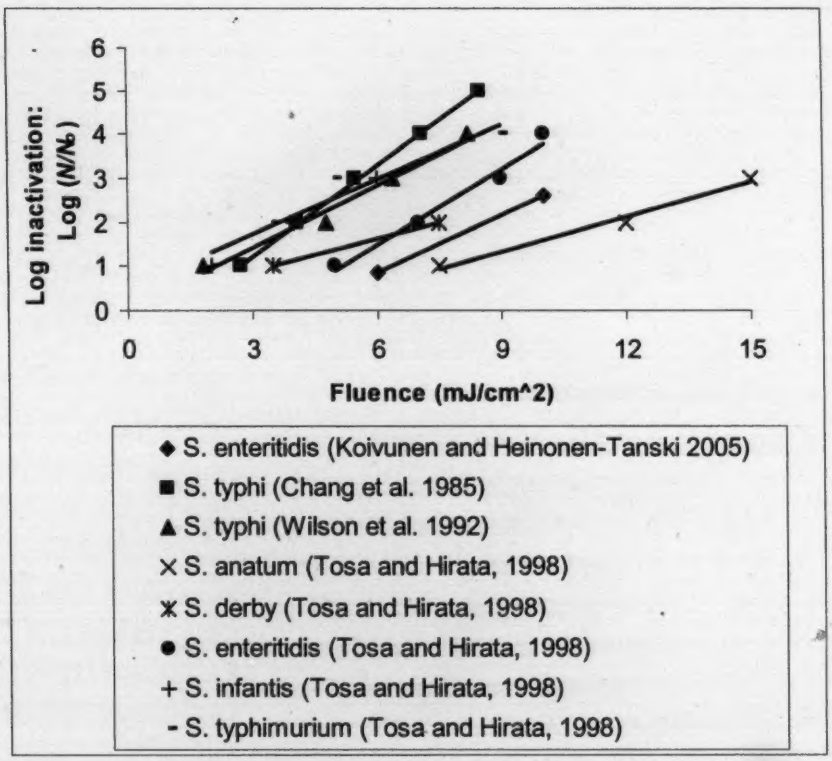

Figure 2.9: Fluence response of *Salmonella* spp.

2.6 Problem Statement and Needs for this Research

MP mercury lamps, which generate polychromatic UV light within the germicidal range from 200 to 300 nm, have been widely used in many water disinfection facilities and water disinfection studies. According to current practice, the relative germicidal effectiveness of these lamps is determined using a *germicidal factor*. In principle, the *germicidal factor* should be the relative action spectrum (usually normalized to 1.00 at 254 nm) of the particular microorganism. Many researchers have characterized the inactivation action spectra for microorganisms including some important water-related pathogens, such as *Cryptosporidium parvum*. The inactivation spectra of the UV-

sensitive microorganisms studied, such as protozoan parasites and bacteria, have been found to be similar to the 'standard' DNA absorbance spectrum. However, the inactivation spectra of some UV-resistant microorganism have been found to diverge significantly from the 'standard' DNA absorbance spectrum, particularly below 240 nm and around 280 nm. The inactivation effect of UV light on microorganisms may be attributed primarily to lesions of DNA or RNA, including formation of dimers. However, it is possible that the inactivation effect may also be attributed partially to the photon absorbed by other components in a cell, such as the inhibition of some important proteins and DNA-protein crosslinks, especially at high fluence levels.

When the action spectrum of a specific microorganism is not available, the germicidal factor is usually estimated from the 'standard' DNA absorbance spectrum. This factor, along with other factors, such as the emission spectrum of the MP lamp and the transmittance spectrum of the quartz sleeve, is used to evaluate the efficiency of a UV reactor that uses polychromatic UV lamps. This approach may be problematic because of possible differences between the actual inactivation spectrum and the 'standard' DNA absorbance spectrum. It has also been postulated that the DNA absorbance spectra of different organisms may differ. It may be necessary to compare the inactivation action spectrum of a microorganism to its own DNA absorbance spectrum, rather than to the 'standard' one. Although a number of studies have determined the UV action spectra of various microorganisms, there have been few, if any, careful comparisons to the absorbance spectra of DNA isolated from the microorganisms actually studied.

B. subtilis spores are often used to evaluate the performance of UV reactor systems used for disinfection of drinking water, and the UV inactivation characteristics of

B. subtilis have been well studied. There are two published papers available in which the UV inactivation action spectrum of *B. subtilis* spores was determined. The results of these two studies are similar with peaks in the action spectra at around 265 nm. Both of these spectra, however, diverge significantly from the 'standard' DNA absorbance spectrum in only one region, around 280 nm. This is different from other UV resistant microorganisms, such as adenovirus and MS2 coliphage, whose inactivation spectra diverge significantly from DNA absorbance in two regions, around 280 nm and below 240 nm. Furthermore, spore DNA is unique because it is saturated with a group of SASPs and is surrounded with DPA, which alter the DNA conformation and possibly protect the DNA from UV-induced damage. The binding of the SASPs to DNA may also influence DNA repair mechanisms and may explain the relatively high resistance of spores to UV light, in comparison to the vegetative cells. Given the high absorbance of proteins below 240 nm, the possible role of proteins in spore UV resistance, the action spectrum of *B. subtilis* spores in this range could be enhanced over the 'standard' DNA absorbance spectrum arising from excitation energy transfer. Besides, DPA in the spore core can affect the photochemistry of *B. subtilis* spores. Thus, it also may alter the action spectrum, so that it deviates from DNA absorbance spectrum. A rigorous characterization of the inactivation spectrum of spores needs to be conducted for comparison. In this study, the DNA absorbance spectrum and the action spectrum will be measured and compared side-to-side.

Salmonella spp. are very important pathogens in the water and food industries. UV treatment has been found to inactivate this pathogen very effectively. However, the inactivation action spectrum of *Salmonella* spp. has not been reported. It is necessary to

characterize its inactivation spectrum and measure its DNA absorbance spectrum. In this study, an avirulent strain of *S. typhimurium* LT2 was selected as a surrogate for the virulent *Salmonella* spp.

3 COMPARISON OF THE ACTION SPECTRUM AND THE DNA ABSORBANCE SPECTRUM OF *BACILLUS SUBTILIS* SPORES

3.1 Introduction

Ultraviolet (UV) treatment is an increasingly popular technology for the disinfection of drinking water and secondary or tertiary wastewater effluents. Although low pressure UV lamps are commonly used for small UV disinfection reactors, medium pressure mercury lamps, which produce polychromatic germicidal UV light, are commonly used in large-scale UV disinfection reactors for drinking water and wastewater treatment. As well, many UV disinfection studies have been carried out using MP lamps (Bolton et al. 1998;Bukhari et al. 1999; Craik et al. 2000; Linden et al. 2005).

Different methods have been reported in the literature for the determination of the germicidally weighted fluence (UV dose) for polychromatic UV sources. A standardized method that uses a germicidal factor to calculate the germicidal fluence (UV dose) from a polychromatic source in bench-scale UV experiment has been proposed (Bolton and Linden 2003). In the validation of a UV reactor equipped with MP lamps using biodosimetry, the evaluation of the reactor efficacy can be affected by the action spectra of challenge microorganisms and target pathogens used (USEPA 2003). Moreover, studies have reported that the germicidal efficacy of microorganisms is highly dependent on wavelength and might vary from microorganism to microorganism (Gates 1929; Rauth 1965; Linden et al. 2001; Linden et al. 2005). A 'standard' DNA absorbance spectrum, reported by von Sonntag (1986), has been used as a surrogate when the inactivation action spectrum was not available.

B. subtilis spores are a surrogate microorganism commonly used to measure and validate UV reactor performance (USEPA 2003; DVGW 1997) and for fundamental UV disinfection studies (Sommer and Cabaj 1993; Uvbiama and Craik 2005). It has been reported that *B. subtilis* spores have their own unique photochemistry and repair mechanisms, which accounts for their greater resistance to UV light than vegetative bacterial cells (Setlow 2001). The novel photochemistry has been discussed as arising from: 1) low water content in the spore core (Rahn and Hosszu 1969; Partrick and Gary 1976); 2) binding of DNA with α/β small acid soluble proteins (SASP) (Setlow et al. 1992; Douki et al. 2005b); and 3) photosensitization of DNA by dipicolinic acids (DPA) in the spore core (Douki et al. 2005a). The inactivation action spectrum for *B. subtilis* has been determined for spores produced from liquid-cultivated (Cabaj et al. 2002) and from surface-cultivated (Mamane-Gravetz et al. 2005) sporulation media. Both studies reported a similar wavelength dependence for the first-order spore inactivation rate. *B. subtilis* spore inactivation, however, is also characterized by a shoulder region at low fluence (UV dose), where little or no inactivation is observed. This shoulder region must also be considered carefully when determining the spore action spectrum. Careful determination of the microorganism action spectrum is crucial for accurate determination of the germicidal fluence (UV dose) when polychromatic lamps are used for UV disinfection studies and for interpreting the results of MP UV reactor bioassays. Moreover, in the previous studies the action spectra of *B. subtilis* spores differed from the 'standard' DNA absorbance spectrum. However, it was not clear what organism and methods were used for measuring the 'standard' DNA absorbance by von Sonntag (1986). Different

organisms may have a different ratio of nucleotide bases, and thus could exhibit different spectral absorbance characteristics.

The objectives of the study in this chapter were to determine the action spectrum of *B. subtilis* spores and compare it to the absorbance spectrum of decoated spores and DNA purified from spores, and to compare these spectra to previously published inactivation action spectra.

3.2 Materials and Methods

3.2.1 *Bacillus subtilis* Spores Production, Preparation of Test Suspensions, and Enumeration

All sterile media, reagents and materials were prepared by autoclaving at 121°C for 15 min or were purchased pre-sterilized. The stock solution of *B. subtilis* spores was kindly provided by Dennis Uvbiama at University of Alberta. Procedures for preparation of *B. subtilis* spores (ATCC 6633) stock solution by growth and sporulation in liquid culture have been described elsewhere (Uvbiama and Craik 2005; Craik and Uvbiama 2005; Uvbiama 2006). The concentration of the stock solution was determined using a nutrient agar pour plate technique as described later. Sterile phosphate-buffered (0.05 M) deionized water (PBDI) was prepared by adding in 0.02 M Na_2HPO_4 and 0.03 M KH_2PO_4 to de-ionized water produced from a Milli-Q ultrapure water system and the adjusting the pH to 7.0 using either 1 M NaOH or 1 M HCl. The PBDI and was then autoclaved at 121°C for 15 min. The experimental spore suspensions were prepared by adding an aliquot of stock spore suspension to a volume of sterile PBDI water to yield a spore concentration of approximately 10^6 Colony Forming Units (CFU) per mL. The actual

concentration of this suspension was determined by enumeration as described later. The spore suspension was stored at 4°C and was used in exposure experiments within 2 weeks of preparation.

A nutrient agar pour plate technique was used to determine the spore concentration (in CFU/mL) in the stock solution, test suspensions and experimental samples. Briefly, a 1 mL aliquot of stock or experimental suspension was transferred into a sterile test tube with 9 mL of a sterile PBDI water. The diluted suspension was mixed using a vortex mixer (Genie 2 Fisher Vortex, Fisher Scientific, Bohemia, NY) for about 30 s at a medium-high setting. A decimal dilution series was prepared by repeating this procedure. The test tubes containing the series were immersed in a water bath at 80°C for 15 min. This heat pasteurization step is sufficient to kill most vegetative bacterial cells that may have entered the sample without inactivating the spores. One mL of each enumerated dilution was aseptically transferred into a sterile 150 x 15 mm pre-sterilized polystyrene Petri dish (Fisher Brand). Approximately 15 mL of sterile nutrient agar, prepared according to the procedure in Appendix A-1, was aseptically poured onto the 1 mL suspension. The contents of the covered Petri dish were gently but thoroughly mixed using back and forth and swirling motions of the dish. For each enumerated dilution, triplicate plates were produced as described above. Agar plates were left to solidify for approximately 10 min and were then inverted and incubated at 37°C for 48 h. The number of colonies on each plate were then counted and recorded and the concentration of spores in the original samples (in CFU/mL) was calculated.

3.2.2 UV Exposure

A collimated beam apparatus (Calgon Carbon Corporation, USA) was used for all UV exposures. To generate monochromatic UV radiation at 254 nm, spore suspensions were exposed to a low pressure (LP) mercury arc lamp (Ster-L-Ray Germicidal Lamp, 10 W, model G12T6L 15114, Atlantic Ultraviolet Corporation, USA). A set of ten band-pass filters (Andover Corporation, Salmen, NH) were housed on the top of collimated tube (Figure 2.1) to isolate narrow bands of UV light produced from a MP lamp (HNG, 1 kW, Strahler, Germany). The relative spectral irradiance for each wavelength band was produced through the combination of the MP lamp output spectrum and the spectral transmission spectrum of the filter. The relative spectral irradiance of each wavelength band was measured directly using a spectroradiometer (USB2000, Ocean Optics, Dunedin, FL). Then, a relative photon flux was calculated by relative irradiance multiplying the averaged wavelength of a 0.38 nm interval which matched the resolution of the spectroradiometer. The weighted average wavelength of each band was calculated by the sum of product of relative photon flux and wavelength divided by the sum of relative photon flux of all 0.38 nm intervals. The characteristics of each wavelength band are presented in Table 3.1.

Table 3.1 Characteristics of the narrow band UV light produced by the MP lamp and the band-pass filters

Nominal Wavelength of BPF (nm)	Weighted Average Wavelength (nm)	Half Peak Bandwidth (nm)
214	222	10.3
220	224	9.1
228	231	9.9
239	243	13.3
248	251	6.8
260	262	9.1
270	269	7.2
280	279	3.4
290	291	9.7
300	302	9.7

Triplicate UV exposures were carried out for each fluence and for each wavelength band. During the experiment for a specific wavelength band, the UV lamp was preheated for more than 10 min. The experimental spore suspension was removed from the refrigerator and pre-warmed to room temperature in an Erlenmeyer flask with continuous stirring with a magnetic stir bar. A 21 mL aliquot of the experimental spore suspension was withdrawn from the flask and transferred into a sterile glass Petri dish (4.73 cm in diameter) that contained a 10 mm × 3 mm Teflon-coated magnetic stir bar. After more than 30 s of gently stirring, a 1 mL aliquot of the unirradiated suspension was transferred from the Petri dish into a test tube containing 9 mL of sterile PBDI. A dilution series was prepared and to determine and the concentration of viable *B. subtilis* spores in the Petri dish before UV exposure (N_0) was determined as described above. The rest of the suspension was exposed to UV by opening and closing the pneumatic shutter located beneath the UV lamp. The exposure time was measured using a stopwatch (Fisher Scientific). Once the pre-determined exposure time for the first fluence level target was

reached, the shutter was closed and the stopwatch was paused. A 1 mL aliquot of suspension was removed from the Petri dish and enumerated as described above to determine the concentration of viable *B. subtilis* spores in the Petri dish after the first UV fluence exposure (*N*). The shutter was then re-opened and the timing was continued until the second target fluence level target was reached. Another 1 mL aliquot of the suspension was collected and enumerated to determine the concentration of viable *B. subtilis* spores in the Petri dish determined. This procedure was repeated until all UV fluence levels were completed. The absorbance of the experimental suspensions was less than 0.05 cm^{-1} over the experimental wavelength range (220 to 320 nm). The fluence rate in the suspension varied only slightly with the water depth. For example, in the experiment with the 222 nm wavelength band, the depth of water changed from 1.14 cm to 0.85 cm, and the average fluence rate varied from 0.0436 at the surface of the liquid 0.0430 to mW/cm^2 at the bottom of the Petri dish (a change of less than 1.5%). In addition, the suspension was continuously mixed. The small variation in fluence rate with depth and stirring ensured that all microorganisms were exposed to a similar fluence. The average fluence (UV dose) for each subsample was then corrected using linear interpolation because of the sub-sampling.

3.2.3 Fluence (UV Dose) Determination

Calculations of the unweighted depth-averaged fluence rate at each wavelength band were based on the protocol proposed by Bolton and Linden(2003). A modified version of the spreadsheet developed by Bolton (2004) was used for the wavelength bands from the medium pressure lamp. For each wavelength band, the fluence rate at the centre surface of the suspension in the Petri dish was measured at wavelength intervals of

0.38 nm using the spectroradiometer. Also, for each wavelength band, the total irradiance incident at the centre of the surface of the suspension was measured using an International Light radiometer (Model IL 1400A) with a SEL 240 detector (International Light, Newburyport, MA). The detector sensor factor which accounts for the wavelength dependence of the sensor response, was determined using a ferrioxalate chemical actinometry protocol provided by Bolton (2006) and which is described in detail in Appendix A-2. The results for detector sensor factor measurement were presented in Table A-1 in Appendix A-2. A reflection factor was used to take account for an incident UV beam from one medium to another. For air to water, the reflection factor is 0.975 in the 200-300 nm region (Bolton and Linden 2003). Because the irradiance of incident beam over a test suspension was not identical, the Petri factor was determined by scanning the radiometer detector every 5 mm along two perpendicular imaginary lines that intersect at the center point of the beam. The water factor was used to take account for the irradiance attenuation through a suspension. The spectral absorbance between 200 and 300 nm of each test suspension was measured in a 1 cm quartz cell using a spectrophotometer (UV-2401PC, Shimadzu Corp., Columbia, MD). For each 0.38 nm interval of a wavelength, the absorbance factor was calculated from Beer's law. The overall absorbance was determined by the sum of the products of all relative photon flux and the absorbance factor divided by the sum of all relative photon flux of 0.38 nm intervals. To account for the beam divergence through a suspension, the divergence was determined by the length from the lamp to the surface of the suspension divided by the sum of the length and the depth of the suspension. For the LP lamp, the spreadsheet proposed by Bolton (2005) was used for fluence rate calculations and the absorbance

factor was directly determined from the absorbance at 254 nm. For each wavelength band, the unweighted, depth-averaged fluence rate was calculated by multiplying the incident irradiance by a Petri factor, a reflection factor, a water absorbance factor and a beam divergence factor.

3.2.4 Data Analysis and Modeling

The initial concentration (N_0) of viable *B. subtilis* spores was determined from enumeration of the un-irradiated test suspensions, and the concentration (N) of viable spores after a given UV exposure as determined from enumeration of an irradiated sample. Both N and N_0 were calculated from the geometric mean colony count of three plates, and the survival ratio (N/N_0) was computed. For each wavelength band, the fluence-inactivation relationship was mathematically modeled using the multi-target model (Severin et al. 1983) given by:

$$\frac{N}{N_0} = 1 - (1 - 10^{-kH'})^{n_c} \qquad \text{Eqn. (3.1)}$$

where H' is the unweighted fluence, n_c is the number of critical targets and k is the first-order inactivation rate constant. The number of critical targets, n_c, is directly related to the shoulder in the fluence-inactivation curve. As n_c increases, the size of the shoulder increases. When n_c is unity, Eqn. (3.1) reduces to a simple first-order model. For each wavelength band, k and n_c, were estimated using non-linear regression (the least sum of residual squares criteria) carried out with the Solver tool in Microsoft Excel™ 2003. The inactivation action spectrum was then obtained by plotting the ratio $k_{rel} = k_\lambda / k_{254}$ where

k_{254} is the rate constant determined at 254 nm and k_λ is the rate constant determined for the particular wavelength band.

To know the precision of the estimates of k and n_c, the 95% Joint Confidence Rejoins (JCR) were constructed. These two parameters in the model were considered simultaneously and their correlation in parameter estimates was described. The critical sum of squares values that bounded 95% JCR was given by:

$$S_c = S_R(1 + \frac{p}{n-p} \times F_{p,n-p,5\%}) \qquad \text{Eqn. (3.2)}$$

where p was the number of parameters estimates (here p was 2), n is the number of experimental data used, and $F_{p, n-p, 5\%}$ is the upper 5% percent value of the F distribution with p and $n - p$ degree of freedom, and S_R is the sum of residual squares. The sum of squares in function of k and n_c were calculated using "Table" of "Data" and the 95% JCR was obtained by plotting S_c using "Contour Surface" of "Chart" in Excel™ 2003.

3.2.5 Measurement of Absorbance Spectra of *B. subtilis* DNA and Decoated Spores

B. subtilis spores in the stock solution were suspended in Milli-Q® water and the suspension was centrifuged at 7500 × *g* for 10 min at 4°C. The supernatant was removed and the pellet was resuspended in clean Milli-Q® water. The wash step was repeated twice more. The purified spores were re-suspended in spore decoating solution [8 M urea, 50 mM Tris-Base (pH 10), 1% sodium dodecyl sulfate, 50 mM dethiothreitol], and then incubated at 50°C for 90 min (Slieman and Nicholson 2000). Decoated spores were centrifuged at 7500 × *g* for 10 min at 4°C, and the pellet was resuspended in STE buffer (10 mM Tris-HCl [pH 8], 10 mM EDTA, 150 mM NaCl, Fisher scientific) three times.

After a final centrifugation step, the pellet was resuspended in lysis buffer (50 mM NaCl, 100 mM EDTA). For preparation of vegetative cells before lysis, an isolated colony of *B. subtilis* growing on a solidified agar plate was aseptically inoculated into 100 mL sterile nutrient broth solution in a 250 mL Erlenmeyer flask (1 μM $FeSO_4$, 10 μM $MnCl_2$, and 8 g nutrient broth/L [BBL Nutrient Broth, Benton Dickinson Microbiology Systems, Cockeysville MD]). The broth was incubated at 37°C at 180 rpm on an incubator shaker (Innova 4080, New Brunswick Instruments Co. Inc., Edison, NJ) for 6 h to produce vegetative cells. Vegetative *B. subtilis* cells were then harvested by centrifugation at 7500 × *g* for 10 min at 4°C. The supernatant was decanted. The pellet was centrifuge for 7500 × *g* for 10 min at 4°C and re-suspended STE buffer three times with and once in lysis buffer. The suspensions of decoated spores or the vegetative cell in lysis buffer were treated with 0.5 mL lysozyme (Sigma), incubated at 37°C for 30 min, and then treated with 0.1 mL proteinase K (DNeasy®, Germany). The lysed spores were incubated at 75°C for 30 min.

Chromosomal DNA, in either the lysed spores solution or the lysed vegetative cells solution, was extracted and purified by phenol-chloroform extraction and ethanol precipitation according to "Current Protocols in Molecular Biology" (Ausuvel et al. 1992). The DNA precipitate was dried in air to evaporate the ethanol for more than 12 h and then dissolved in TE buffer (10 mM Tris-HCl [pH 8.0] and 1 mM EDTA). The absorbance spectrum of the spore DNA was measured using a spectrophotometer (UV-2401PC, Shimadzu Corp., Columbia, MD). A solution of TE buffer served as the reference for the spectrophotometry.

To measure the absorbance spectrum of decoated spores, the decoated spore suspension was centrifuged at 7500 x *g* for 5 min at 4°C. The supernatant was removed and the pellet was re-suspended in Milli-Q® water to a final volume of approximately 10 mL. This wash step was repeated twice more. The pellet was then dissolved by the addition of 1 mL of 1 M HCl followed by incubation at 75°C for 30 min (Tsuboi 1950). The dissolved spore solution was neutralized by adding 1 ml of 1 M NaOH and was buffered to pH 7.0 by addition of with 8 mL 0.05 M PBDI. The absorbance spectrum of decoated spores was measured as described above. The solution prepared using the same procedure, excluding the decoated spore pellet, was served as the reference for the spectrophotometry.

3.3 Results and Discussion

3.3.1 UV Fluence-Inactivation Response Curves

Spore enumeration data are presented from Table B-1 to Table B-11 in Appendix B-1. The UV inactivation responses of *B. subtilis* spores versus fluence for each wavelength band are presented in Figure 3.1 using semi-log plot. Inactivation responses for the 289 nm and 302 nm bands are presented separately using a different horizontal scale for convenience. Each response curve exhibited a shoulder effect at low UV fluence that is characteristic of *B. subtilis* spores. The resistance of the spores to low UV fluences has been attributed to the self-repair capability of double-stranded DNA (Harm 1980). When the log inactivation was greater than 4, tailing effects were observed in some of the response curves (e.g., at 225, 231 and 262 nm), probably due to experimental artifacts such as spore clumping. Since the multi-target model does not accommodate tailing behaviour, data in the tailing regions (i.e., greater than 4 log inactivation) were omitted

from the least-squares estimation of the parameters k and n_c. The inactivation curves were derived from the estimated k and n_c from the best fit to the multiple-target model.

The 95% JCRs of k and n_c for all wavelength bands are presented from Figure B-1 to Figure B-11 in Appendix B-3. All JCRs indicate these two parameters were highly correlated, and a small change in the estimated value of k leads to a significant change in the estimated value of n_c. When k goes up, n_c goes up quickly. Table 3.2 presents k and n_c values of all wavelength bands estimated from the multi-target model. The lower and upper values were derived from their JCRs. It was clearly shown that k values varied mostly within ±10% in 95% statistical confidence. However, the values of another parameter n_c varied significantly. For example, the n_c value for the 269 nm wavelength band varied from 11 to 66. Even on a $\log(n_c)$ scale, the variation was still significant.

3.3.2 Wavelength Dependence of Inactivation Rate Constant, Number of Critical Targets and Threshold Fluence

As demonstrated in Table 3.2, the inactivation rate constants (k) determined in this study varied from 0.0018 to 0.176 mJ/cm^2 within the germicidal UV range. The significant variation of k confirmed that the UV sensitivity of *B. subtilis* spores is highly wavelength dependent. According to the multi-target model, the shoulder effect in the *B. subtilis* spore inactivation curves is present because a minimum number of critical targets, given by n_c, must absorb photons and react photochemically before an individual microorganism is effectively inactivated. The n_c values varied from 4 to 24 with no apparent trend with wavelength. The average value for all wavelength bands was 11. This variation may be attributed to the mathematic model used.

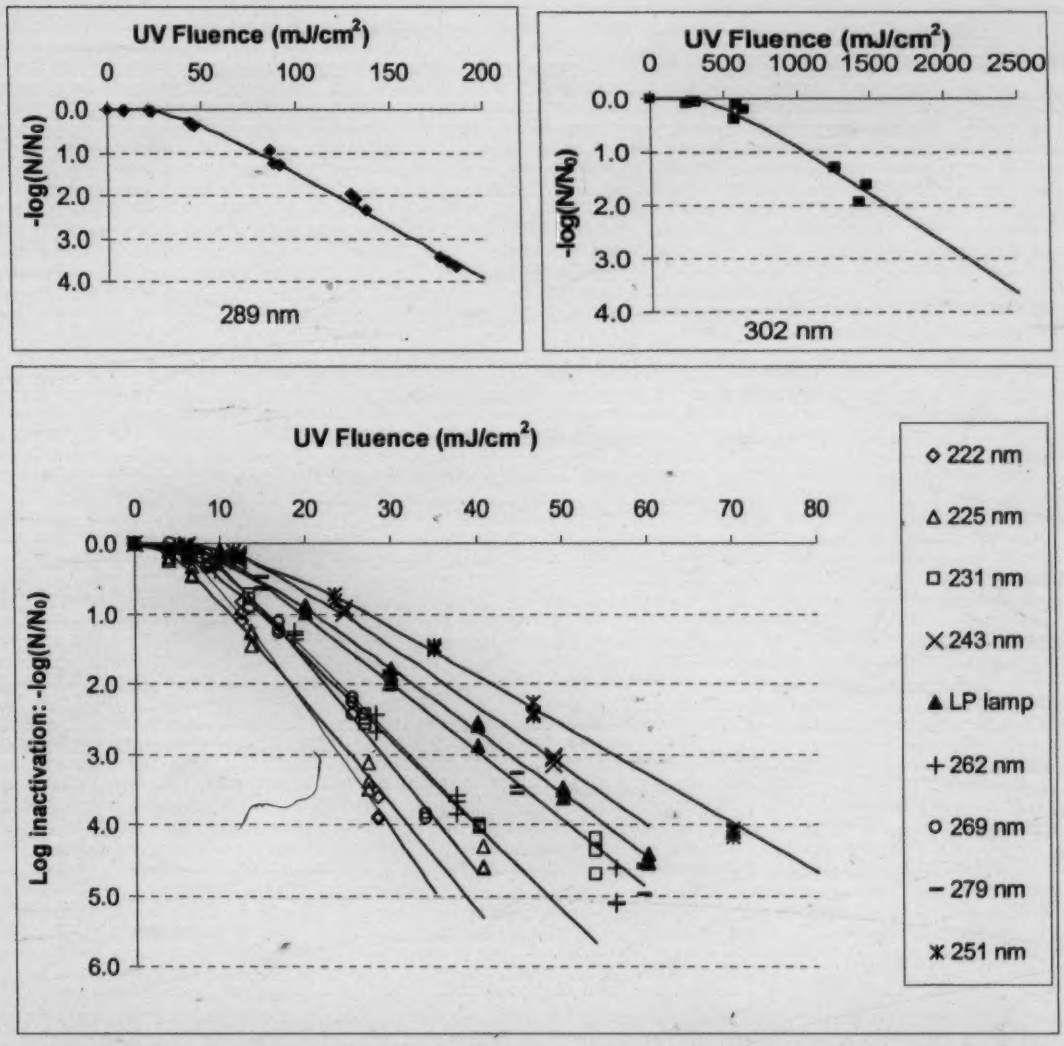

Figure 3.1: UV fluence-inactivation response of *B. subtilis* spores (ATCC 6633) in 0.05 M phosphate buffered de-ionized water at different wavelengths and curves derived from k and n_c of the multiple targets model best-fit to experimental data

To simplify the multiple-target model, as shown in Figure 3.2, Harm (1980) proposed that k represents the slope of the linear portion of fluence response curve in a semi-log plot and the shoulder effect coefficient $\log(n_c)$ is the point at which the

extrapolation of the linear portion of the inactivation curve intercepts with the inactivation (vertical) axis. The model thus can be rewritten as a linear model:

$$-\log(N/N_0) = kH - \log(n_c) \qquad \text{Eqn. 3.2}$$

The threshold fluence H_t, which is obtained from the intercept of the linear portion of the inactivation curve with the fluence (horizontal) axis, was then obtained from $\log(n_c)$ divided by k. H_t varied from 4.4 mJ/cm^2 at 224 nm to 517.9 mJ/cm^2 at 302 nm. The values of H_t are almost the reverse those of k. This indicates that UV light with lower inactivation rate may also need a higher threshold fluence (UV dose) to cause lethal action in *B. subtilis* spores.

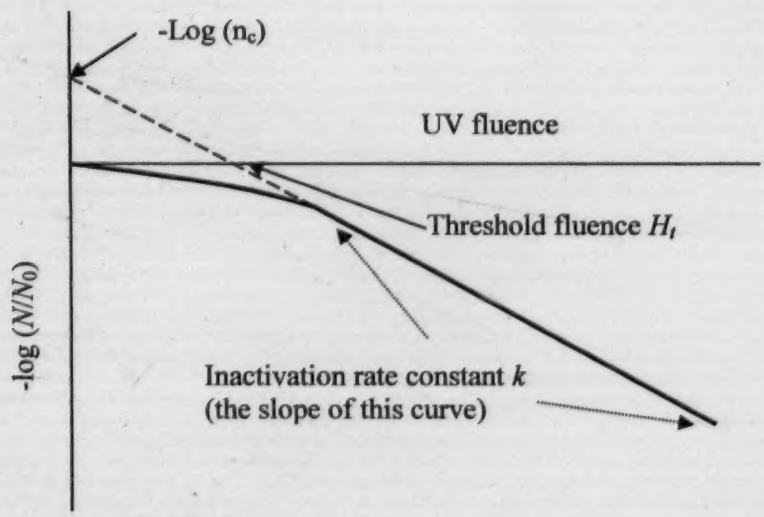

Figure 3.2: Approximation of the shouldered inactivation curves by linear functions

Table 3.2 Wavelength dependence of the inactivation rate vonstant (k), number of critical targets (n_c) and threshold fluence (H_f) of *B. subtilis* spores (ATCC 6633)

Weighted Average Wavelength (nm)	Inactivation rate constant k (cm^2/mJ)			Number of critical targets n_c			Threshold Fluence (H_t) (mJ/cm^2)
	Estimated	Lower	Upper	Estimated	Lower	Upper	
222	0.176	0.169	0.191	15	6	38	5.4
225	0.146	0.135	0.159	4	3	8	3.2
231	0.120	0.116	0.125	6	5	9	6.7
243	0.085	0.082	0.090	13	9	18	13.0
251	0.070	0.078	0.080	8	6	12	13.1
254	0.089	0.084	0.094	8	5	14	9.9
262	0.125	0.118	0.132	10	6	16	7.9
269	0.152	0.141	0.168	24	11	66	9.1
279	0.097	0.092	0.103	9	5	14	9.5
291	0.025	0.023	0.027	11	7	20	41.6
302	0.0018	0.0017	0.0025	9	7	71	520

Note: Estimated values of k and n_c were derived from the multiple target model with non-linear regression by minimizing the sum of square errors, and lower and upper values were derived from 95% JCR in Appendix B-2.

3.3.3 Comparison of the Inactivation Action Spectra of *B. subtilis* Spores

A first-order inactivation rate law has been used to characterize the action spectra for *B. subtilis* spores (Cabaj et al. 2002; Mamane-Gravetz et al. 2005). The reported values of the first-order inactivation rate constant for *B. subtilis* ATCC 6633 spores, determined in LP lamp studies differ considerably, possibly due to differences in the spore cultivation methods (Sommer and Cabaj 1993; Cabaj et al. 2002; Mamane-Gravetz et al. 2005). Austria Standard Institute (2001) summarized that the inactivation rate constant (k) for spores cultivated in liquid media using LP exposure was 0.065 cm^2/mJ with a 20% variation, whereas the k for those spores grown on solid agar was 0.134 cm^2/mJ. In the present study, the *B. subtilis* spore inactivation rate constant k for spores exposed to monochromatic (254 nm) radiation generated using the LP lamp was 0.089

cm^2/mJ with ±6% variation at 95% confidence level. In comparison, Cabaj et al. (2002) reported a *k* value of 0.0612 cm^2/mJ for spores exposed to LP (254 nm) UV for the same strain (ATCC 6633) of *B. subtilis* spores produced using a similar broth cultivation/sporulation procedure. The difference among the reported *k* values may have been the result of batch-to-batch variation in the UV sensitivity of spores, which has been observed in other studies (Uvbiama 2006). The *k* value for spores exposed to LP (254 nm) UV in this study was similar to that observed by Uvbiama (2006) using the same batch of *B. subtilis* spores.

Figure 3.3 demonstrates the action spectrum for *B. subtilis* spores determined in this study to the action spectra reported previously in the literature for the same species of microorganism. The inactivation action spectrum generated in this study indicates the presence of a large peak at wavelengths less than 222 nm, a minimum at around 250 nm and a smaller peak around 270 nm. The spectrum then declines to nearly zero at 302 nm. Intuitively, the action spectrum determined in this study was distinctly different from those reported by Cabaj et al. (2002) and by Mamane-Gravetz et al. (2005), particularly in the wavelength region below 240 nm and in the region of the peak at 270 nm. To compare the action spectrum from this study to other two, the relative *k* values at each aliquot 5 nm were interpolated from 220 to 290 nm for all three action spectra. The relative values were listed in Table B-23, Appendix B-6. Paired t-Test also concluded that the action spectrum determined in this study was different from other two with 95% statistical confidence. The results of the paired t-Test are demonstrated in Table B-23 in Appendix B-6. Possible explanations for the differences between studies include:

- *Differences in the method use to measure absolute fluence rate.* Ferrioxalate chemical actinometry was used in this study, versus a spectroradiometer measurement in previous studies;

- *Differences in the source of narrowband UV light.* Band-pass filters were used to generate narrowband UV in this study while monochromator were used in previous studies;

- *Differences in the methods used to interpret and model the inactivation curves.* In this study a non-linear multi-target model that accounts for the shoulder effect was used to model the inactivation curves of Figure 3.1, while data from the shoulder regions were not included either for a linear model by Mamane-Gravetz et al. (2005) or for non-linear model by Cabaj et al. (2005). In addition, data in the trailing region of the inactivation curves in Figure 3.1 was omitted from the modeling analysis in this study. In previous studies data in the tailing region might be included, thus resulting in biased and less accurate estimates of the first-order rate constant. If the data in the tailing region are excluded from the analysis of the UV fluence response at 265 nm reported by Mamane-Gravetz et al. (2005), the value of k_{rel} generated by linear regression would match the value from other study well. This will result in an action spectrum that is closer to that reported in the present study in the region above 250 nm. Cabaj et al. (2002) used the k values from at least two previous papers in the literature to generate their action spectrum. And the action spectrum and *B. subtilis* spores might not be from the same batch. This might be problematic to characterize their action spectrum because the sensitivity of *B. subtilis* spores could vary from batch to batch (Uvbiama 2006).

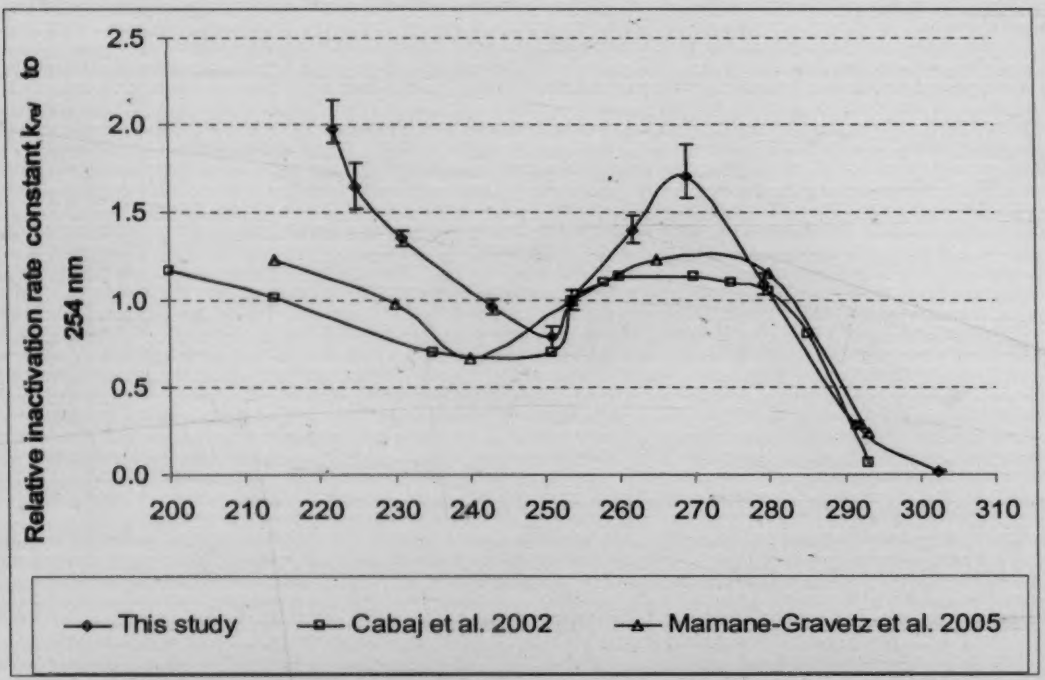

Figure 3.3: Comparison of action spectra of *B. subtilis* spores (ATCC 6633)

Note: Error bars were derived from upper and lower k values in 95% JCR.

3.3.4 Comparison of Wavelength Dependence of the Shoulder Effects

The wavelength dependence of the parameter n_c determined in this study and the two previous studies are compared on a log scale in Figure 3.4. In the case of the present study, n_c was relatively constant over the 220 to 300 nm wavelength range. This makes intuitive sense, since the number of UV sensitive targets within the microorganism, which are presumably sites of adjacent pyrimidines on the DNA, should be independent of wavelength. The finding that the value of $\log(n_c)$ is relatively independent of wavelength also agrees with a previous study by Munakata and coworkers (Munakata et al. 1991), in which the UV inactivation of *B. subtilis* spores suspended in a vacuum was studied between 50 and 300 nm. In the Cabaj et al. (2002) study, the value of $\log(n_c)$ (the

same as intercept d of the linear part of the fluence response curve in their study) increased with increasing wavelength. In the Mamane-Gravetz et al. (2005) study, $\log(n_c)$ varied considerably in an *ad hoc* way and included a physically unrealistic negative value at 265 nm. Possible explanations of the different wavelength dependence of $\log(n_c)$ from this study to the other two may be due to different data processing [e.g., inclusion from data the tailing region in the study by Mamane-Gravetz et al. (2005)]. As well, different water matrices were used between this study (using clean PBDI) and the other two studies (using simulated drinking water, which contained particulate matters). One may expect that the initial resistance of *B. subtilis* spores can also be associated with shielding behaviors by particles. This may increase the uncertainty for estimates of shoulder coefficient. In addition, it should be considered that the parameters k and n_c are highly correlated and, in particular, the least-squares estimate of n_c is sensitive to the estimate of k as indicated by the JCRs. In these two previous studies, only one run was conducted for each level fluence. With a low level of replication, the estimate of k would be less precise, which in turn affected the estimate of $\log(n_c)$ through the correlation. Because of the variable nature of UV disinfection for microorganisms, more replications should improve the precision of the estimates of k and n_c.

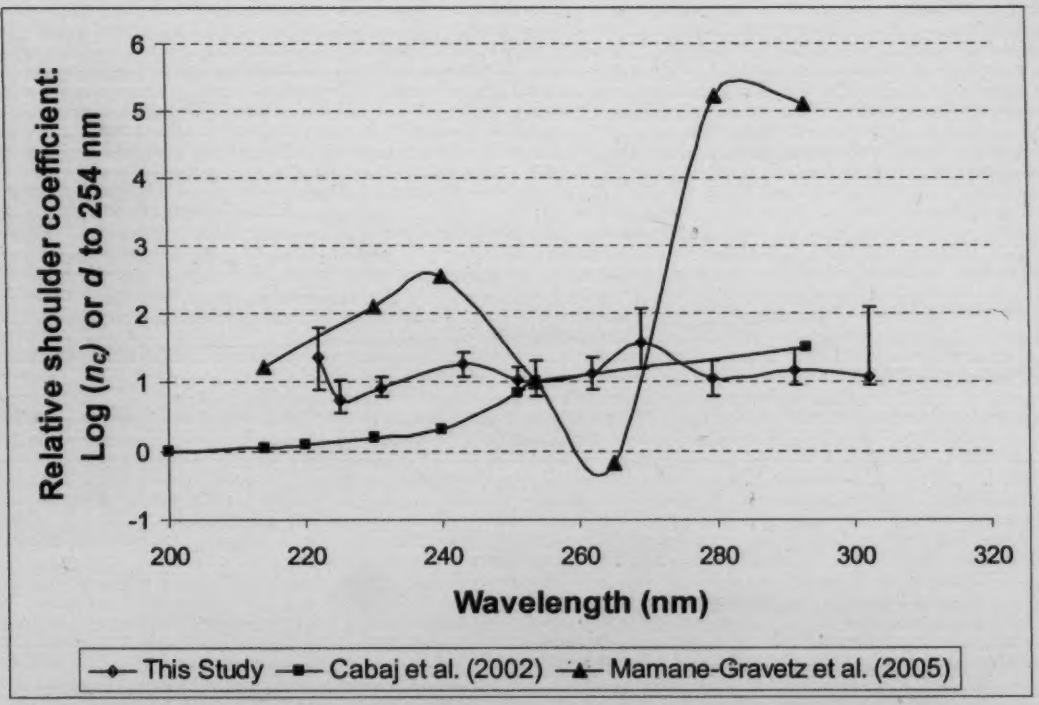

Figure 3.4: Relative shoulder coefficients for inactivation of *B. subtilis* spores (ATCC 6633) as a function of wavelength as determined in this and previous studies

Note: Error bars were derivate from the n_c values in Table 3.2.

3.3.5 Absorbance Spectra of *Bacillus subtilis* DNA and Decoated Spores

The original results for the spectrophotometry of purified DNA and decoated spores are shown in Figure B-23, Appendix B-5. The absorbance spectra (normalized to 254 nm) of purified DNA extracted from spores and vegetative cells of *B. subtilis* are presented in Figure 3.5. These two spectra almost coincide each other. This is understandable, since the chromosomal DNA in the spores or in vegetative cells should be identical. In comparison, a 'standard' DNA absorbance spectrum originally reported by von Sonntag (1986), which has been used as a polychromatic weighting tool in UV disinfection studies (Bolton and Linden 2003), is also plotted in Figure 3.5. Only a slight

difference was observed between the DNA absorbance spectra of *B. subtilis* and the 'standard' DNA absorbance spectrum. The following two possible explanations are offered. First, the five nucleotide bases found in DNA and RNA have unique and slightly different UV absorbance spectra and DNA or RNA from different microorganisms may differ in the composition of nucleotide bases. The overall DNA or RNA spectral absorbance therefore, can be expected to vary from microorganism to microorganism. Secondly, the DNA or RNA absorbance spectra can be slightly affected by ionic strength of the purified DNA solution (Wilfinger 1997).

There are several levels of structure in *B. subtilis* spores. The coat layer has been reported to have little effect on UV inactivation at 254 nm (Riesenman and Nicholson 2000). The inner core of the spores contains DNA, ribosomes, DPA (pyridine-2, 6-dicarboxylic acid), and proteins such as α/β type SASP and spore photoproduct (SP) lyase, which are important in establishing spore resistance to UV light. The absorbance spectrum is significantly different from that of the purified spore DNA absorbance.

In particular, as shown in Figure 3.4, the relative absorbance observed for the decoated spores was significantly greater than that of the purified DNA in the region below 240 nm. This may arise from protein absorbance in this region. The relative absorbance was also found to be distinctly higher than the relative absorbance of purified DNA in the region between 260 and 280 nm. However, the molar absorption coefficient of protein is typically much less (10 to 20 times less) than that of DNA (Harm 1980). Presumably, other components such as DPA may contribute to the distinct difference of relative absorbance in the region from 260 to 280 nm. On the other hand, proteins may partially contribute to the difference since the concentration of SASP alone is

significantly greater (4 to 5 times) than that of DNA in the spore core (Setlow et al. 1992), and the proteins usually have a secondary peak at around 280 nm (Jagger 1967).

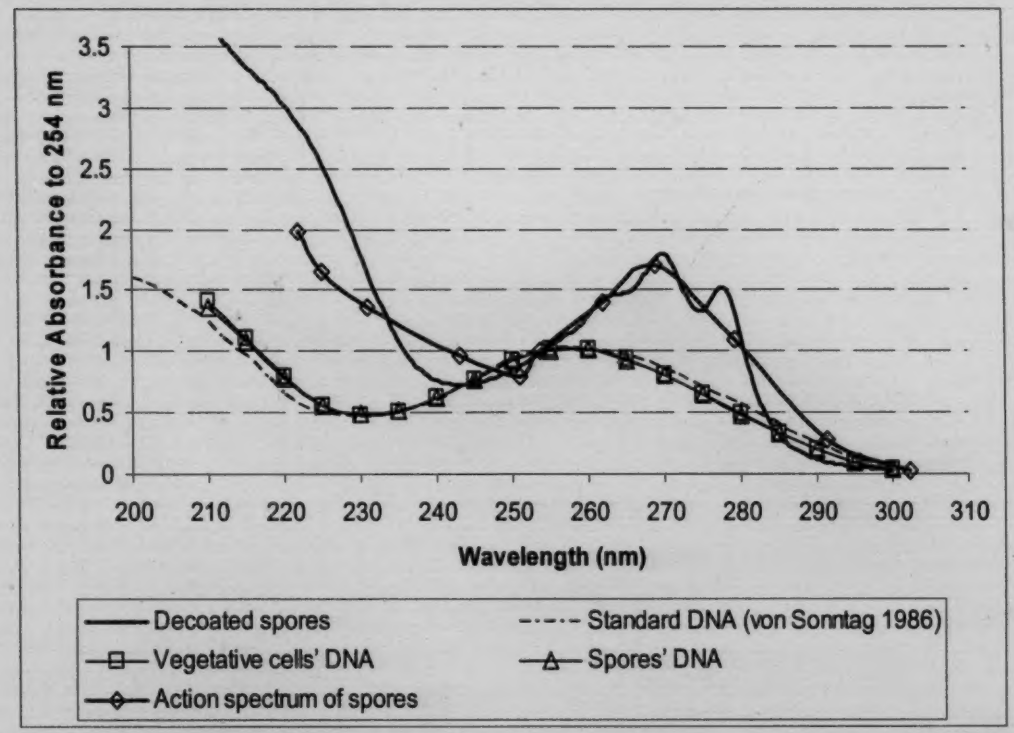

Figure 3.5 Comparison of the absorbance spectra of DNA extracted and purified from *B. subtilis* spores and vegetative cells, the absorbance spectrum of decoated *B. subtilis* spore and the spore action spectrum measured in this study. The 'standard' DNA absorbance spectrum reported by von Sonntag (1986) is also shown. All spectra have been normalized to 1.000 at 254 nm.

3.3.6 Comparison of the Action Spectrum of *B. subtilis* Spores and the DNA Absorbance Spectra of *Bacillus subtilis*

As clearly demonstrated in Figure 3.5, the *B. subtilis* spore action spectra deviate significantly from their own DNA absorbance spectrum and the standard DNA absorbance spectrum. Previous studies also found that the action spectra of *B. subtilis* spores did not match the 'standard' absorbance spectrum (Cabaj et al. 2002; Mamane-

Gravetz et al. 2005). Mamane-Gravetz et al. (2005) suggested that other factors may be involved in the inactivation of *B. subtilis* spores by UV light. If the quantum yield of DNA lesion by DNA absorbance is independent of wavelength, this result strongly indicates that the photons absorbed by other components in the spores may contribute to inactivation. In this study, it was shown that the observed action spectrum coincides with the absorbance spectrum of decoated *B. subtilis* spores much better than it coincides with the absorbance spectrum of DNA from either the spore or vegetative cell DNA. The action spectra of *B. subtilis* spores reveals that the spores are much more sensitive to UV at wavelengths less than 240 nm and around 270 nm than is predicted by the DNA absorbance spectra. It has been reported that the UV resistance of spores is elevated by a group of α/β type SASP that bind to the DNA (Setlow et al. 1992). This binding alters the spore DNA photochemistry and the DNA repair mechanisms. Indeed, when these proteins are removed from *B. subtilis* spores in vitro, it was observed that the photochemistry of DNA and the UV sensitivity are similar to those of the vegetative cells (Mason and Setlow 1986). Also, certain aromatic amino acids in proteins, such as phenylalanine, tyrosine, and tryptophan, show a strong absorbance peak below 240 nm and a weaker peak in the 260 to 280 nm region. In addition, two DNA repair mechanisms can efficiently remove SP in the early minutes of spore germination and outgrowth. These two repair mechanisms also support a higher UV resistance of *B. subtilis* spores compared to that of vegetative cells (Setlow 2001). It was reported that enzymes can also be inhibited by UV light (Setlow 1960). Nonetheless, a much higher fluence (UV dose) may be required to inhibit the DNA repair enzymes at 254 nm than is required to induce DNA lesions. Together, these two previous studies suggest that proteins may play a role

in the UV inactivation of microorganism by polychromatic UV when protein absorbance is not negligible (Rauth 1965).

Moreover, a more recent study reported that the unique photochemistry of *B. subtilis* spores may also be associated with DPA (Douki et al. 2005a). Thus, one may conclude that the novel photochemistry of DNA in *B. subtilis* spores may be attributed to the combined effects of SASP and DPA in the spore core. These two components bind spore DNA tightly and change the DNA conformation (Setlow 2001). The mechanism for the effects of SASPs and DPA on the novel photochemistry of *B. subtilis* spores can be explained by a photosensitized triplet energy transfer (Lamola et al. 1970; Charlier and Helene 1972). The photon energy absorbed by either SASPs or DPA in the spore core may be transferred to the DNA strands and thus cause DNA damage.

The combined effects of proteins, DPA and/or other possible content are thus a possible cause of the novel photochemistry of DNA in spores. Therefore, the absorbance of photons by proteins, DPA and/or possible other components may contribute to the inactivation of *B. subtilis* spores by UV light in a minor way. These mechanisms explain, partly at least, why the action spectrum of *B. subtillis* spores matches the absorbance spectrum of decoated spore solution better than the DNA absorbance spectra. The former contains DPA, SASPs and other proteins such as SP lyase while the latter does not.

3.3.7 Effect of Inactivation Spectra on Germicidal Fluence Determination

In a standard bench-scale UV inactivation study, knowledge of the action spectrum of the microorganism under study is required in order to calculate the germicidal UV fluence accurately (Bolton and Linden 2003). Conventionally, the

'standard' DNA absorbance spectrum has been used as a substitute for the actual microorganism action spectrum when the latter is not known. The effect of using the 'standard' DNA absorbance spectrum instead of the actual *B. subtilis* spore action spectrum for calculating germicidal dose delivery from a MP lamp could be significant. Mamane-Gravetz et al. (2005) compared the inactivation spectra of *B subtilis* spores and MS2 coliphage to the 'standard' DNA absorbance spectrum as weighting tools for determining the germicidal fluence rate in bench-scale using a simulation of MP UV lamp. They concluded that the values of the wavelength weighted average fluence rate using the microorganism's action spectra were >20% greater than those obtained using the relative DNA absorbance spectrum as a weighting factor for both deionized water and simulated drinking water. Therefore, using the 'standard' DNA absorbance spectrum may result in an underestimate of the germicidal fluence for both microorganisms. The results from this study suggest that the error may be even greater.

The action spectrum of *B. subtilis* spores determined in this study was also used to calculate the germicidal fluence from a polychromatic MP UV light source. Although Mamane-Gravetz et al. (2005) used both k and shoulder coefficients to determine a germicidal fluence, the value of k alone can be used to represent the spectral sensitivity of *B. subtilis* spores because $\log(n_c)$ was found to be fairly constant compared with other studies and essentially independent of wavelength in this study. For a collimated beam exposure, the determination of germicidal fluence has been standardized based on the 'standard' DNA absorbance (Bolton and Linden 2003). Using the standardized spreadsheet provided by Bolton (2004), if the germicidally weighted fluence calculated using the standard DNA absorbance spectrum was 40 mJ/cm^2, the fluence calculated

using the *B. subtilis* action spectrum would be 60 mJ/cm^2, or 50% greater. In comparison, the unweighted fluence would be 51 mJ/cm^2.

Regulatory agencies have proposed using *B. subtilis* spores as a surrogate microorganism in reactor bioassays (USEPA 2003; DVGW 1997). The bioassays are used to evaluate the inactivation of target pathogens by the UV reactor under flow-through test conditions using a surrogate microorganism because the direct inactivation measurement of target pathogens is not allowed. Evaluation of reactor performance involves determination of the Reduction Equivalent Fluence (REF) in a bioassay experiment. The determination of REF for MP lamp reactors includes calculating a polychromatic bias and is thus more complex than that for LP lamp reactors. The polychromatic bias accounts for the spectral differences in the lamp output, lamp sleeve UV transmittance, water UV transmittance, and action spectra between a target pathogen and a surrogate microorganism. USEPA (2003) used germicidal outputs of a target pathogen and a surrogate microorganism to determine a correction factor because of the difference between the action spectra. To obtain an accurate REF, the true action spectrum of the surrogate should be known accurately. Using the 'standard' DNA absorbance spectrum instead of the inactivation spectrum of *B. subtilis* spores may result in inaccurate calculation of the REF for MP lamp UV reactors. Accurate knowledge of the inactivation action spectrum of *B. subtilis* spores will improve the prediction of MP lamp UV reactor performance, and consequently help in the design and optimization of UV reactors equipped with MP lamps.

3.4 Conclusions

The inactivation action spectrum of *B. subtilis* spores determined in this study was found to be different from those published in two previous studies. The difference may have arisen from differences in the source of narrowband UV light, methods for UV irradiance measurement and data analysis procedures. The absorbance spectrum of either spores or vegetative cells of *B. subtilis* was appreciably different from the 'standard' DNA absorbance spectrum. The inactivation action spectrum deviated from the 'standard' DNA absorbance spectrum and the absorbance spectra of DNA of *B. subtilis*, but matched the absorbance spectrum of decoated spores fairly well. This strongly indicates that the photons absorbed by components other than DNA in spores may be involved in the inactivation effect by germicidal UV light, when the absorbance of these components is not negligible. The use of the 'standard' DNA absorbance spectrum as an alternative to the action spectrum of the microorganism of interest will result in inaccurate determination of the weighted germicidal fluence in UV disinfection studies. This, in turn, may result in a systematic error when evaluating the performance of a polychromatic UV light reactors using bioassays.

4 COMPARISON OF THE ACTION SPECTRUM AND THE DNA ABSORBANCE SPECTRUM OF *SALMONELLA TYPHIMURIUM* LT2

4.1 Introduction

In drinking water and wastewater treatment facilities, the use of UV technologies in a multi-barrier treatment train can provide an effective barrier against many pathogens such as *Cryptosporidium* and *Giardia*. Polychromatic UV light is a common source used for UV disinfection reactors. UV germicidal effectiveness of a specific pathogen is dependent on wavelength, which is be characterized as an action spectrum. The action spectra of some health-important pathogens have been characterized including *E coli*. (Gates 1930), *Cryptosporidium* (Linden et al. 2001) and adenovirus (Linden et al. 2005). The knowledge of action spectra of health-important pathogens can be used to predict the performance for these pathogens and help future design of a UV reactor equipped with polychromatic UV light source such as MP lamps. If the action spectrum of a specific pathogen is unknown, the 'standard' DNA absorbance spectrum (von Sonntag 1986) was conventionally used as the surrogate (Bolton and Linden 2003). However, the action spectra of some pathogens such as adenovirus differ much from the 'standard' DNA absorbance from von Sonntag (1986). Thus, use of the 'standard' DNA absorbance may be improper for some pathogens.

Salmonella is a very important pathogen in food industry. In the food industry, crops can be contaminated by irrigation water. In water scarce regions, reclaimed municipal water is often used for agricultural irrigation (York et al. 2002). UV treatment

has been reported to be a favorable technology as a barrier for a pathogen's pathway from municipal wastewater to food (Yoon et al. 2004).

Salmonella spp. is an important waterborne pathogen in drinking water. Most UV disinfection studies of *Salmonella* spp have been carried out using monochromatic UV light (Chang et al. 1985; Wilson et al. 1992; Tosa and Hirata 1998; Koivunen and Heinonen-Tanski 2005). These studies have shown that sensitivity to LP UV light might vary from strain to strain. However, little study has been carried out using polychromatic UV light. Nonetheless, *Salmonella* spp. was found to be relatively susceptible to UV treatment. The most resistant strain reported by far was *S. anatum*, which requires 15 mJ/cm^2 to achieve 3-log inactivation (Tosa and Hirata 1998). Both *Salmonella* and *E. coli* belong to the family *Enterobacteriaceae*. These two members possess similar DNA base composition. The spectrum action of *E. coli* has been well characterized by Gates (1930). It was hypothesized that these two similar microorganisms should have a very similar action spectrum. The inactivation action spectrum of *Salmonella* spp. has not yet been reported. Moreover, *Salmonella* DNA might have its own unique absorbance spectrum.

Some strains of *Salmonella* with mutations are avirulent. The strain of *Salmonella typhimurium* LT2 has a highly attenuated virulence and has been commonly used as a surrogate for virulent *Salmonella* spp. in laboratory studies. This strain was selected for this study. The objectives for the study of this chapter were to characterize the inactivation action spectrum of *S. typhimurium* LT2 and to measure its DNA absorbance spectrum for comparison. Moreover, the effect on the germicidal fluence (UV dose) determination using the 'standard' and these two action spectra was to be evaluated.

4.2 Materials and Methods

4.2.1 *S. typhimurium* LT2 Production, Preparation of Test Suspensions, and Enumeration

The strain of *S. typhimurium* LT2 (SL3770 from the *Salmonella* Genetic Stock Centre (SGSC) at University of Calgary) was kindly provided by Dr. Diane Taylor's laboratory, at the Department of Medical Microbiology, University of Alberta. *Salmonella* culture medium was prepared by dissolving 30 g of Tryptone Soya Broth (TSB, Oxid CM129) per liter of Milli-Q® water. Then the liquid medium was autoclaved at 121°C for 15 min. After cooling down the liquid medium to room temperature, an isolated colony of *Salmonella* on the agar plate prepared from Dr. Diane Taylor's laboratory or a solidified MacConkey agar plate was aseptically inoculated into the culture liquid medium. The medium was incubated at 35°C in an incubator shaker (Innova 4080, New Brunswick Instruments Co. Inc., Edison, NJ) at 180 RPM for 24 h (Wilson et al. 2003). After incubation, *Salmonella* was harvested by centrifugation at 7500 × g for 20 min at 4°C. The supernatant was decanted and the pellet was re-suspended in sterile PBDI water and was homogenized with a homogenizer (PowerGen 700, Fisher Scientific). The centrifugation and wash steps were repeated until the supernatant was clear. The final pellet was then suspended in sterile 0.05 M PBDI water and homogenized. The homogenized solution was diluted in sterile PBDI water. The *Salmonella* concentration (CFU/mL) in the diluted solution was enumerated as described later. The test suspension was prepared with *Salmonella* concentration at approximate 10^7 CFU/mL by again diluting the calculated solution into sterile PBDI water with a Teflon®

coated magnetic stir bar. The test suspension was stored at 4°C for further UV exposure experiments within 2 weeks.

A spread plate method was employed to enumerate the CFU of a sample. The detailed procedures were described elsewhere (Maier et al. 2000; Pepper et al. 1995). Briefly, an aliquot 1 mL of a sample was aseptically transferred into 9 mL sterile PBDI water in a test tube. The first dilution was mixed thoroughly using a vortex mixer. A second dilution was prepared by continuing to dilute the first dilution. Likewise, a series of decimal dilutions were prepared. A 0.1 mL aliquot of a selected dilution or sample was uniformly spread on top of a solidified MacConkey agar (Difco™, Becton Dickson and Company, MD) with a sterile glass rod. The detailed procedures for preparing a solidified MacConkey Agar were described in Appendix A-3. Three replicates of a selected dilution were carried out for each enumeration. The plates with seeded agar were incubated at 32°C for 24 h. Colonies on each plate, yielding approximately 30-300 colonies per plate, were counted and recorded. Relative consistency of a sample was found among dilutions. The counting of approximate 30-300 colonies per plate for the same dilution was selected for further data processing. The geometric mean of the replicated counting was recorded as the averaged count for a sample. The concentration of *Salmonella* in a sample was calculated from the average counting as CFU per 1 mL sample by taking account into the dilution factor.

4.2.2 UV Exposures

The collimated beam apparatus, the method of selecting wavelength bands of UV light, pre-warming of the UV lamp and the spectral absorbance measurement of a test

suspension were same as described in Chapter 3. For a given wavelength band, five fluence levels and triplicate UV exposures for each fluence level were carried out. During the UV exposure experiments, all the runs and three samplings of an un-irradiated test suspension were randomized. A 1 mL aliquot of un-irradiated test suspension (continuingly stirred) was aseptically transferred into an autoclaved test tube containing 9 mL of PBDI water. The concentration of an un-irradiated test suspension (N_0) was then determined as described previously. For a given exposure run, a 10 mL test suspension was aseptically withdrawn and transferred into the autoclaved Petri dish with a 10 mm × 2 mm Teflon-coated magnetic stir bar. To prevent potential contamination and spill of test suspension, the Petri dish was immediately covered with an autoclaved quartz dish. The UV exposure was initiated by opening the pneumatic shutter and the counting of the exposure time began by simultaneously starting a stopwatch (Fisher Scientific). Once the pre-determined exposure time was reached, the shutter was closed. A 1 mL aliquot of irradiated suspension or approximately 5 mL for the highest fluence (UV dose) level was sampled to determine the concentration of the sample.

4.2.3 Fluence (UV dose) Determination

Calculations of the unweighted depth-averaged fluence rate at each wavelength band were detailed in Chapter 3. The difference was the measurement of irradiance was accomplished using the radiometer. At each wavelength band, the incident irradiance on the liquid surface band was measured by covering a quartz dish over the SED 240 detector (International Light, Newburyport, MA). The unweighted, depth-averaged fluence rate was calculated by multiplying the incident irradiance by a sensor factor by

ferrioxalate actinometry, a Petri factor, a reflection factor, a water absorbance factor and a beam divergence factor as described in Chapter 3.

4.2.4 Data Analysis and the Statistical Method

Chromosomal DNA of *Salmonella* spp. is double-helical. The fluence-inactivation relation of *S. typhimurium* LT2 could also be mathematically modeled using the multi-target model (Eqn. 3.1) (Harm 1980). Therefore, the inactivation rate k and the number of critical targets n_c were determined using non-linear regression as described in Chapter 3. JCR plots with 95% confidence regions were constructed and the action spectrum of *S. typhimurium* LT2 was characterized using as described in Chapter 3.

4.2.5 Measurement of the Absorbance Spectrum of *Salmonella typhimurium* LT2 DNA

The production of *S. typhimurium* LT2 for DNA extraction was described previously. *Salmonella* cells ($< 2 \times 10^9$) was harvested in a microcentrifuge tube by centrifugation at 5000 × g for 10 min and the supernatant was decanted The pellet was resuspended in Milli-Q® water and mixed by vortex. The cells were washed and purified by centrifugation at 5000 × g at 4°C for 10 min three times. *Salmonella* genomic DNA was extracted and purified using a DNeasy® kit (QIAGEN, Germany). The detailed protocol for the DNA extraction and purification was provided by the manufacturer. Briefly, the purified cells pellet was suspended in Buffer ATL and added to proteinase K. The mixture was then vortexed and incubated at 55°C for 3 h. The solution was then treated with Buffer AL and incubated at 70°C for 10 min. The DNA was precipitated by adding ethanol and was bound onto the DNeasy® membrane by centrifugation. The

remaining contaminants and enzyme inhibitors were removed by two wash steps using Buffer AW1 and Buffer AW2. The DNA precipitate was incubated in AE buffer for 1 min and eluted by centrifugation at 7500 × g for 1 min twice. The eluted solution contained dissolved DNA in AE buffer. The absorbance spectrum of *Salmonella* DNA was measured by scanning the DNA solution with AE buffer as the reference using a spectrophotometer (UV-2401PC, Shimadzu Corp., Columbia, MD). The relative DNA absorbance spectrum was then obtained by plotting the ratio $A_{rel} = A_\lambda/A_{254}$ as described in Chapter 3.

4.3 Results and Discussion

4.3.1 UV Fluence-Inactivation Response Curves

The CFU enumeration data for *S. typhimurium* LT2 are presented in Tables B-12 to B-22 in Appendix B-3. Curves of log UV inactivation responses of *S. typhimurium* LT2 versus UV fluence for each wavelength band are presented in Figure 4.1. The inactivation response for the 291 nm and 302 nm bands are presented separately using a different horizontal scale for convenience. Each fluence response also exhibited a shoulder effect at low UV fluence that is characteristic of *S. typhimurium* LT2. These fluence response curves were plotted using the parameters estimated from the multiple-target model. The initial resistance to low UV fluence has been attributed to the self-repair capability of double-stranded DNA and microorganisms, which can recover from lesions when exposed to UV light below a threshold fluence (Harm 1980). When the log inactivation was greater than 4, slight tailing effects were observed in some of the response curves (i.e., at 225, 289 and 302 nm), probably due to experimental artifacts such as microorganism clumping (Craik et al. 2001). Since the multi-target model does

not accommodate tailing behaviour, data in the tailing region were omitted from the least-squares estimation of the parameters k and n_c.

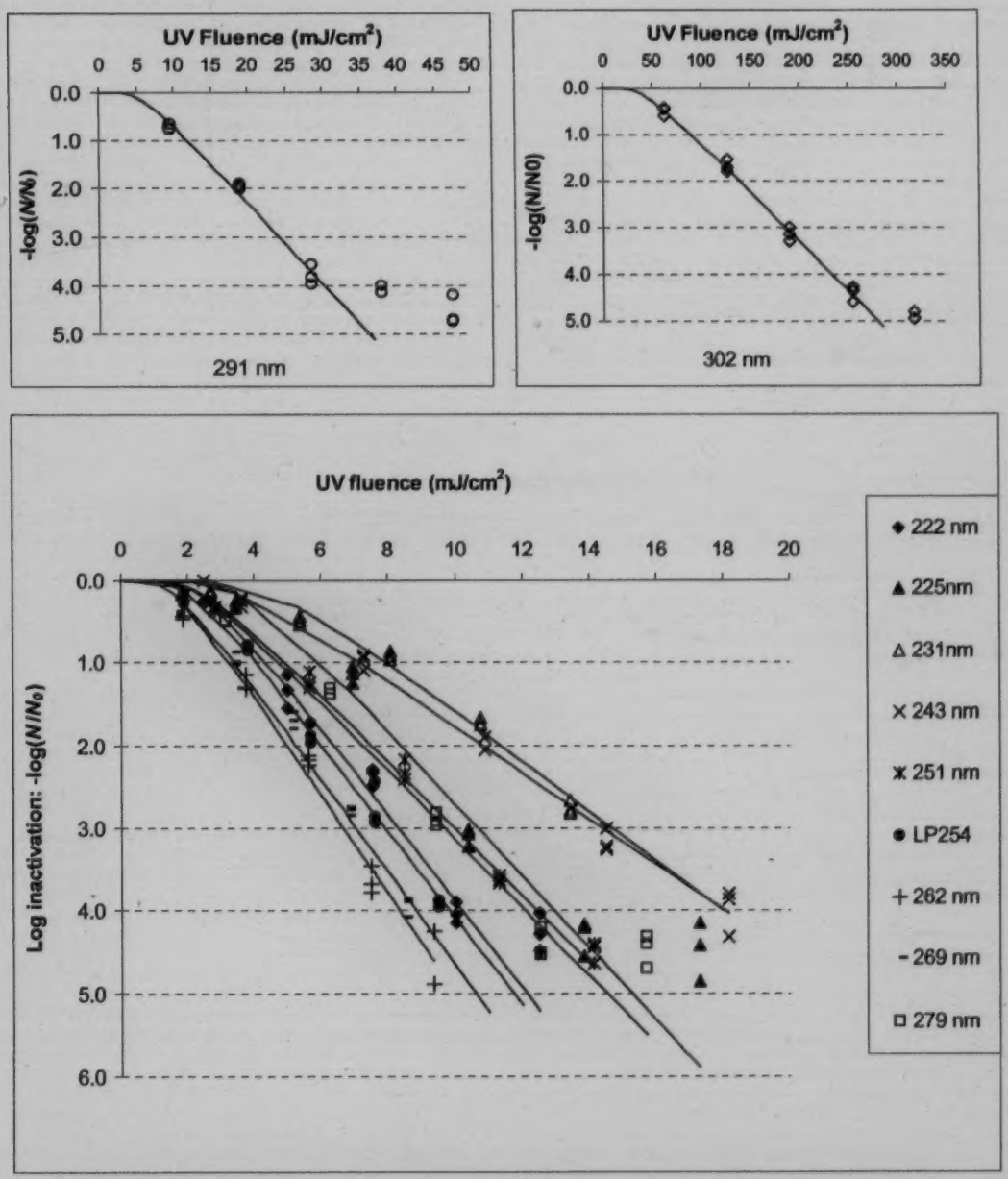

Figure 4.1: UV fluence-inactivation responses of *Salmonella typhimurium* LT2 (SGSC SL 3770) in 0.05 M phosphate buffered de-ionized water at different wavelengths

4.3.2 Wavelength Dependent of Inactivation Rate Constant, Number of Critical Targets and the Threshold Fluence

As shown in Table 4.1, the inactivation rate constants (k) determined in this study varied from 0.021 to 0.594 mJ/cm^2 within the germicidal UV range. Like other microorganisms, the UV germicidal efficiency of *S. typhimurium* LT2 was also highly dependent on wavelength. As reviewed in Chapter 2, the first-order inactivation rate constant of *Salmonella* might vary from species to species within the same study or even from study to study for the same species. Using a LP lamp, the inactivation rate k of *S. typhimurium* determined from the study by (Tosa and Hirata 1998) was 0.667 cm^2/mJ. In this study, k was 0.525 cm^2/mJ varying from 0.486 to 0.571 cm^2/mJ with 95% statistical confidence level for the LP lamp. This value is close to 0.515 cm^2/mJ calculated from the combination of the previous studies for *Salmonella* spp. (Hijnen et al. (2006). All the data indicate that *Salmonella* spp. are relatively susceptible to UV light.

According to the multi-target model, the shoulder effect in the *S. typhimurium* LT2 inactivation curves is present because a minimum number of critical targets, given by n_c, must absorb photons and react photochemically before an individual microorganism is effectively inactivated. As described in Chapter 3 for *B. subtilis* spores, n_c for *S. typhimurium* LT2 in Table 4.1 varied from 9 to 43 with an average of 16 for different wavelength bands. The shoulder coefficients $\log(n_c)$ of *S. typhimurium* LT2 thus varied from 0.94 to 1.63 and did not vary much. Again, this variation might be attributed to the mathematic model used. The JCRs of k and n_c (see Appendix B-4) indicate these two parameters are also correlated, and a change of k leads to a significant change of n_c. This further confirms that the number of critical targets is likely independent of

wavelength for a microorganism in the same suspension. Using the multiple-target model, replication of experimental runs is necessary to improve the precision of parameters estimated.

As described in Chapter 3, threshold fluences (H_t) were also estimated from k and n_c, in which k is the slope of linear portion of a semi-log fluence response curve and $\log(n_c)$ is the intercept on the inactivation axis. The threshold fluence can be determined for a given wavelength using $\log(n_c)$ divided by k. These three parameters are also presented in Table 4.1 for all the wavelength bands tested. The threshold fluence H_t which is an estimate of the minimum fluence level required order to inactivate *S. typhimurium* LT2, varied from 1.6 mJ at 262 nm to 45.7 mJ at 302 nm.

Table 4.1 Wavelength dependence of inactivation rate constant (k), number of critical targets (n_c) and threshold fluence of *S. typhimurium* LT2 (SGSC SL 3770)

Weighted Average Wavelength (nm)	Inactivation rate constant (k) (cm^2/mJ)			Number of critical targets (n_c)			Threshold fluence (H_t) (mJ/cm^2)
	Estimated	Lower	Upper	Estimated	Lower	Upper	
222	0.522	0.468	0.606	21	10	95	2.5
225	0.434	0.402	0.500	43	28	395	3.8
231	0.301	0.270	0.343	26	16	102	4.7
243	0.277	0.250	0.302	10	5	27	3.6
251	0.405	0.381	0.431	11	7	19	2.6
LP 254	0.525	0.486	0.571	14	8	31	2.2
262	0.594	0.539	0.661	9	5	28	1.6
269	0.560	0.510	0.625	9	5	23	1.7
279	0.414	0.398	0.496	10	6	73	2.4
291	0.166	0.155	0.180	10	7	21	6.1
302	0.021	0.020	0.023	9	5	25	45.7

Note: Estimated values of k and n_c were derived from the multiple target model with non-linear regression by minimizing the sum of square errors, and the lower and upper values were derived from 95% JCR in Appendix B-4.

4.3.3 Comparison of the Inactivation Action Spectra of *S. typhimurium* LT2 with that of *E. coli*

As shown in Figure 4.2, the overall shape of the action spectrum of *S. typhimurium* LT2 characterized in this study decreases from 222 nm with a low valley around 240 nm, then increases up to a peak around 265 nm, and declines to nearly zero at 302 nm. The *Salmonella* DNA base composition is similar to that of *Escherichia* genera. The *Salmonella* genera are most closely related to *Escherichia*, *Shigella* and *Citrobacter* genera. The UV fluence-response of *E. coli* is found to be similar to that of *Salmonella* and both are fairly sensitive to UV light. The inactivation action spectrum of *E. coli* has well been characterized by Gates (1930). Therefore, the action spectrum of *S. typhimurium* LT2 is presented and is compared to that of *E. coli* in Figure 4.2. Intuitively, these two action spectra show a high degree of consistency across the germicidal wavelength range. To compare the action spectrum of *Salmonella* and that of *E. coli* in statistics, the relative k value at each aliquot 5 nm from 230 to 300 nm were interpolated for both action spectra as presented in Table B.4, Appendix B-6. The paired t-Test results also concluded that these two action spectra were not statistically different with 95% confidence. This indicates that the microorganisms with similar characteristics should have similar inactivation action spectra. The action spectrum of *Salmonella* determined in this study might suitably be used as a surrogate for other waterborne pathogens such as *Shigella*, *Citrobacter, coliform* and even possibly for those of some other UV susceptible bacteria reviewed by Hijnen et al. (2006) such as *Cabopylobacter* and *Yersinia.*

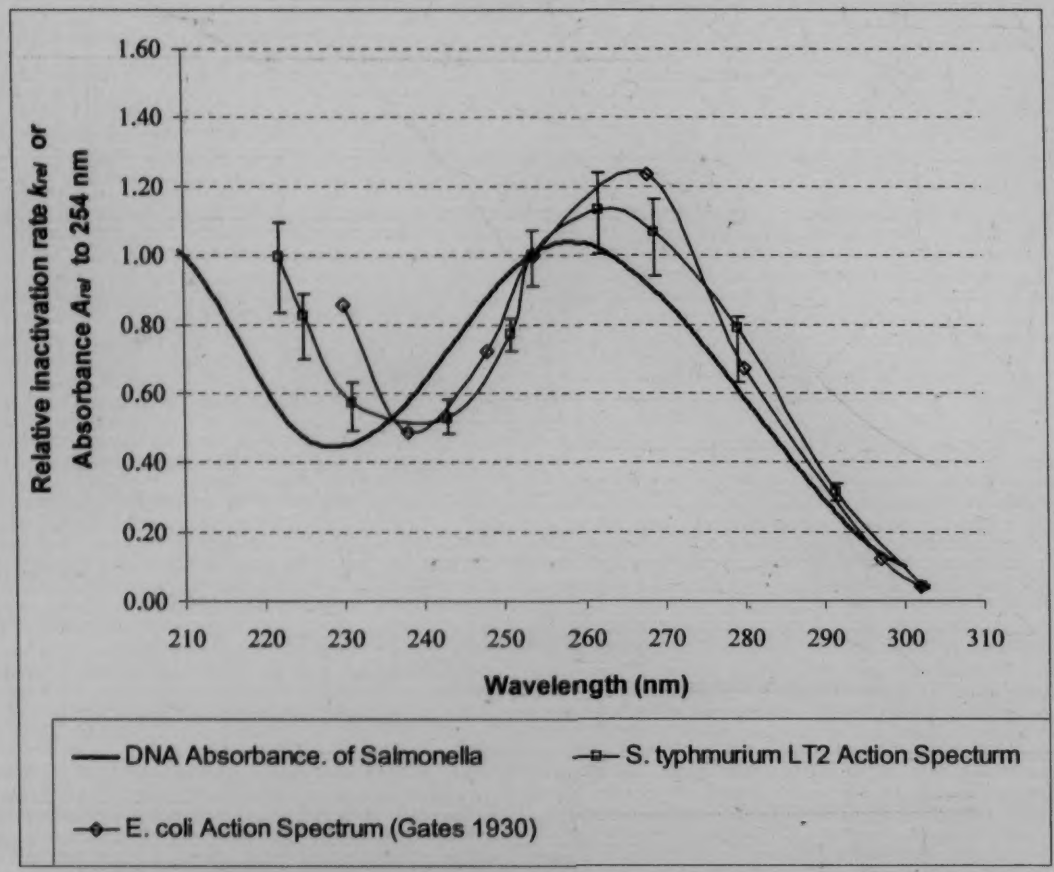

Figure 4.2: Action spectra of *S. typhimurium* LT2 (SGSC SL 3770), its DNA absorbance spectrum, and *E. coli* action spectrum, and the 'standard' DNA absorbance spectrum

Note: Error bar were derived from the upper and lower values of k and were to relative to the estimated value of LP 254nm in Table 4.1

4.3.4 Comparison of the Action Spectrum and the DNA Absorbance Spectrum of *S. typhimurium* LT2

The original result for DNA absorbance measurement was shown in Figure B-24 in Appendix B-4. For comparison, the absorbance spectra of *Salmonella* DNA relative to 254 nm and the 'standard' DNA are also presented in Figure 4.2. These two absorbance spectra match well. Only a slight difference was observed between the DNA absorbance

spectra of *S. typhimurium* LT2 and the 'standard' DNA absorbance spectrum. Possible explanations of this difference were discussed as in Chapter 3. The action spectrum of *S. typhimurium* LT2 was close to its own DNA absorbance spectrum over most of the wavelength range. This indicates that the absorbance of photons by DNA is the main mechanism of *Salmonella* spp. inactivation by UV light. An appreciable difference between the two spectra, however, was observed below 230 nm, where the inactivation was greater than that predicted based on DNA absorbance alone. This suggests that proteins may also be involved and may play a minor role in the inactivation mechanism, since proteins absorb more strongly in this region. One possible explanation is the formation of DNA-protein crosslinks induced by UV light (Smith et al. 1966), although these researchers used monochromatic UV light (253.7 nm) in which the absorbance of proteins was much lower than that of nucleic acids. However, the intrinsic sensitivity of *E. coli* cells was directly correlated to the amount of DNA crosslinked to protein. As well, in Figure 4.2 the comparison of the action spectrum of *E. coli* and DNA absorbance spectrum agrees with this evidence.

4.3.5 Effect of Action Spectra on Germicidal Fluence Determination

In the bioassay methods for MP reactor validation, knowledge of the action spectra of both surrogate organisms and target pathogens is important to evaluate accurately the performance of a UV reactor. The USEPA "Draft UV Disinfection Guidance Manual" proposes bias safety factors to be applied during a reactor validation using a bioassay test (USEPA 2003). For a UV reactor with polychromatic UV light, the polychromatic bias factor should be determined. One important factor is the difference of the action spectra between a challenge microorganisms and target pathogen. For a

collimated beam exposure, the determination of germicidal fluence has been standardized (Bolton and Linden 2003). Simulation was conducted for calculating the weighted germicidal fluence using *Salmonella* action spectrum and *E. coli* action spectrum in comparison to using the 'standard' DNA absorbance using spreadsheet provided by Bolton (2004). As discussed in Chapter 3, the relative inactivation rate constant k alone can be used for weighted germicidal efficiency. The wavelength range from 220 to 300 nm obtained in this study was used for *Salmonella*. The relative spectrum and incident irradiance of a polychromatic UV light, the spectral absorbance and volume of a sample were the same as Bolton (2004). If the fluence calculated using the 'standard' DNA absorbance spectrum was 40 mJ/cm^2, the fluence calculated using the action spectrum *S. typhimurium* LT2 would be 42.5 mJ/m^2. Similarly, the germicidal fluence calculated from 220 to 300 nm using the action spectrum of *E. coli* by Gates (1930) would be 43.5 mJ/cm^2. There is no significant difference when using the 'standard' DNA absorbance spectrum instead of the action spectrum of *S. typhimurium* LT2 or that of *E. coli*. This suggests that using the 'standard' DNA absorbance instead of the action spectrum of some microorganisms such as *S. typhimurium* LT2 or *E. coli* may be acceptable.

4.4 Conclusions

The inactivation action spectrum of *S. typhimurium* LT2 determined in this study was similar to that of *E. coli*, which both belong to the same *Enterobacteriaceae* family. Furthermore, the action spectrum of *S. typhimurium* LT2 matched its own DNA absorbance spectrum and the 'standard' DNA absorbance spectrum fairly well. This evidence suggests that the germicidal action of *Salmonella* cells by UV light primarily resulted from photons absorbed by DNA rather than by other components. In terms of the

weighted germicidal fluence calculation for polychromatic UV light for either *Salmonella* or *E. coli*, results using the 'standard' DNA absorbance spectrum as a surrogate were not significantly different from those using the actual action spectra for that microorganism. This means that the use of the 'standard' DNA absorbance spectrum as a surrogate for some microorganisms such as *Salmonella* and *E. coli* may be acceptable to predict the inactivation of target pathogens when using conducting bioassay tests for a UV reactor validation.

5 GENERAL DISCUSSION, CONCLUSIONS AND RECOMMENDATIONS

5.1 General Discussion

5.1.1 DNA and RNA Absorbance Spectra

The chromosomal nucleic acids in some microorganisms, such as *B. subtilis*, *Salmonella* and adenovirus are DNA, whereas those in MS2 bacteriophage are single-stranded RNA. The nucleotide bases of DNA are adenine, guanine, thymine and cytosine, whereas the counterpart of thymine is uracil in RNA. The absorption spectra of the component bases differ to some extent (Davidson 1965). The UV absorbance spectrum of nucleic acids from different organisms, therefore, is expected to differ to some degree as the relative compositions of the bases differ. As discussed in previous chapters, absorbance spectra of the DNA purified from *S. typhimurium* LT2 and *B. subtilis* spores characterized in this study was consistent with the standard DNA absorbance spectrum (von Sonntag 1986). As well, the comparison in Figure 5.1 shows that the DNA absorbance spectra of widely different species, such as *E. coli* (Setlow 1960) and the mouse liver (Tsuboi 1950) may not be significantly different. Moreover, as illustrated in Figure 5.1, the absorbance spectra from different nucleic acids (DNA or RNA) from organisms (either animal or bacteria) are also similar. This suggests that the difference between uracil and thymine absorbance appears not to affect the overall absorbance spectrum of DNA or RNA significantly. Although the source of DNA that was studied by von Sonntag (1986) is not clear, the 'standard' DNA absorbance spectrum may indeed suitably represent the DNA or RNA absorbance spectra of other organisms.

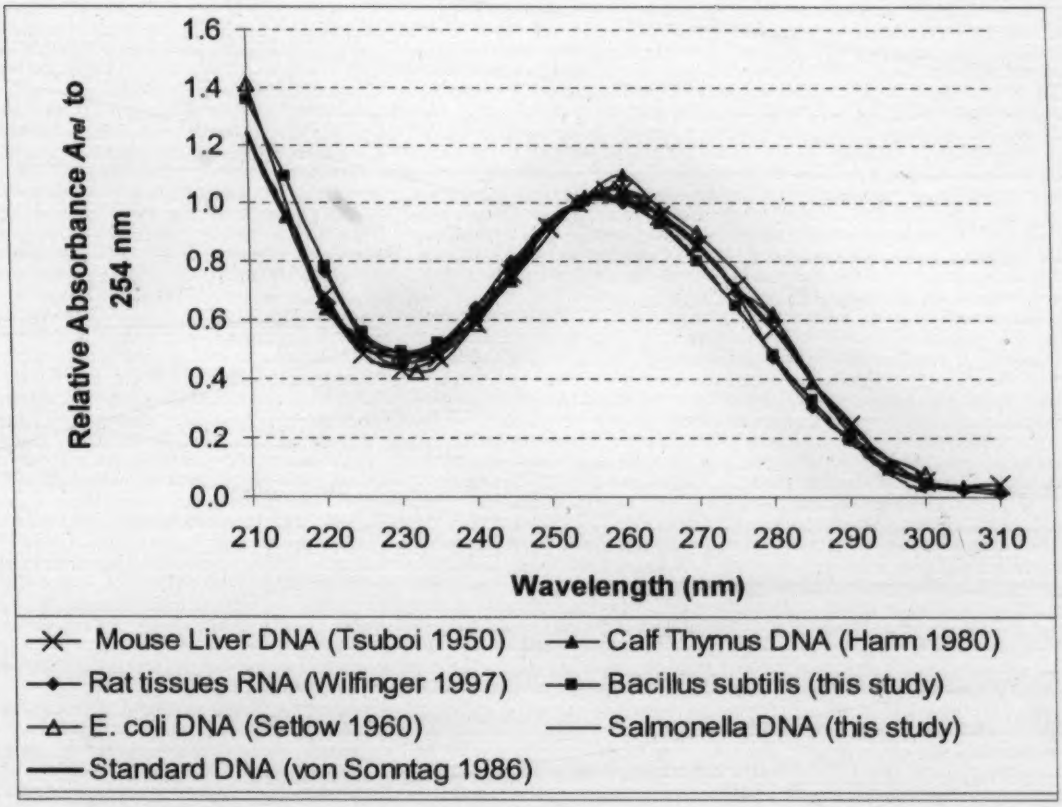

Figure 5.1: Absorbance spectra of nucleic acids (DNA or RNA) from different organisms

5.1.2 Inactivation Action Spectra of Surrogate or Challenge Microorganisms

The common surrogate microorganisms for UV disinfection studies or challenge microorganisms in UV reactor validation for bioassay tests are MS2 bacteriophage and *B. subtilis* spores. The action spectra of MS2 or *B. subtilis* spores have been characterized using different UV light sources and methods for isolating UV wavelengths (monochromators versus band-pass filters) and different fluence measurement methods (spectroradiometer versus chemical actinometry).

The action spectra of MS2 were reported previously (Rauth 1965; Linden et al. 2000; Mamane-Gravetz et al. 2005). Figure 5.2 compares these previously-reported action spectra and the 'standard' DNA absorbance spectrum of von Sonntag (1986). The most pronounced difference in spectra occurs in the wavelength region around 265 nm. Linden et al. (2000) used band-pass filters to generate wavelength bands and ferrioxalate chemical actinometry to measure the irradiance of the incident UV light. The other two studies used monochromators to generate wavelength bands and used spectroradiometers to measure the irradiance of the incident UV light. Mamane-Gravetz et al. (2005) argued that the difference in action spectra between the studies might be attributed to the use of different methods to obtain the wavelength bands (monochromator vs. band-pass filter). They thought the band-pass filters could be problematic because of the reduction of overall incident irradiance and a half-peak bandwidth of more than 10 nm. However, in this particular case, this explanation does not make sense. In the 265 nm wavelength region, all the action spectra showed a secondary peak of germicidal efficiency. The relative germicidal efficiency for broader bandwidth radiation produced from the band-pass filters by Linden et al. (2000) was greater than those of the narrower bandwidth radiation produced using the monochromator from the other two (Mamane-Gravetz et al. 2005). If their explanation was valid, the result should have been the reverse because broader band can offset the peak and make the relative germicidal efficiency less. Therefore, another question can be raised: "Does the difference arise from the measurement methods of incident irradiance?" As discussed in Chapter 3, the action spectrum of *B. subtilis* spores determined in this study was significantly different from that measured in previous studies. One of the possible explanations for this difference

may be the different methods used for fluence measurement. The action spectra of *B. subtilis* spores in this study and that of MS2 by Linden et al. (2000) were both determined using ferrioxalate actinometry. The spectra both had significantly higher relative germicidal efficiency than the action spectrum that was determined by Mamane-Gravetz (2005) using spectroradiometry. These findings highlight the need to compare ferrioxalate chemical actinometry and physical radiometry for fluence (UV dose) measurements.

As illustrated in Figure 5.2 and Figure 3.3, the action spectra of *B. subtilis* spores and MS2 are significantly different from the absorbance spectrum of the 'standard' DNA. This difference may lead to significant differences in calculating germicidal fluences in UV disinfection studies. The use of the 'standard' DNA absorbance spectrum, instead of the action spectrum of *B. subtilis* spores, to calculate the weighted germicidal fluence could induce large inaccuracies in fluence determinations (Mamane-Gravetz et al. 2005). For example, in a bench-scale UV disinfection study using a polychromatic UV light source, if the weighted germicidal fluence (UV dose) using the 'standard' DNA absorbance spectrum is 40 mJ/cm^2, the weighted germicidal fluence (UV dose) would be 53 mJ/cm^2 when using the action spectrum of MS2 determined by Linden et al. (2000). In comparison, the fluence (UV dose) calculated using the *B. subtilis* action spectrum (this study) would be 60 mJ/cm^2.

5.1.3 Action Spectra of Waterborne Pathogens

The action spectra of some important waterborne pathogens are illustrated in Figure 5.3. Clearly, the action spectra of *E. coli*, *Salmonella* and *C. parvum* oocysts do

not vary significantly across the germicidal wavelength range, especially above 230 nm. The consistency of the action spectra for these three microorganisms with the DNA

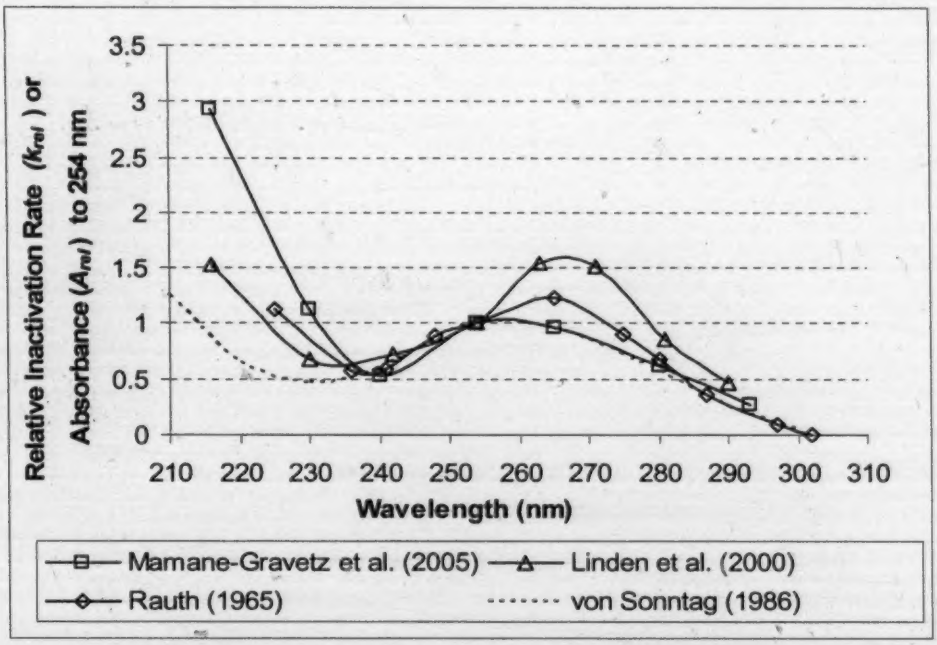

Figure 5.2: Comparison of action spectra of MS2 bacteriophage and the standard DNA absorbance spectrum of von Sonntag (1986)

absorbance spectra strongly suggests that UV inactivation action of sensitive microorganisms is primarily induced by photons absorbed by nucleic acids, where chromosomal DNA or RNA are the primary targets in terms of UV inactivation. Adenoviruses are double-stranded DNA viruses and have been identified as the most UV resistant microorganisms thus far. The DNA absorbance spectrum of adenoviruses might, therefore, be similar to the 'standard' DNA absorbance spectrum. However, the action spectrum of adenoviruses determined by Linden et al. (2005) differed most from the 'standard' DNA absorbance spectrum and the action spectra of the other pathogenic

microorganisms (see Figure 5.3). Linden et al. (2005) reported that germicidal UV light from a MP lamp was more effective than that from a LP lamp for inactivating adenovirus even when the wavelengths below 230 nm were filtered out. This evidence strongly indicates that other mechanisms, in addition to adsorption of photons by DNA, may be involved in the UV inactivation of adenoviruses.

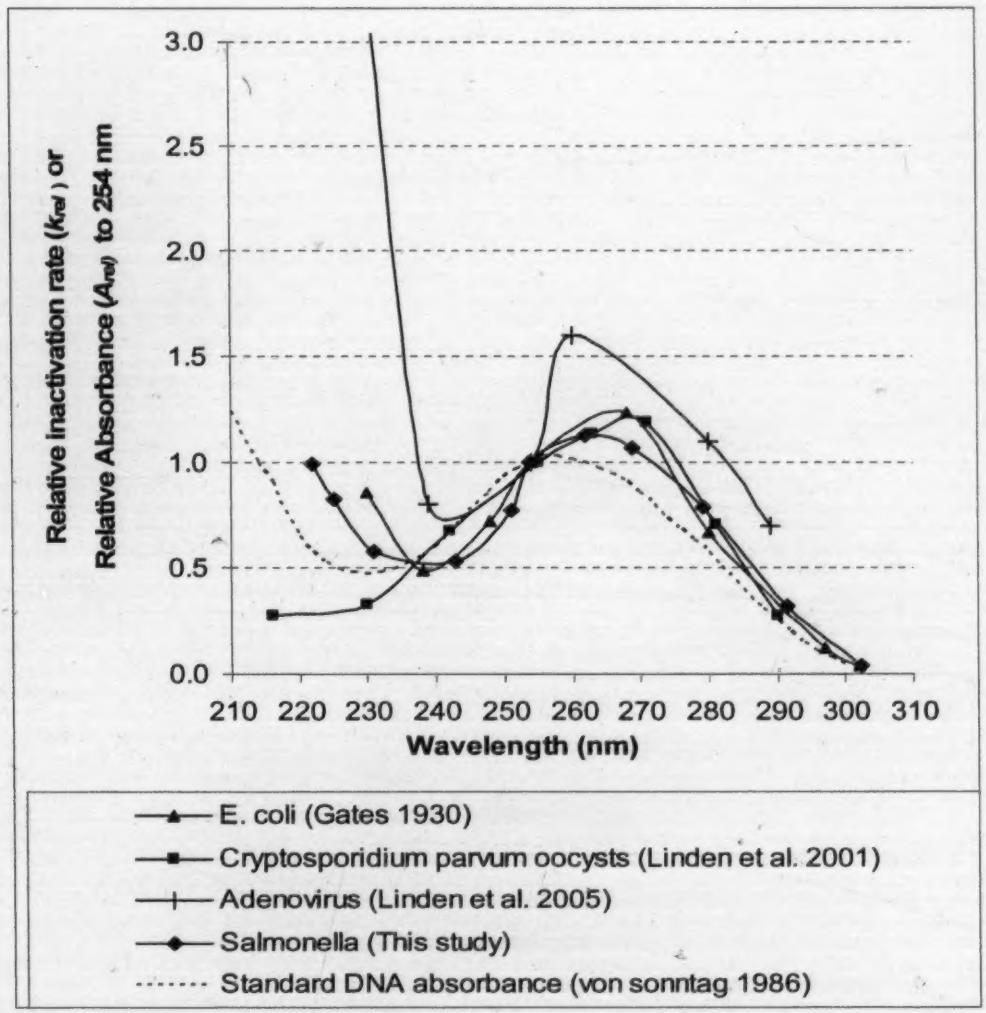

Figure 5.3: Comparison of action spectra of some waterborne pathogens and the 'standard' DNA absorbance spectrum

5.1.4 Differences between the Action Spectra of UV-Sensitive Microorganisms and UV-Resistant Microorganisms

For some UV sensitive protozoan parasites and bacteria, such as *E. coli*, *Salmonella* and *C. parvum* oocysts, protein involvement and/or other factors may be negligible in terms of UV inactivation. The action spectra of these microorganisms are close to the 'standard' DNA absorbance spectrum (Figure 5.3). However, viruses and *B. subtilis* spores exhibit action spectra significantly different from their nucleic acid absorbance spectra. The nucleic acids of MS2 bacteriophage and adenovirus are a small percentage of the total viral material, and the inactivation of these viruses usually requires relatively high UV fluences. The action spectrum of MS2 differs significantly from the 'standard' DNA absorbance spectrum, particularly below 230 nm. It has been suggested that this effect may arise from protein absorption, and that proteins may apparently be involved in the inactivation, since proteins absorb at wavelengths below 230 nm (Rauth 1965). The UV resistance of *B. subtilis* spores may be greater than other bacteria due to the unique protein binding to DNA that occurs in spores (Setlow 2001). In addition, there are large amounts of DPA in the spore core (Douki et al. 2005a) during sporulation. As discussed in Chapter 3, the action spectra of *B. subtilis* spores, as determined in this study, matches the absorbance spectrum of decoated spores, which contain critical components that make spores resistant to UV light. This strongly indicates that absorbance of photons by components other than DNA in spores may contribute to inactivation. Furthermore, one might consider that the quantum yield for photoproduct formation and the quantum yield for photoproduct repair are different at different wavelengths. The distinct difference of the action spectra between UV-sensitive

microorganisms and UV-resistant microorganisms suggests that higher UV fluence may induce more involvement of factors other than photons absorbed by nucleic acids in terms of the inactivation mechanism.

In Chapter 4, the weighted germicidal UV fluences, calculated using the action spectrum of either *E. coli* or *Salmonella*, were close to those calculated using the standard DNA absorbance spectrum. Using the same approach, when the germicidal fluence calculated from the standard DNA absorbance spectrum was 40 mJ/cm^2, that calculated from the action spectrum of *C. parvum* oocysts would be 42 mJ/cm^2, and that calculated using the action spectrum of adenovirus would be approximately 75 mJ/cm^2. Obviously, the 'standard' DNA absorbance spectrum can be a surrogate for the action spectrum of *C. parvum* oocysts, but not for that of adenovirus in bench-scale UV disinfection studies. It might be reasonable that the 'standard' DNA absorption spectrum can be used as a surrogate for the action spectra of other UV sensitive pathogens, such as *Giardia* cysts. However, for UV-resistant microorganisms, the degree of protein involvement and/or other factors in the mechanisms of inactivation is uncertain and difficult to estimate. Therefore, the action spectra of UV resistant microorganisms need to be characterized individually.

5.1.5 Effect of Action Spectra on Polychromatic UV Reactor Validation Using Bioassay

To validate a polychromatic UV reactor using bioassay, ideally the action spectrum of the test microorganism should be similar to that of a target pathogen to provide an accurate estimate of inactivation. Otherwise, a fluence rate correction factor should be considered. In the USEPA's "Draft Ultraviolet Disinfection Guidance

Manual", the action spectra of MS2 (Rauth 1965) and *B. subtilis* spores (Cabaj et al. 2002) were used to determine correction factors for *Cryptosporidium* (USEPA 2003). In their protocol, the measured REF of a test microorganism should be greater than the calculated REF of *Cryptosporidium* for the target inactivation determined from the literature. The calculated REF accounted for some factors such as a safety factor and polychromatic bias. For the polychromatic UV light, the correction factor for the difference of action spectra was multiplied to obtain a calculated REF. According to their result, the germicidal outputs of a MP lamp for these three microorganisms were close to each other and the correction factor was negligible. However, the action spectrum of *B. subtilis* spores from this study and that of MS2 by Linden et al. (2000) are significantly different from those determined by Cabaj et al. (2002) and by Rauth (1965). These differences may lead to a needed correction factor.

Here, a simulation is presented to determine a correction factor (using the fluence rate in stead of the germicidal output) to account for the greater inactivation of the challenge microorganism that arises from the differences in action spectra. A UV reactor equipped with a single MP lamp was considered. The weighted average path length was assumed to be 5 cm and the test water was thoroughly and continuingly mixed across fluence rate gradients. Table 5.1 presents weighted average germicidal fluence rate for this reactor calculated using the reported action spectrum of different surrogate microorganisms. The ratios of the output and the germicidal fluence rates relative to those of *Cryptosporidium* are also shown. If a MP reactor is intended to inactivate *Cryptosporidium*, and the correction factor for the challenge microorganism is greater than one, then this correction factor should be applied to calculate germicidal fluence

rate. This factor will account for the greater inactivation of the challenge organism that arises from the differences in action spectra. For example, if the fluence rate in the reactor based on a *B. subtilis* spores bioassay was 1.32 mW/cm^2 (determined in this study), the effective *Cryptosporidium* fluence rate would be 1.00 mW/cm^2. If the action spectra of MS2 (Linden et al. 2000) was used, the correction factor would 1.24. The ratio determined using the action spectrum of MS2 by Mamane-Gravetz et al. (2005) is 0.98, and hence a correction factor is not necessary (this is a conservative measure), respectively. These ratios determined using the action spectra of *B. subtilis* spores (this study) and MS2 (Linden et al. 2000) are significantly larger than those for most microorganisms, with the exception of adenovirus. This indicates that a correction factor should be assessed when using these two action spectra. This contradicts the USEPA (2003) recommendation to use the action spectra of MS2 by Rauth (1965) and *B. subtilis* spores by Cabaj et al. (2002). However, this simulation may be not good enough for a true reactor in which fluence rate distribution and the flow are complex and complete mixing across fluence rate gradients does not occur. Modeling a reactor with a Computational Fluid Dynamic (CFD) program and using these action spectra will improve the accuracy for determining a correction factor.

In Table 5.1, the ratio for the 'standard' DNA absorbance spectrum is slightly less than that for UV-sensitive pathogens such as *Cryptosporidium*, *Salmonella* and *E. coli*. This suggests that use of the 'standard' DNA absorbance spectrum is slightly conservative for these pathogens. It is thus reasonable to use the 'standard' DNA absorbance spectrum as a surrogate for other UV sensitive pathogens such as *Giardia*, for which an action spectrum is not known. If a reactor is designed to inactivate adenovirus,

the correction factor can be less than one, since the ratio for adenovirus is 1.54, which is higher than both challenge microorganisms.

Table 5.1 Weighted germicidal fluence delivered to microorganisms by a MP lamp

Microorganism or DNA absorbance	References	Weighted Average Germicidal Fluence Rate for 5 cm pathlength	
		Absolute (mW/cm^2)	Relative to *Cryptosporidium* (no units)
Cryptosporidium	Linden et al. (2001)	0.507	1.00
MS2	Linden et al. (2000)	0.631	1.24
MS2	Mamane-Gravtz et al. (2005)	0.498	0.98
B. subtilis spores	This study	0.671	1.32
E. coli	Gates (1930)	0.531	1.05
Salmonella	This study	0.502	0.99
Adenovirus	Linden et al. (2005)	0.779	1.54
DNA absorbance	von Sonntag (1986)	0.479	0.94

5.2 Conclusions and Recommendations

The results from this study provide insight into the application of action spectra to UV disinfection reactors using polychromatic light sources. This section summaries the

significance of this study. Furthermore, recommendations will be proposed for future research.

The absorbance spectra of nucleic acids from different organisms did not differ significantly. The 'standard' DNA absorbance spectrum determined by von Sonntag (1986) may, therefore, be suitable as a surrogate for other nucleic acids absorbance spectra of other microorganisms. The inactivation action spectra for *B. subtilis* spores or MS2 bacteriophage have been found to differ from study to study. These differences might be attributed to the methods used for measuring the fluence (chemical actinometry versus radiometry). Future studies are recommended to compare the fluence determination between the ferrioxalate chemical actinometry and that using a spectroradiometer.

The action spectra of some UV-sensitive waterborne pathogens, such as bacteria and protozoan parasites, have been found to match the 'standard' DNA absorbance spectrum fairly well. However, the action spectra of UV-resistant microorganisms differed significantly from the 'standard' DNA absorbance spectrum. The action spectrum of adenovirus (the most UV-resistant of the known waterborne pathogens that have been studied) differed most. Therefore, the action spectra of UV-resistant microorganisms, such as viruses and bacterial spores, should be characterized individually and rigorously. Simulations of the calculation of germicidal fluence using a MP lamp in bench-scale UV disinfection studies and reactor validation using bioassay suggested that the 'standard' DNA absorbance spectrum might be a suitable surrogate for UV-sensitive microorganisms, such as *Giardia*. The results also suggested that a correction factor should be considered when either MS2 or *B. subtilis* spores are used as

surrogates for a UV-sensitive pathogenic target, such as *Cryptosporidium* oocysts, during validation of a MP lamp UV reactor. Finally, it is recommended that the effect of the action spectra on UV fluence delivered in a real UV reactor be studied more closely using CFD analysis.

REFERENCES

Angulo, F. J.; Tippen, S.; Sharp, D. J.; Payne, B. J.; Collier, C.; Hill, J. E.; Barrett, T. J.; Clark, R. M.; Geldreich, E. E.; Donnell, H. D. and Swerdlow, D. L. (1997), A community waterborne outbreak of salmonellosis and the effectiveness of a boil water order. *Am. Journ. Public Health*, **87**(4), 580-584.

Arvanitidou, M.; Papa, A.; Constantinidis, T. C.; Danielides, V. and Katsouyannopoulos, V. (1997), The occurrence of *Listeria* spp. and *Salmonella* spp. in surface waters. *Microbiol. Res.*, **152**(4), 395-397.

Austria Standards Institute (2001), In Austrian national standard, Plants for disinfection of water using ultraviolet radiation, Requirements and testing, Part 1. Low-pressure mercury lamp plants, ONORM M 5873-1, Vienna, Austria.

Ausuvel, F. M.; Brent, R.; Kingston, R. E.; Moorw, D. D.; Seidman, J. G.; Smith, J. A. and K, S. (1992) *Current Protocols in Molecular Biology,* Jihn Wiley and Sons, Inc., New York.

Bolton, J. R.; Dussert, B.; Bukhari, Z.; Hargy, T. M. and Clancy, J. L. (1998), Inactivation of *Cryptosporidium parvum* by medium-pressure Ultraviolet light in finished drinking water. *Proceedings of the American Water Works Association Water Quality Technology Conference*, November 1-5, San Diego, CA, US, 1998

Bolton, J. R. (2001), Ultraviolet Applications Handbook, 2nd Ed., Bolton Photosciences Inc., Edmonton, AB, Canada.

Bolton, J. R. and Linden, K. G. (2003), Standardization of methods for fluence (UV dose) determination in bench-scale UV experiments. *J. Environ. Eng.*, **129**(3), 209-215.

Bolton, J. R. (2004) Unweighted Fluence (UV Dose) Calculations for a Medium Pressure UV Lamp, *Personal Communication*, 628 Cheriton Cres., NW, Edmonton, AB, Canada T6R 2M5

Bolton, J. R. (2005) Germicidal Fluence (UV Dose) Calculations for a Low Pressure UV lamp, *Personal Communication*, 628 Cheriton Cres., NW, Edmonton, AB, Canada T6R 2M5

Bolton, J. R. (2006) Protocol for the measurement of the irradiance using the ferrioxalate actinometry, *Personal Communication*, 628 Cheriton Cres., NW, Edmonton, AB, Canada T6R 2M5

Britt, A. B. (2004), Repair of DNA damage induced by solar UV. *Photosynthe. Res.*, **81** 105-112.

Bukhari, Z.; Hargy, T. M.; Bolton, J. R.; Dussert, B. and Clancy, J. L. (1999), Medium-pressure UV for oocyst inactivation. *J. Am. Water Works Assoc.*, **91**(3), 86-94.

Cabaj, A.; Sommer, R.; Pribil, W. and Haider, T. (2001), What means "dose" in UV-disinfection with medium pressure lamps? *Ozone: Sci. Engng.*, **23**(3), 239-244.

Cabaj, A.; Sommer, R.; Pribil, W. and Haider, T. (2002), The spectral UV sensitivity of microorganisms used in biodosimetry. *Wat. Sci. and Technol.: Water Supply*, **2**(3), 175-181.

Cameron, K. R. (1973), Ultraviolet Irradiation of Herpes Simplex Virus: Action Spectrum for the Survival of Infectivity in Relation to the Small-plaque Effect. *J. Gener. Virol.*, **8**, 51-54.

Cerf, O. (1977), Tailing of survival curves of bacterial-spores. *J. Appl. Bacteriol.*, **42**(1), 1-19.

Chang, J. C. H.; Ossoff, S. F.; Lobe, D. C.; Dorfman, M. H.; Dumais, C. M.; Qualls, R. G. and Johnson, J. D. (1985), UV Inactivation of Pathogenic and Indicator Microorganisms. *Appl. Environ. Microbiol.*, **49**(6), 1361-1365.

Charlier, M. and Helene, C. (1972), Photochemical reactions of aromatic ketones with nucleic acids and their components-III. Chain breakage and thymine dimerization in benzophenone photosensitized DNA. *Photochem. Photobiol. Sci.*, **51**, 527-536.

Craik, S. A.; Finch, G. R.; Bolton, J. R. and Belosevic, M. (2000), Inactivation of *Giardia muris* cysts using medium-pressure ultraviolet radiation in filtered drinking water. *Wat. Res.*, **34**(18), 4325-4332.

Craik, S. A.; Weldon, D.; Finch, G. R.; Bolton, J. R. and Belosevic, M. (2001), Inactivation of *Cryptosporidium parvum* oocysts using medium- and low-pressure ultraviolet radiation. *Wat. Res.*, **35**(6), 1387-1398.

Craik, S. A. and Uvbiama, R. D. (2005), Effect of Aggregation on UV Inactivation of Microorganisms in Filtered Drinking Water. *Proceedings of the American Water Works Association Water Quality Technology Conference*, November 7-11, Quebec City, QC, Canada, 2005

Davidson, J. N. (1965), *The biochemistry effect of nucleic acids*, Methuen and Co., Ltd., London.

Donnellan, J. E. and Setlow, R. B. (1965), Thymine photoproducts but not thymine dimers are found in ultraviolet irradiated bacterial spores. *Science*, **149**, 308-310.

Douki, T.; Setlow, B. and Setlow, P. (2005a), Photosensitization of DNA by dipicolinic acid, a major component of spores of *Bacillus* species. *Photochem. Photobiol. Sci.*, **4**(8), 591-597.

Douki, T.; Setlow, B. and Setlow, P. (2005b), Effects of the binding of alpha/beta-type small, acid-soluble spore proteins on the photochemistry of DNA in spores of *Bacillus subtilis* and in vitro. *Photochem. and Photobiol.*, **81** (1), 163-169.

DVGW (1997) *UV systems for Disinfection in Drinking Water Supplies - Requirements and Testing*, Deutscher Verein des Gas- und Wasserfaches e.V, Bonn, Germany

Fluke, D. J. and Pollard, E. C. (1949), Ultraviolet Action Spectrum of T1 Bacteriophage. *Science*, **110**, 274-275.

Friedberg, E., R.; Walker, G. C. and Siede, W. (1995) *DNA Repair and Mutagenesis*, WSM Press, Washington, D.C.

Gates, F. L. (1929), A study of the bactericidal action of ultra violet high II. The effect of various environmental factors and conditions. *J. of Gen. Physiol.*, **13**(2), 249-260.

Gates, F. L. (1930), A study of the bactericidal action of ultra violet light III. The absorption of ultra violet light by bacteria. *J. of Gen. Physiol.*, **14**(1), 31-42.

Harm, M. (1980) *Biological Effects of Ultraviolet Radiation*, Cambridge University Press, Westford, Massachusetts.

Heering, W. (2004), UV Source - Basics, properties and application. *IUVA NEWS*, **6**(4), 7-12.

Hijnen, W. A. M.; Beerendonk, E. F. and Medema, G. J. (2006), Inactivation credit of UV radiation for viruses, bacteria and protozoan (oo)cysts in water: A review. *Wat. Res.*, **40**, 3-22.

Jagger, J. (1967) *Introduction to Research in Ultraviolet Photobiology*, Prentice-Hall Inc, New Jersey.

Koivunen, J. and Heinonen-Tanski, H. (2005), Inactivation of enteric microorganisms with chemicla disinfectants, UV irradiation and combined chemical/UV treatments. *Wat. Res.*, **39**,1529-1526.

Lamola, A. A. Longworth, J. W. and Gratzer W. B. (1970), Biological molecules in their excited states. *Nature*, **226**, 113-118.

Lindberg, C. and Horneck, G. (1991), Action spectra for survival and spore photoproduct formation of *Bacillus subtilis* irradiated with short wavelength (200-300 nm) UV at atmospheric pressure and *in vacus*. *Photochem. Photobiol. Sci.*, **11**, 69-80.

Linden, K. G. (1998), UV acceptance. *Civil Engineering*, **68**(3), 58-61.

Linden, K. G.; Shin, G. A. and Sobsey, M. D. (2000). In comparison of monochromatic and polychromatic UV light for disinfection efficiency. *Proceedings of the American Water Works Association Water Quality Technology Conference*, November, Salt Lake City, Utah

Linden, K. G.; Shin, G. and Sobsey, M. D. (2001), Comparative effectiveness of UV wavelengths for the inactivation of *Cryptosporidium parvum* oocysts in water. *Wat. Sci. and Technol.*, **43**(12), 171-174.

Linden, K. G.; Johnson, S. and Malley, J. P. (2005). Importance of Wavelength for UV Inativation of Adenovirus in Water. *Proceedings of 3rd International Congress on Ultraviolet Technologies*, May 24–27, Whistler, BC, Canada, 2005

Maier, R. M.; Pepper, I. L, and Gerba, C. P. (2000) *Environmental Microbiology*, Academic Press, Orlando, Florida

Mamane-Gravetz, H. and Linden, K. G. (2005), Relationship between physiochemical properties, aggregation and UV inactivation of isolated indigenous spores in water. *J. Appl. Microbiol.*, **98**(2), 351-363.

Mamane-Gravetz, H.; Linden, K. G.; Cabaj, A. and Sommer, R. (2005), Spectral sensitivity of *Bacillus subtilis* spores and MS2 Coliphage for validation testing of ultraviolet reactors for water disinfection. *Environ. Sci. Technol.*, **39**(20), 7845-7852.

Mason, J. M. and Setlow, P. (1986), Essential role of Small, Acid-Soluble spore proteins in resistance of *bacillus subtilis* spores to UV-Light. *J. Bacteriol.*, **167**(1), 174-178.

Munakata, N. and Rupert, C. S. (1972), Genetically controlled removal of "spore photoproduct" from DNA of ultraviolet *Bacillus subtilis* spores. *J. Bacteriol.*, **111**,192-198.

Munakata, N. and Rupert, C. S. (1975), Effect of DNA-polymerase-defective and recombination-deficient mutations on ultraviolet sensitivity of *Bacillus subtilis* spores. *Mutat. Res.*, **21**,157-169.

Munakata, N., Saito, S. and Hieda, K. (1991), Inactivation action spectra of *Bacillus subtilis* spores in extended ultraviolet wavelengths (50-300 nm) obtained with synchrotron radiation. *Photochem. Photobiol.*, **54**(5), 761-768.

Nagaraju, D. and Sastri, J. C. V. (1999), Confirmed faecal pollution to bore well waters of Mysore city. Environmental Geology, 38 (4), 322-326.

NCI (1976) Report on the Carcinogenesis Bioassay of Chloroform, NTIS PB-264-018. National Cancer Institute, Bethesda, Md,

Nicholson, W. L.; Setlow, B. and Setlow, P. (1990), Binding of DNA *in vitro* by a small, acid-soluble spore protein from *Bacillus subtilis* and the effect of this binding on DNA Topology. *J. Bacteriol.*, **172**(12), 6900-6906.

Nicholson, W. L. and Setlow, P. (1990), Dramatic increase in negative superhelicity of plasmid DNA in the forespore compartment of sporulating cells of *Bacillus subtilis*. *J. Bacteriol.*, **169**(6), 3633-3637.

Oguma, K.; Katayama, H. and Ohgaki, S. (2003). Effects of UV Spectral Sensivity on Inactivation and Photoreactivation of *Escherichia coli*. Proceedings of *2nd International Congress on Ultraviolet of Technologies*, Vienna, Austria,

Partrick, M. H. and Gary, D. M. (1976), Independence of photoproduct formation on DNA conformation. *Photochem. Photobiol.*, **24**, 507-513.

Pepper, I. L.; Gerba, C. P. and Brendecke, J. W. (1995) *Environmental Microbiology: A laboratory Manual*, Academic Press, San Diego, CA.

Rahn, R. O. and Hosszu, J. L. (1969), Influence of relative humiduty on the photochemistry of DNA films. *Biochi. Biophys. Acta*, **190**, 126-131.

Rauth, A. M. (1965), Physical state of viral nucleic acid and sensitivity of viruses to ultraviolet light. *Biophysical Journal*, **5**(3), 257-265

Riesenman, P. J. and Nicholson, W. L. (2000), Role of the spore coat layers in *Bacillus subtilis* spore resistance to hydrogen peroxide, artificial UV-C, UV-B, and solar UV radiation. *Appl. Environ. Microbiol.*, **66**(2), 620-626.

Ross, M. A. and Setlow, P. (2000), The *Bacillus subtilis* HBsu protein modifies the effects of alpha/beta-type, small acid-soluble spore proteins on DNA. *J. Bacteriol.*, **182**(7), 1942-1948.

Setlow, B..; Xu, D. and Setlow, P. (1992), Interaction between DNA and a/b-Type small, acid-soluble spore proteins: a new class of DNA-binding protein. *J. Bacteriol.*, **174**(7), 2312-2322.

Setlow, B. and Setlow, P. (1993a), Binding of small, acid-soluble spore proteins to DNA plays a significant role in the resistance of *Bacillus subtilis* spores to hydrogen-peroxide. *Appl. Environ. Microbiol.*, **59**(10), 3418-3423.

Setlow, B. and Setlow, P. (1993b), Dipicolinic acid greatly enhances the production of spore photoproduction in bacterial spores upon ultraviolet irradiation. *Appl. Environ. Microbiol.*, **59**, 640-643.

Setlow, P. (1988), Small, acid-soluble spore proteins of *Bacillus* Species - structure, synthesis, genetics, function, and degradation. *Ann. Review Microbiol.*, **42**, 319-338.

Setlow, P. (1992a), I will survive - protecting and repairing spore DNA. *Appl. Environ. Microbiol.*, **174**(9), 2737-2741.

Setlow, P. (1992b), DNA in dormant spores of *Bacillus* species is in an A-Like conformation. *Molecul. Microbiol.*, **6**(5), 563-567.

Setlow, P. (1995), Mechanisms for the prevention of damage to DNA in spores of *Bacillus* species. *Ann. Review Microbiol.*, **49**, 29-54.

Setlow, P. (2001), Resistance of spores of *Bacillus* species to ultraviolet light. *Environ. Molecul. Mutagenes.*, **38**(2-3), 97-104.

Setlow, R. (1960), Ultraviolet wave-length-dependent effects on proteins and nucleic acids. *Radiat. Res.*, **Suppl. 2**, 276-289.

Severin, B. F.; Suidan, M. T. and Engelbrecht, R. S. (1983), Kinetic modeling of UV disinfection of water. *Wat. Res.*, **17**(11), 1669-1678.

Shin, G. A.; Linden, K. G. and Sobsey, M. D. (2005), Low pressure ultraviolet inactivation of pathogenic enteric viruses and bacteriophages. *J. Environ. Engng. Sci.*, **4**, 7-11.

Sime, E. H. and Bedson, H. S. (1973), Comparison of ultraviolet action spectra for vaccinia virus and T2-Bacteriophage. *J. Gener. Virol.*, **18**(Jan), 55-60.

Slieman, T. A. and Nicholson, W. L. (2000), Artificial and solar UV radiation induces strand breaks and cyclobutane pyrimidine dimers in *Bacillus subtilis* spore DNA. *Ann. Review Microbiol.*, **66**(1), 199-205.

Slieman, T. A.; Rebeil, R. and Nicholson, W. L. (2000), Spore photoproduct lyase from *Bacillus subtilis* specifically binds to and cleaves SP but not cyclobutane pyrimidine dimers in UV radiation DNA. *J. Bacteriol.*, **182**, 6412-6417,

Smith, K. C.; Hodgkins, B. and Oleary, M. E. (1966), Biological importance of ultraviolet light induced DNA-protein crosslinks in *Escherichia coli* 15 Tau. *Biochim. Biophys. Acta*, **114**(1), 1-8.

Sommer, R. and Cabaj, A. (1993), Evaluation of the efficiecy of a UV plant for drinking water disinfection. *Wat. Sci. Technol.*, **27**(3/4), 357-362.

Tosa, K. and Hirata, T. (1998). HRWM-39: Photoreactivation of *Salmonella* following UV disinfection. *IAWQ 19th Biennial International Conference*, August 22-25, Vancouver, Canada, 1998

Tsuboi, K. K. (1950), Mouse liver nucleic acids. II. Ultraviolet absorption studies. *Biochim. Biophys. Acta*, **6**, 202-209.

Tulchinsky, T. H.; Burla, E.; Clayman, M.; Sadik, C.; Brown, A. and Goldberger, S. (2000), Safety of community drinking-water and outbreaks of waterborne enteric disease: Israel, 1976-97. *Bulletin of the World Health Organization*, **78**(12), 1466-1473.

USEPA (2003) Ultraviolet Disinfection Guidance Manual, EPA 815-D-03-007. Office of Water, Washington, DC.

USEPA (2006) Long Term 2 Enhanced Surface Water Treatment Rule, EPA 816-F-06-008. Washington, DC,

Uvbiama, R. D. and Craik, S. A. (2005). The effect of upstream treatment processes on UV inactivation of microorganisms in filtered water. Proceedings of *third congress of the International Ultraviolet Association*, May 24-27, Whistler, BC, Canada

Uvbiama, R. D. (2006) The effect of upstream treatment processes on UV inactivation of microorganisms in filtered drinking water. *Msc. Thesis*, Department of Civil and Environmental Engineering, University of Alberta, Edmonton, AB, Canada

Varghese, A. (1970), 5-thyminyl-5, 6-dihydrothymine from DNA irradiated with ultraviolet light. *Bioch. Biophys. Res. Commun.*, **38,** 484-490.

Von Sonntag, C. (1986), Disinfection by free radicals and UV inactivation. *Water Supply*, **4**, 11-18.

Wetlaufer, D. B. (1962), Ultraviolet spectra of proteins and amino acids. *Advance in Protein Chemistry*, 303-383, Academic Press Inc, New York.

Wilfinger, W. (1997), Effect of pH and ionic strength on the spectro-photometric assessment of nucleic acid purity. *Bio. Techniques*, **22**, 474-481.

Wilson, B. R.; Roessler, P. F.; Van Dellen, E.; Abbaszadegan, M. and Gerba, C. P. (1992). Coliphage MS2 as a UV Water Disinfection Efficiency Test Surrogate and Viral Pathogens. *Proceedings of American Water Works Association Water Quality Technology Conference*, November 15-19, Toronto, ON, Canada

Wilson, P. D. G.; Wilson, D. R.; Brocklehurst, T. F.; Coleman, H. P.; Mitchell, G.; Waspe, C. R.; Jukes, S. A. and Robins, M. M. (2003), Batch growth of *Salmonella typhimurium* LT2: stoichiometry and factors leading to cessation of growth. International *J Food Microbiol.*, **89**, 195-203.

Wolfe, R. L. (1990), Ultraviolet disinfection of potable water. *Environ. Sci. Technol.*, **24**(6), 768-773.

Xue, Y. and Nicholson, W. L. (1996), The two major DNA repair pathways, nuclcotide excision repair and spore photoproduction lyase, are sufficient for resistance for *Bacillus subtillis* spores to artificial UV-C and UV-B but not to solar radiation. *Appl. Environ. Microbiol.*, **62**, 2221-2227.

Yoon, C. G.; Chuang, K. M.; Ham, J. H. and Jeon, J. H. (2004), Feasibility study of UV disinfection for agricultural reuse of secondary level effluent in Korea. *J. Environ. Sci. Health*, **A39**(3), 835-846.

York, D. W.; Walker, L. C. and Ferraro, C. (2002). Florida's water reuse program past, present and future directions. *Water reuse Assoc. symp.*, Orlando, FL

Zelle, M. R. and Hollaender, A. (1954), Monochromatic ultraviolet action spectra and quantum yields for inactivation of T1 *Escherichia* and T2 *Escherichia-Coli* Bacteriophages. *J. Bacteriol.*, **68**(2), 210-215.

APPENDIX-A: DETAILED EXPERIEMENTAL METHODS

Appendix A-1: Preparation of Nutrient Agar for *B. subtilis* Spores Enumeration

1. Weigh out and transfer 8 g nutrient broth (Difco™, Detroit, MI) and 16 g Solidified Agar (Difco™, Detroit, MI) per liter Milli-Q® water into a clean Erlenmeyer flask. Immerse a Teflon® coated magnetic stir bar.
2. Heat the agar solution in the flask with continuing stirring on a stirrer plate.
3. Place a set of clean 20 mL test tubes onto test tube racks vertically.
4. Stop heating when the nutrient agar is boiling.
5. Transfer each approximate 15 mL liquid agar into a test tube and cap the test tube.
6. Autoclave the agar at 121°C for 15 min.
7. After autoclave, keep the agar in an isotherm water bath at 50°C for future use less than one week.

Appendix A-2: Protocol for the Measurement of Irradiance Using the Ferrioxalate Actinometer

Provided by Dr. James R. Bolton
Bolton Photosciences Inc., 628 Cheriton Cres., NW, Edmonton, AB, Canada T6R 2M5

Background

An actinometer is a solution that is photosensitive, and by absorption of light generates photoproducts with a known quantum yield. By measuring that product generated, it is possible to determine the photon flow (einstein/s).

The potassium ferrioxalate actinometer is the 'gold' standard actinometer, which is based on the photo-reduction of iron, according to the following equation:

$$Fe(C_2O_4)_3^{3-} + h\nu \longrightarrow Fe^{2+} + 2.5\ C_2O_4^{2-} + CO_2 \qquad \text{Eqn (A-1)}$$

The quantum yield of Fe^{2+} production is essentially independent of wavelength in the range 220 – 320 nm at 1.25, but decreases sharply at longer wavelengths, for example, to 0.013 at 577 nm. The quantum yield of ferrioxalate actinometer has been determined at 254, 297, 302 and 313 nm and is 1.25 (Murov et al., 1993). No published data are available below 254 nm, although the quantum yield probably remains independent of wavelength down to about 200 nm. For the photon flow measurements within 200-300 nm range, a quantum yield value of 1.25 has been used in many studies.

The amount of iron (II) produced is measured via spectrophotometric determination of its 1,10-phenenthroline complex at 510 nm. At this wavelength, the molar absorption coefficient of the complex is 11,182 $M^{-1}\ cm^{-1}$.

Ferrioxalate absorbs strongly in the range from 200 to 600 nm. This makes it impossible to use in the daylight (room-light); therefore, the ferrioxalate actinometry experiments must be conducted with red 'safety' photographic lamps.

Solutions

Materials and Chemicals requirements

1 L volumetric flask
250 mL volumetric flask
100 mL volumetric flask
at least ten 10 mL volumetric flasks
250 mL brown reagent bottle
250 mL reagent bottle
100 mL graduated cylinder
0 – 1 mL variable pipette
0 – 5 mL variable pipette
two red "safety" photographic lamps
a room that can be completely darkened

All chemicals must be analytical reagent grade.
distilled water
conc. (96-98%) H_2SO_4
at least 200 g ferric sulfate [$Fe_2(SO_4)_3$] – usually comes as a hydrate
at least 400 g potassium oxalate [$K_2C_2O_4 \cdot H_2O$]
at least 250 g sodium acetate [$CH_3COONa \cdot 3H_2O$]
at least 0.5 g 1,10-phenanthroline
at least 100 mL of a concentrated solution of hydroxyl amine hydrochloride [$NH_2OH \cdot HCl$]

Solution A - 0.2 M Ferric Sulfate Solution in 2 N H_2SO_4

Weigh out 25 g $Fe_2(SO_4)_3$ (solid containing 21-23% Fe) and transfer it into a 250 mL volumetric flask. Add ~100 mL distilled water, and mix. The salt does not dissolve. Immerse the volumetric flask in a large beaker with cold tap water, and add slowly, while mixing carefully, 14 mL concentrated H_2SO_4 (96-98%, density = 1.84 g/mL). The role of tap water in the beaker is to cool down the ferric sulfate solution in H_2SO_4, since while adding the concentrated acid, the solution temperature increases.

Add about 25 mL distilled water to the solution washing the neck of the volumetric flask, and keep mixing the solution until the solid is dissolved. Bring the solution to the 250 mL mark with distilled water, add a small magnetic stir bar, stopper the flask and mix the solution on a stir plate until completely homogeneous.

Transfer the solution into a brown bottle, label it and store at the room temperature in a dark place. The ferric sulfate solution is light sensitive. Under the specified conditions, the solution can be stored for at least 3 months.

Solution B - 1.2 M Potassium Oxalate Solution

Weigh out 55.26 g $K_2C_2O_4 \cdot H_2O$ and transfer it into a 250 mL volumetric flask. Add distilled water slowly, while mixing, to dissolve the solid. Bring the solution to the 250 mL mark with distilled water and homogenize. Transfer the solution in a reagent bottle, label and store it at room temperature. The solution can be stored at least 3 months.

Solution C - Sodium Acetate – Sulfuric Acid Buffer Solution pH 4.5

Weigh out 20.5 g $CH_3COONa \cdot 3H_2O$ and transfer it in a 250 mL volumetric flask. Add 100 mL distilled water and mix until the solid is dissolved. Add slowly 2.5 mL of concentrated H_2SO_4 (96-98%) to the solution, while gently mixing. Add distilled water to the mark, homogenize the solution and transfer it in a storage bottle.

Solution D - 0.2% 1,10-Phenanthroline Solution

Weigh out 0.5 g 1,10-phenanthroline and transfer it into a 250 mL volumetric flask. Add distilled water to the mark, then, immerse a magnetic stir bar and stopper the flask. Keep stirring the mixture on a stir plate until all solid is completely dissolved. Transfer the solution to a brown bottle and store in a dark place.

Solution E - 1 M Hydroxylamine Hydrochloride Solution

Dissolve 6.95 g of $NH_2OH \cdot HCl$ (1 M solution) in 100 mL of distilled water.

Solution F – 2 N H_2SO_4

In a 250 mL volumetric flask add 125 mL distilled water, then, immerse the flask in a large beaker containing cold tap water, and add carefully, under continuous mixing, 14 mL of concentrated H_2SO_4 (96-98%, d = 1.85 g/mL). To the cold solution of sulfuric acid, add the rest of distilled water up to the 250 mL mark. Mix to homogenize. Transfer it into a reagent bottle and label it.

Experimental Procedure

Standardization of Ferric Sulfate Solution

Take exactly 0.300 mL of Solution A into a 100 mL volumetric flask and add distilled water to the mark. Mix the solution thoroughly. Take 0.80 mL of this solution into a 10 mL volumetric flask, add 2 mL of distilled water and 1 mL of Solution E. Mix and wait for 2 min. Add 2 mL of Solution C and 2 mL of Solution D, and keep the volumetric flask for 40 min in a dark place. Then, add distilled water to the mark, mix thoroughly and read the absorbance of the solution at 510 nm in a 1 cm path quartz cell. Note this absorbance as *A* (sample).

Repeat the above procedure without adding Solution E. Note the absorbance of this solution at 510 nm as *A* (blank).

The concentration of Fe(III) in Solution A is:

$$[Fe^{3+}]/M = [A\ (\text{sample}) - A\ (\text{blank})] \times 0.3754$$

Attach a label to the Solution A bottle stating its molarity.

Ferrioxalate Actinometry Experiments

Prior to proceeding with the ferrioxalate actinometry experiments, make sure that the desired experimental configuration is properly set up. The following instructions apply to the use of a 10 mL beaker.

For experiments in a "*quasi* collimated beam" apparatus, a 10 mL beaker should be used over which is placed a black cardboard or plastic "mask", in which a 1.78 cm OD circular hole has been cut in the center (this must be cut very accurately). One can also use a large "washer" for this purpose. The beaker should be filled with no more than 5 mL of solution so that the solution is well below the top of the dish, so that the "mask" can be placed without touching the solution. This procedure will avoid any "edge" effects from the beaker.

Prior to starting the irradiations, prepare a set of labeled 10 mL volumetric flasks. The number of these flasks should correspond to twice the number of the irradiations including blanks. A typical set of runs would consist of a 'blank' run and 3-4 'exposure' runs. Calibrate each volumetric flask by weighing each flask 'dry' and filled to the mark with distilled water. The density of pure water is given in Table 1. Carry out the calibration three times for each flask and record the average 'calibrated volume' for each flask made up to the mark (bottom on the meniscus should be at the mark).
To each calibrated 10 mL volumetric flask, add 2 mL of Solution C and 2 mL of Solution D. Set these aside for the analysis of each exposure.

All of the following steps should be carried out in very subdued light or with red 'safety' photographic lamps:

1. The experiments must be conducted in a "dark room", with strong precautions to prevent any (even small) leaks of visible and UV light. It is particularly important to stop any light leaks from the collimated beam apparatus.
2. In a 1 L volumetric flask, add 15 mL of Solution B, approximately 800 mL distilled water, and 35 mL of Solution F. Mix gently, then, add 6/[Fe(III)] mL of Solution A, where [Fe(III)] is the concentration of ferric ions in Solution A, as determined above. Mix and add distilled water up to the 1 L mark. Mix thoroughly, and transfer the solution quickly to a brown bottle. Label the bottle as 0.006 M potassium ferrioxalate in 0.1 N H_2SO_4. This solution is very photosensitive. Keep it away from any light (except for the red light) at all times.

This is the solution to be used for the determination of photon flow; call it the "FeOx Solution".

3. Weigh the selected 10 mL beaker (empty and dry) (no mask) with a small magnetic stir bar.

4. Add a 5 mL (with a 5 mL pipette) of the "FeOx Solution" to the 5 mL beaker and weigh again. The difference is the weight of the FeOx solution. The density of this solution is 0.9986 g/mL; hence, one can determine the volume of the FeOx solution very accurately. Place the 10 mL beaker (with mask on top) on the stir plate in the collimated beam setup, and start the stirring (gently so as not to disturb the surface of the water with a 'vortex'). Leave the solution on that spot with the shutter CLOSED for the longest chosen irradiation time in the ferrioxalate actinometry experiments. Monitor the time accurately with the stopwatch.

5. Before and after each run with a UV exposure, position the radiometer detector head so that the "calibration plane" is at the level of the top of the washer or cardboard plate, and record the radiometer irradiance value.

6. Repeat Step 3 for each of the UV exposure runs, except accurately determine the time of the exposure with a stop watch and record the radiometer irradiance before and after each run.

7. For the analysis of the "control" runs, weigh one of the 10 mL volumetric flasks containing Solutions C and D. Then add 1 mL of the FeOx solution and weigh again. From the difference in weight and the density of the FeOx solution, a very accurate determination of the volume of the FeOx solution added can be determined. Add ~1 mL distilled water and hide it in a dark place for 40 min. Then, add distilled water to the mark and read the absorbance at 510 nm [A(blank)] in a 1 cm cuvette. If the light precautions were properly taken, the absorbance of the "blank" solution should not exceed 0.015.

8. For each "light-exposed" experiment, add a known volume of the "FeOx Solution" to the sample container to be employed for the irradiation experiments.

In the case of a dish, add a small magnetic stir bar, place it on the stir plate in the collimated beam setup, and start the stirring at a very slow rate, so that the surface of the solution is not disturbed. Open the lamp shutter and start the stopwatch. Irradiate for 2 min, if the center irradiance (with the quartz window in place) is ~1 mW/cm^2. If the incident irradiance is significantly different from ~1 mW/cm^2, increase or decrease the exposure time accordingly. Close the shutter and stop the timer. Please be aware that the exposure time must be very accurately monitored.

Increase the speed of stirring for a few seconds, then stop the stirring. Carry out the analysis as in Step 7. After 40 min, bring the volume to the 10 mL mark with distilled water, homogenize and take the absorbance reading at 510 nm, A(sample).

9. Repeat step 8 for the remaining exposure times (for example, 30, and 20 min). Make sure that the absorbance readings of the irradiated samples are not larger than 1.3-1.4 ($\lambda = 510$ nm).

10. The moles of Fe^{2+} generated from a single measurement is obtained from:

$$\text{Moles } Fe^{2+} = \frac{[A(\text{sample}) - A(\text{blank})] \times 10 \times V}{11182 \times V_1} \qquad \text{Eqn. A-2}$$

where, V (mL) is the total irradiated volume (e.g., 10.0 mL), V_1 (mL) is the volume withdrawn from the irradiated solution (e.g., 1.0 mL).

11. The UV irradiance measured by the Ferrioxalate Actinometry is given by:

$$E = \frac{V_3 \times C_\lambda}{0.975 \times \Phi \times A_{cs} t} \qquad \text{Eqn. A-3}$$

where

E = UV irradiance (mW/cm^2);

0.975 is the reflection factor;

Φ_λ = quantum yield of ferrous production (1.25 mole/Einstein);

V_1 = volume, mL, of irradiated actinometer solution withdrawn (5 mL);

V_2 = volume, L, of actinometer irradiated (0.015 L);

V_3 = volume, mL, of volumetric flask used for dilution of irradiated aliquot (25 mL);

A_{cs} = cross-sectional area, cm^2, of irradiated actinometer solution;

t = exposure time (second);

C_λ = constant used to convert Einstein into radiance energy (mJ / Einstein).

12. The sensor factor is obtained by dividing the value from the Ferrioxalate Actinometry and the value of the radiometer reading.

Table A-1 Sensor factor for the International Light Radiometer

Weighted Average Wavelength (nm)	Radiometer Reading (mW/cm^2)	Irradiance Measured by the Ferrioxalate Actinometry (mW/cm^2)	Sensor Factor of IL Radiometer
222	0.24	0.506	2.15
224	0.31	0.647	2.10
231	0.68	1.103	1.63
243	0.76	0.933	1.24
251	0.79	0.906	1.14
LP 254	0.70	0.819	1.17*
262	1.80	1.771	0.98
269	1.43	1.363	0.96
280	1.10	1.128	1.03
291	0.66	0.737	1.13
302	0.93	1.599	1.72

*Note: LP lamps also emit light with wavelengths above 300 nm, which can activate the Ferrioxalate Actinometer. The sensor factor of the LP lamp is 1.00 rather than 1.17 obtained here.

Appendix A-3 Method for preparation of MacConkey agar plate for *Salmonella typhimurium* LT2

1. Weigh out 60 g MacConkey agar (Difco™, Sparks, MD) and transfer it into a clean 2 L Erlenmeyer flask. Add 1.2 L Milli-Q® water and immerse a Teflon® coated magnetic stir bar.
2. Seal the flask with aluminum paper and heat the agar in the flask with continuing stirring on a stirrer plate.
3. Stop heating when the nutrient agar is boiling.
4. Autoclave the agar at 121°C for 15 min.
5. Transfer each approximate 10 mL of the agar into a sterile 150 x 15 mm pre-sterilized polystyrene Petri dish (Fisher Brand) with a sterile pipette on a horizontal bench in a clean air cabinet (Canadian Cabinets HEA-7, Ottawa, ON).
6. After solidification of the agar, cover the lid of Petri Dishes.
7. Keep the Petri Dishes containing the MacConkey agar in a covered plastic container and store the agar plate at 4°C for further use.

APPENDIX B RAW DATA AND SUPPORTIVE INFORMATION

Appendix B-1: CFU Enumeration of *Bacillus subtilis* Spores

Table B-1 CFU enumeration of *B. subtilis* spores for the 222 nm band

UV fluence (mJ/cm^2)	Dilution Factor	CFU Counts #1	#2	#3	Geometric Mean	*N* CFU/mL
0	1.00E+04	60	51	56	55.5	5.55E+05
0	1.00E+04	46	47	45	46.0	4.60E+05
0	1.00E+04	50	48	57	51.5	5.15E+05
3.75	1.00E+04	44	49	41	44.5	4.45E+05
3.75	1.00E+04	34	46	43	40.7	4.07E+05
3.75	1.00E+04	37	44	41	40.6	4.06E+05
6.25	1.00E+04	34	34	18	27.5	2.75E+05
6.25	1.00E+04	32	27	40	32.6	3.26E+05
6.25	1.00E+04	34	35	37	35.3	3.53E+05
12.51	1.00E+03	63	55	41	52.2	5.22E+04
12.51	1.00E+03	41	47	35	40.7	4.07E+04
12.51	1.00E+03	86	75	65	74.8	7.48E+04
28.24	1.00E+00	67	56	68	63.4	6.34E+01
28.24	1.00E+00	68	56	78	66.7	6.67E+01
28.24	1.00E+00	140	125	118	127.3	1.27E+02

Table B-2 CFU enumeration of *B. subtilis* spores for the 225 nm band

UV fluence (mJ/cm^2)	Dilution Factor	CFU Counts #1	#2	#3	Geometric Mean	N_o CFU/mL
0	1.00E+04	98	98	107	100.9	1.01E+06
0	1.00E+04	97	116	113	108.3	1.08E+06
0	1.00E+04	112	106	108	108.6	1.09E+06
4.07	1.00E+04	57	57	67	60.2	6.02E+05
4.07	1.00E+04	75	60	72	68.7	6.87E+05
4.07	1.00E+04	97	88	70	84.2	8.42E+05
6.78	1.00E+04	38	29	45	36.7	3.67E+05
6.78	1.00E+04	53	49	45	48.9	4.89E+05
6.78	1.00E+04	39	40	36	38.3	3.83E+05
13.57	1.00E+03	31	43	38	37.0	3.70E+04
13.57	1.00E+03	48	64	55	55.3	5.53E+04
13.57	1.00E+03	51	64	62	58.7	5.87E+04
27.14	1.00E+01	44	41	45	43.3	4.33E+02
27.14	1.00E+01	35	35	32	34.0	3.40E+02
27.14	1.00E+01	77	88	72	78.7	7.87E+02
40.70	1.00E+00	43	42	74	51.1	5.11E+01
40.70	1.00E+00	33	18	35	27.5	2.75E+01
40.70	1.00E+00	17	73	13	25.3	2.53E+01

Table B-3 CFU enumeration of *B. subtilis spores* for the 231 nm band

UV fluence (mJ/cm^2)	Dilution Factor	CFU Counts #1	#2	#3	Geometric Mean	*N* CFU/mL
0	1.00E+04	105	106	101	104.0	1.04E+06
0	1.00E+04	126	127	140	130.8	1.31E+06
0	1.00E+04	126	109	87	106.1	1.06E+06
6.73	1.00E+04	74	70	82	75.2	7.52E+05
6.73	1.00E+04	85	82	82	83.0	8.30E+05
6.73	1.00E+04	84	69	67	73.0	7.30E+05
13.45	1.00E+03	134	142	145	140.3	1.40E+05
13.45	1.00E+03	184	189	170	180.8	1.81E+05
13.45	1.00E+03	182	225	235	212.7	2.13E+05
26.90	1.00E+02	39	45	40	41.3	4.13E+03
26.90	1.00E+02	38	31	36	34.9	3.49E+03
26.90	1.00E+02	25	29	39	30.5	3.05E+03
40.35	1.00E+00	86	87	152	104.4	1.04E+02
40.35	1.00E+00	120	89	119	108.3	1.08E+02
40.35	1.00E+00	166	153	60	115.1	1.15E+02
53.80	5.00E-01	107	55	152	96.4	4.82E+01
53.80	5.00E-01	115	153	169	143.8	7.19E+01
53.80	5.00E-01	39	60	41	45.8	2.29E+01

Table B-4 CFU enumeration of *B. subtilis* spores for the 243 nm band

UV fluence (mJ/cm^2)	Dilution Factor	CFU Counts #1	#2	#3	Geometric Mean	*N* CFU/mL
0	1.00E+04	105	106	101	104.0	1.04E+06
0	1.00E+04	126	127	140	130.8	1.31E+06
0	1.00E+04	126	109	87	106.1	1.06E+06
6.73	1.00E+04	74	70	82	75.2	7.52E+05
6.73	1.00E+04	85	82	82	83.0	8.30E+05
6.73	1.00E+04	84	69	67	73.0	7.30E+05
13.45	1.00E+03	134	142	145	140.3	1.40E+05
13.45	1.00E+03	184	189	170	180.8	1.81E+05
13.45	1.00E+03	182	225	235	212.7	2.13E+05
26.90	1.00E+02	39	45	40	41.3	4.13E+03
26.90	1.00E+02	38	31	36	34.9	3.49E+03
26.90	1.00E+02	25	29	39	30.5	3.05E+03
53.80	1.00E+00	86	87	152	104.4	1.04E+02
53.80	1.00E+00	120	89	119	108.3	1.08E+02
53.80	1.00E+00	166	153	60	115.1	1.15E+02
80.71	5.00E-01	107	55	152	96.4	4.82E+01
80.71	5.00E-01	115	153	169	143.8	7.19E+01
80.71	5.00E-01	39	60	41	45.8	2.29E+01

Table B-5 CFU enumeration of *B. subtilis* spores for the 251 nm band

UV fluence (mJ/cm^2)	Dilution Factor	CFU Counts #1	#2	#3	Geometric Mean	N_o CFU/mL
0	1.00E+05	45		44	44.5	4.45E+06
0	1.00E+05	38	28	41	35.2	3.52E+06
0	1.00E+05					0.00E+00
5.83	1.00E+05	31	43	56	42.1	4.21E+06
5.83	1.00E+05	28	32	47	34.8	3.48E+06
5.83	1.00E+05	43	36	33	37.1	3.71E+06
11.66	1.00E+04	251	291	269	269.8	2.70E+06
11.66	1.00E+04	315	330	289	310.9	3.11E+06
11.66	1.00E+04	285	229	257	256.0	2.56E+06
23.32	1.00E+04	59	61	63	61.0	6.10E+05
23.32	1.00E+04	69	78		73.4	7.34E+05
23.32	1.00E+04	84	64	77	74.5	7.45E+05
34.98	1.00E+03	156	134	142	143.7	1.44E+05
34.98	1.00E+03	121	127	129	125.6	1.26E+05
34.98	1.00E+03	135	116	113	121.0	1.21E+05
46.65	1.00E+02	148	164	152	154.5	1.55E+04
46.65	1.00E+02	134	147	125	135.0	1.35E+04
46.65	1.00E+02	235	215	204	217.6	2.18E+04
69.97	1.00E+01	26	26	29	27.0	2.70E+02
69.97	1.00E+01	33	32	30	31.6	3.16E+02
69.97	1.00E+01	38	34	32	34.6	3.46E+02

Table B-6 CFU enumeration of *B. subtilis* spores for the LP lamp

UV fluence (mJ/cm^2)	Dilution Factor	CFU Counts #1	#2	#3	Geometric Mean	N_0 CFU/mL
0	1.00E+04	105	106	103	104.7	1.05E+06
0	1.00E+04	84	110	102	98.0	9.80E+05
0	1.00E+04	93	108	90	96.7	9.67E+05
0	1.00E+04	81	96	89	88.5	8.85E+05
10	1.00E+04	73	58	57	62.3	6.23E+05
10	1.00E+04	83	89	68	79.5	7.95E+05
10	1.00E+04	78	75	77	76.7	7.67E+05
20	1.00E+03	156	129	108	129.5	1.30E+05
20	1.00E+03	110	101	83	97.3	9.73E+04
20	1.00E+03	142	128	109	125.6	1.26E+05
30	1.00E+02	109	102	136	114.8	1.15E+04
30	1.00E+02	148	181	162	163.1	1.63E+04
30	1.00E+02	107	140	161	134.1	1.34E+04
40	1.00E+01	286	270	256	270.4	2.70E+03
40	1.00E+01	125	147	121	130.5	1.31E+03
40	1.00E+01	226	260	239	241.3	2.41E+03
50	1.00E+01	28	14	33	23.5	2.35E+02
50	1.00E+01	34	38	27	32.7	3.27E+02
50	1.00E+01	42	21	31	30.1	3.01E+02
60	1.00E+00	16	28	43	26.8	2.68E+01
60	1.00E+00	30	48	38	38.0	3.80E+01
60	1.00E+00	34	24	31	29.4	2.94E+01

Table B-7 CFU enumeration of *B. subtilis* spores for the 262 nm band

UV fluence (mJ/cm^2)	Dilution Factor	CFU Counts #1	#2	#3	Geometric Mean	N_o CFU/mL
0	1.00E+05	51	50	42	47.5	4.75E+06
0	1.00E+05	48	58	36	46.5	4.65E+06
0	1.00E+05	47	52	49	49.3	4.93E+06
4.68	1.00E+05	45	54	62	53.2	5.32E+06
4.68	1.00E+05	39	48	41	42.5	4.25E+06
4.68	1.00E+05	54	49	56	52.9	5.29E+06
9.37	1.00E+04	210	222	241	224.0	2.24E+06
9.37	1.00E+04	186	207	228	206.3	2.06E+06
9.37	1.00E+04	196	197	203	198.6	1.99E+06
18.74	1.00E+03	210	218	190	205.7	2.06E+05
18.74	1.00E+03	231	221	259	236.5	2.36E+05
18.74	1.00E+03	274	256	252	260.5	2.60E+05
28.11	1.00E+02	103	112	91	101.6	1.02E+04
28.11	1.00E+02	145	182	207	176.1	1.76E+04
28.11	1.00E+02					
37.48	1.00E+01	52	87	73	69.1	6.91E+02
37.48	1.00E+01	126	129	124	126.3	1.26E+03
37.48	1.00E+01	83	108	122	103.0	1.03E+03
56.22	1.00E+00	106	115	136	118.4	1.18E+02
56.22	1.00E+00	42	30	35	35.3	3.53E+01
56.22	1.00E+00	32	42	40	37.7	3.77E+01

Table B-8 CFU enumeration of *B. subtilis* spores for the 269 nm band

UV fluence (mJ/cm^2)	Dilution Factor	CFU Counts #1	#2	#3	Geometric Mean	*N* CFU/mL
0	1.00E+04	101		86	93.2	9.32E+05
0	1.00E+04	116	109	74	97.8	9.78E+05
0	1.00E+04	84	79	75	79.2	7.92E+05
4.23	1.00E+04	74	83	66	74.0	7.40E+05
4.23	1.00E+04	82	73	46	65.1	6.51E+05
4.23	1.00E+04	90	101	81	90.3	9.03E+05
8.46	1.00E+04	40	46	36	40.5	4.05E+05
8.46	1.00E+04	63	46	81	61.7	6.17E+05
8.46	1.00E+04	40	46	51	45.4	4.54E+05
16.93	1.00E+03	50	49	48	49.0	4.90E+04
16.93	1.00E+03	52	60	51	54.2	5.42E+04
16.93	1.00E+03	58	83	68	68.9	6.89E+04
25.39	1.00E+02	36	32	31	32.9	3.29E+03
25.39	1.00E+02	51	46	52	49.6	4.96E+03
25.39	1.00E+02	49	75	53	58.0	5.80E+03
33.85	1.00E+00		97	129	111.9	1.12E+02
33.85	1.00E+00	101	106	131	111.9	1.12E+02
33.85	1.00E+00	102	166	126	128.7	1.29E+02

Table B-9 CFU Enumeration of *B. subtilis* spores for the 279 nm band

UV fluence (mJ/cm^2)	Dilution Factor	CFU Counts #1	#2	#3	Geometric Mean	N_o CFU/mL
0	1.00E+04	91	122	121	110.3	1.10E+06
0	1.00E+04	139	130	101	122.2	1.22E+06
0	1.00E+04	108	122	141	122.9	1.23E+06
7.43	1.00E+04	90	78	94	87.1	8.71E+05
7.43	1.00E+04	99	99	101	99.7	9.97E+05
7.43	1.00E+04	90	102	116	102.1	1.02E+06
14.86	1.00E+04	47	36	34	38.6	3.86E+05
14.86	1.00E+03	282	296	248	274.6	2.75E+05
14.86	1.00E+03	277	268	242	261.9	2.62E+05
29.73	1.00E+02	186	166	171	174.1	1.74E+04
29.73	1.00E+02	168	151	160	159.5	1.60E+04
29.73	1.00E+02	108	106	75	95.0	9.50E+03
44.59	1.00E+01	36	32	31	32.9	3.29E+02
44.59	1.00E+01	40	42	37	39.6	3.96E+02
44.59	1.00E+01	64	68	56	62.5	6.25E+02
59.45	1.00E+00	33	21	34	28.7	2.87E+01
59.45	1.00E+00	32	26	37	31.3	3.13E+01
59.45	1.00E+00	12	14	11	12.3	1.23E+01

Table B-10 CFU enumeration of *B. subtilis* spores for the 291 nm band

UV fluence (mJ/cm^2)	Dilution Factor	CFU Counts #1	#2	#3	Geometric Mean	*N* CFU/mL
0	1.00E+04	93	97	86	91.9	9.19E+05
0	1.00E+04	83	86	99	89.1	8.91E+05
0	1.00E+04	83	80	95	85.8	8.58E+05
0	1.00E+04	73	85	77	78.2	7.82E+05
9.32	1.00E+04	90	105	99	97.8	9.78E+05
8.98	1.00E+04	91	82	83	85.2	8.52E+05
8.78	1.00E+04	75	74	86	78.2	7.82E+05
23.25	1.00E+04	87	84	66	78.4	7.84E+05
22.39	1.00E+04	76	78	86	79.9	7.99E+05
21.91	1.00E+04	77	87	94	85.7	8.57E+05
46.34	1.00E+03	349	393	352	364.1	3.64E+05
44.62	1.00E+03	383	401	391	391.6	3.92E+05
43.65	1.00E+03	398	424	422	414.5	4.14E+05
92.02	1.00E+02	448	430	447	441.6	4.42E+04
88.59	1.00E+02	481	503	495	492.9	4.93E+04
86.66	1.00E+03	90	107	91	95.7	9.57E+04
137.03	1.00E+01	406	393	392	396.9	3.97E+03
131.92	1.00E+02	77	85	54	70.7	7.07E+03
129.02	1.00E+02	91	91	93	91.7	9.17E+03
185.29	1.00E+00	198	266	126	187.9	1.88E+02
180.77	1.00E+00		246	229	237.3	2.37E+02
176.25	1.00E+01	34	38	28	33.1	3.31E+02

Table B-11 CFU enumeration of *B. subtilis* spores for the 302 nm band

UV fluence (mJ/cm^2)	Dilution Factor	CFU Counts			Geometric Mean	N_o CFU/mL
		#1	#2	#3		
0	1.00E+04	59	68	73	66.4	6.64E+05
0	1.00E+04	74	57	75	68.1	6.81E+05
0	1.00E+04	66	53	65	61.0	6.10E+05
319	1.00E+04	48	65	64	58.4	5.84E+05
635	1.00E+04	38	41	44	40.9	4.09E+05
1252	1.00E+02	366	316	345	341.7	3.42E+04
289	1.00E+04	43	66	63	56.3	5.63E+05
593	1.00E+04	41	49	57	48.6	4.86E+05
1464	1.00E+02	122	158	185	152.8	1.53E+04
257	1.00E+04	43	66	48	51.5	5.15E+05
578	1.00E+04	33	32	20	27.6	2.76E+05
1423	1.00E+02	72	78	74	74.6	7.46E+03

Appendix B-2: 95% JCR of Inactivation Rate Constant k and Number of Critical Targets n_c from the Multiple-Target Model for *B. subtilis* Spores

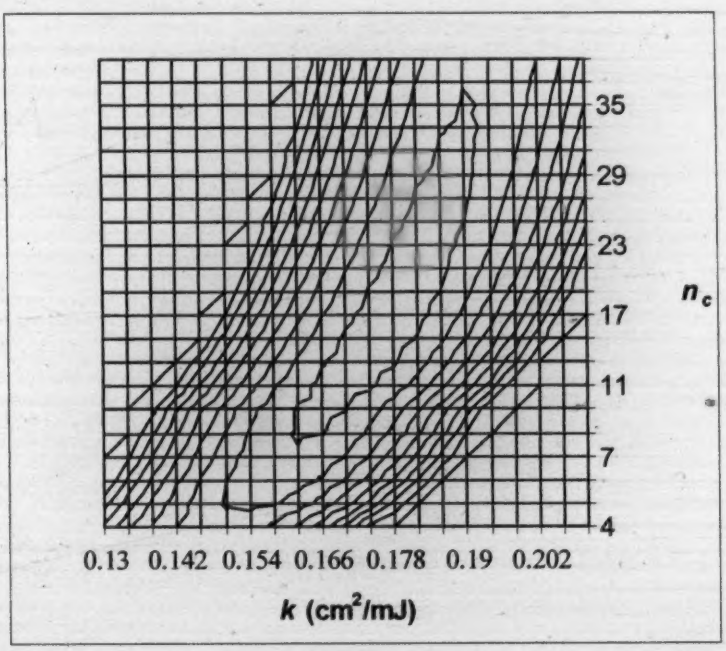

Figure B-1: 95% JCR of k and n_c of 222 nm band for *B. subtilis* spores (the inner region is the 95% JCR)

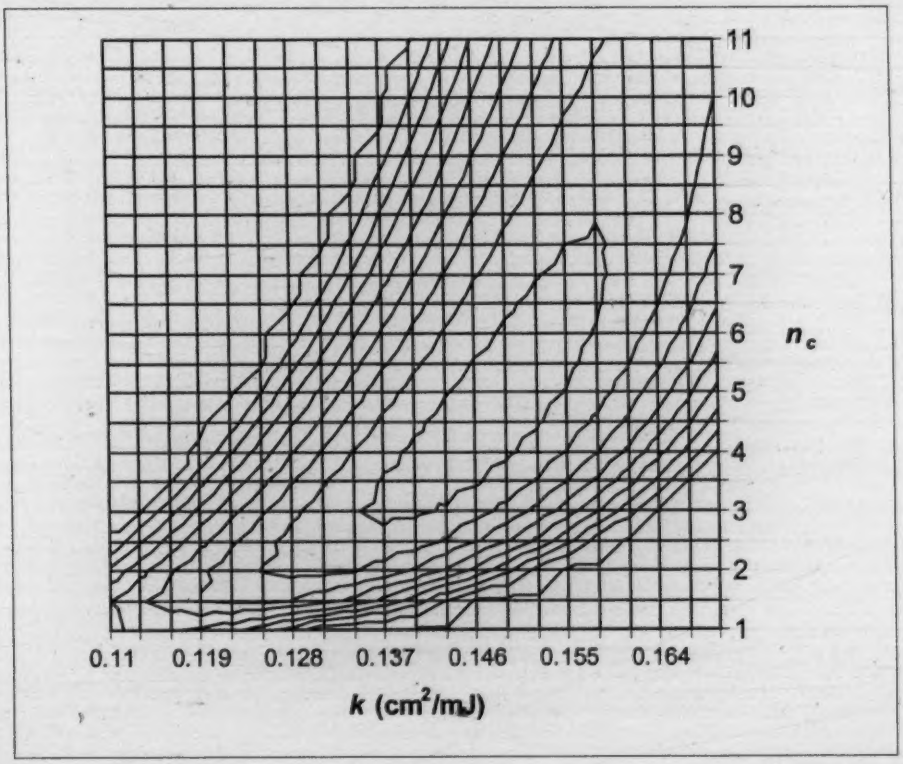

Figure B-2: 95% JCR of k and n_c of 225 nm band for *B. subtilis* spores (the inner region is the 95% JCR)

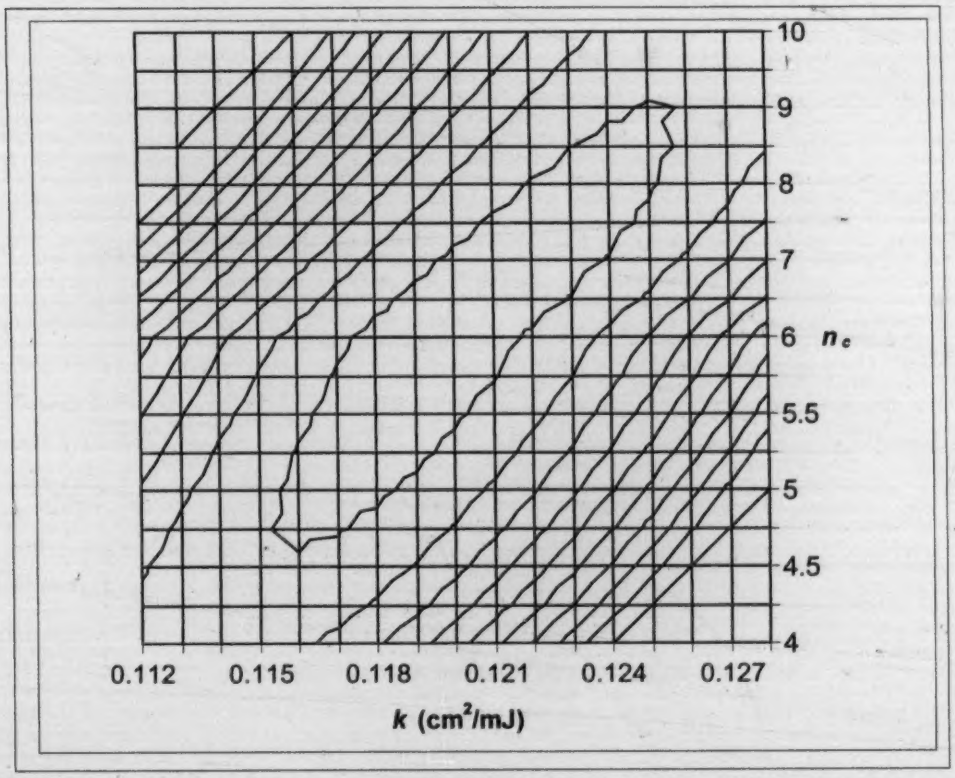

Figure B-3: 95% JCR of k and n_c of 231 nm band for *B. subtilis* spores (the inner region is the 95% JCR)

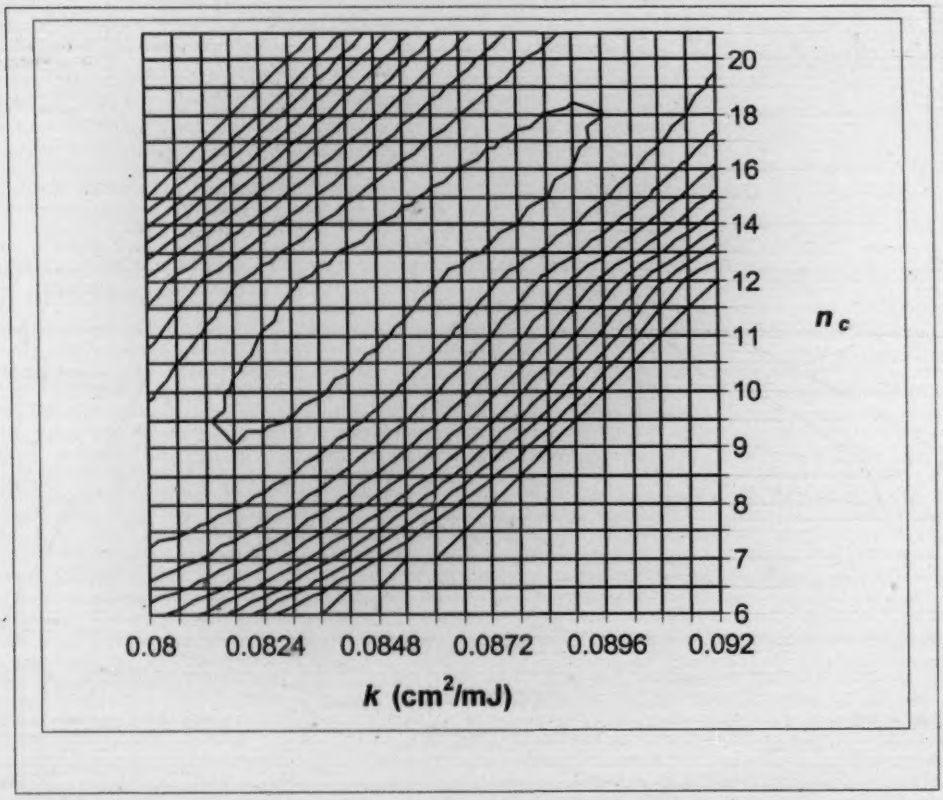

Figure B-4: 95% JCR of k and n_c of 243 nm band for *B. subtilis* spores (the inner region is 95% JCR)

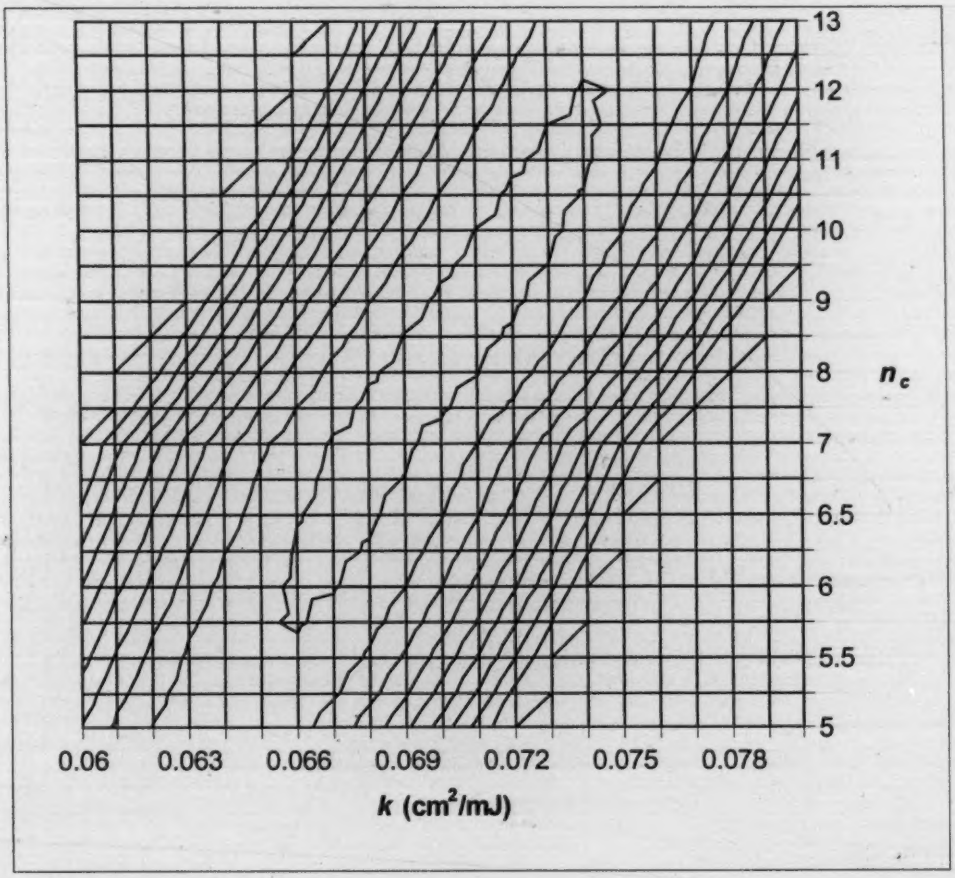

Figure B-5: 95% JCR of k and n_c of 251 nm band for *B. subtilis* spores

(the inner region is 95% JCR)

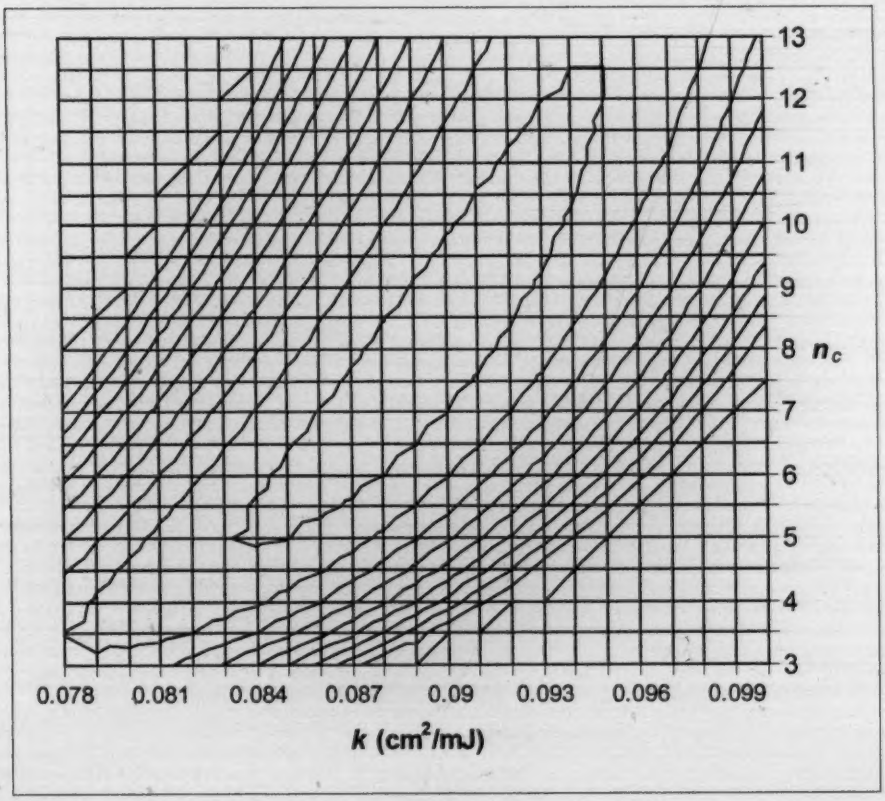

Figure B-6: 95% JCR of k and n_c of LP lamp 254 nm band for *B. subtilis* spores

(the inner region is 95% JCR)

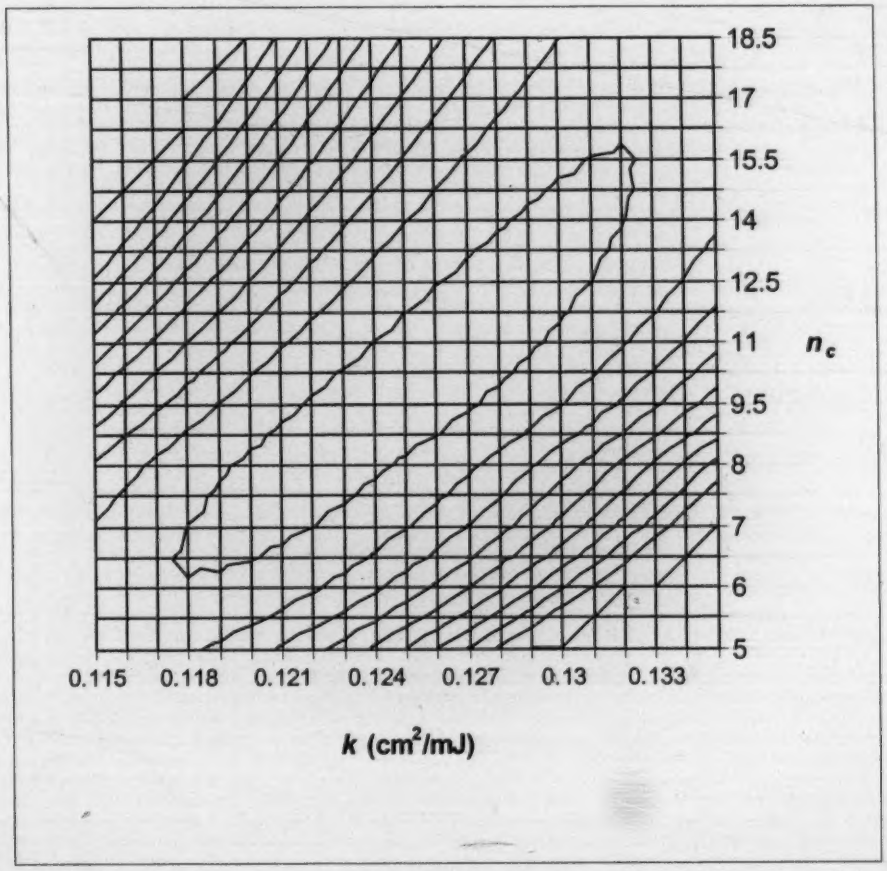

Figure B-7: 95% JCR of k and n_c of 262 nm band for *B. subtilis* spores (the inner region is 95% JCR)

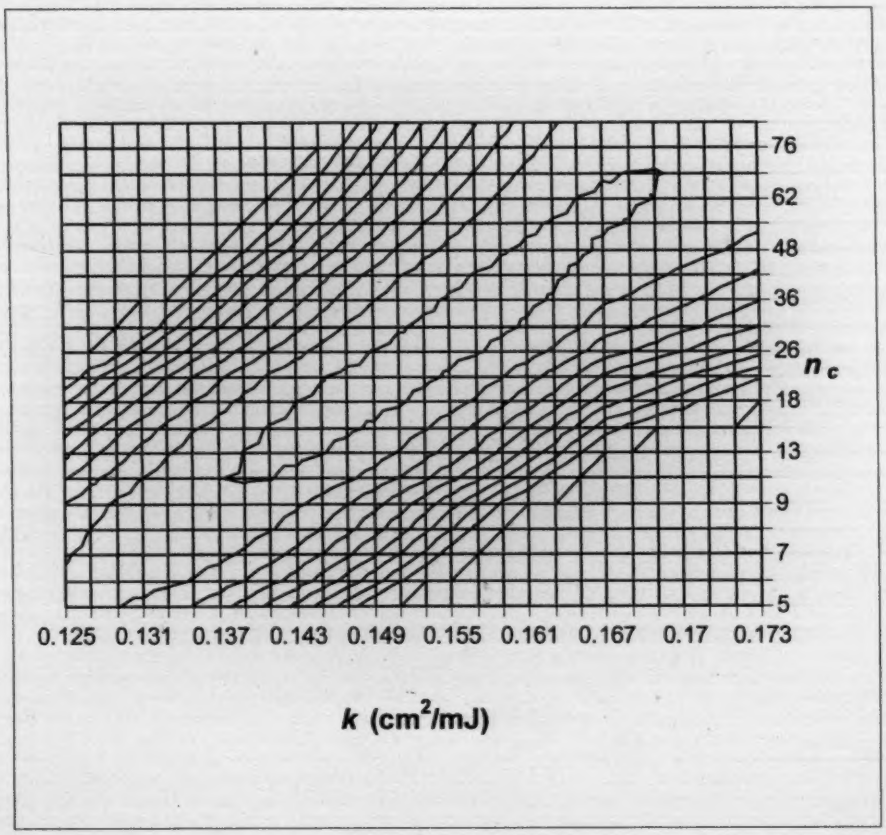

Figure B-8: 95% JCR of k and n_c of 269 nm band for *B. subtilis* spores (the inner region is 95% JCR)

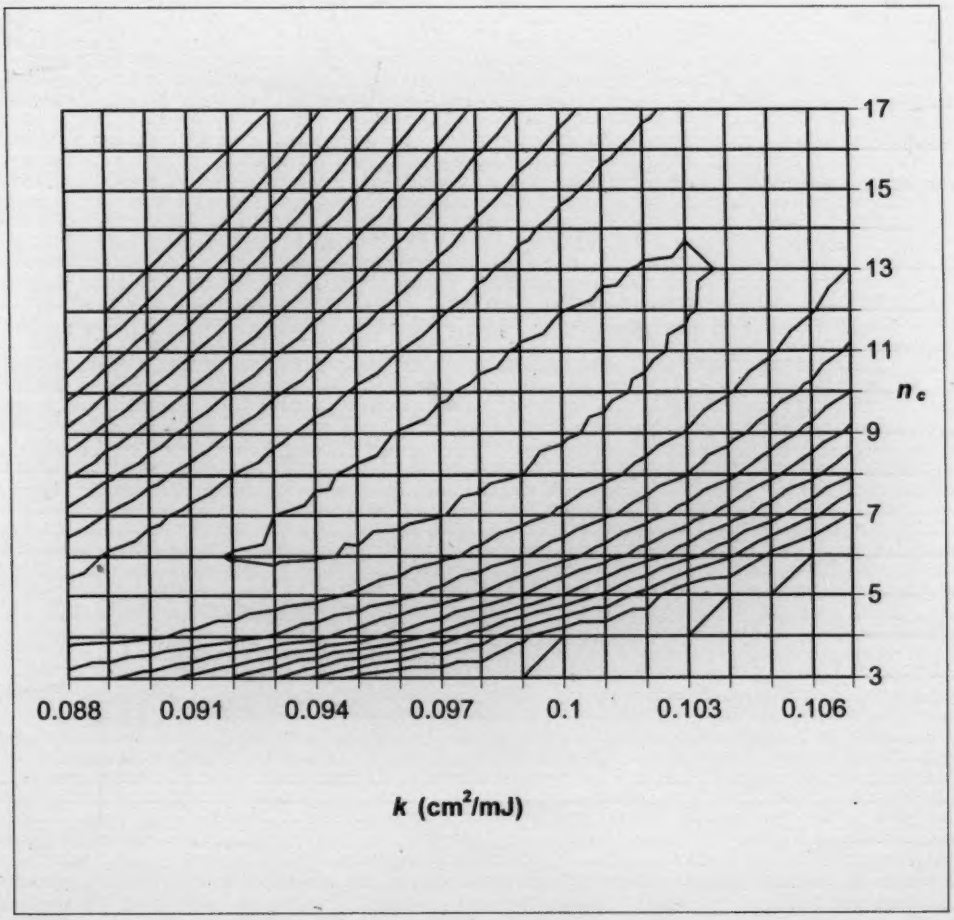

Figure B-9: 95% JCR of k and n_c of 279 nm band for *B. subtilis* spores (the inner region is 95% JCR)

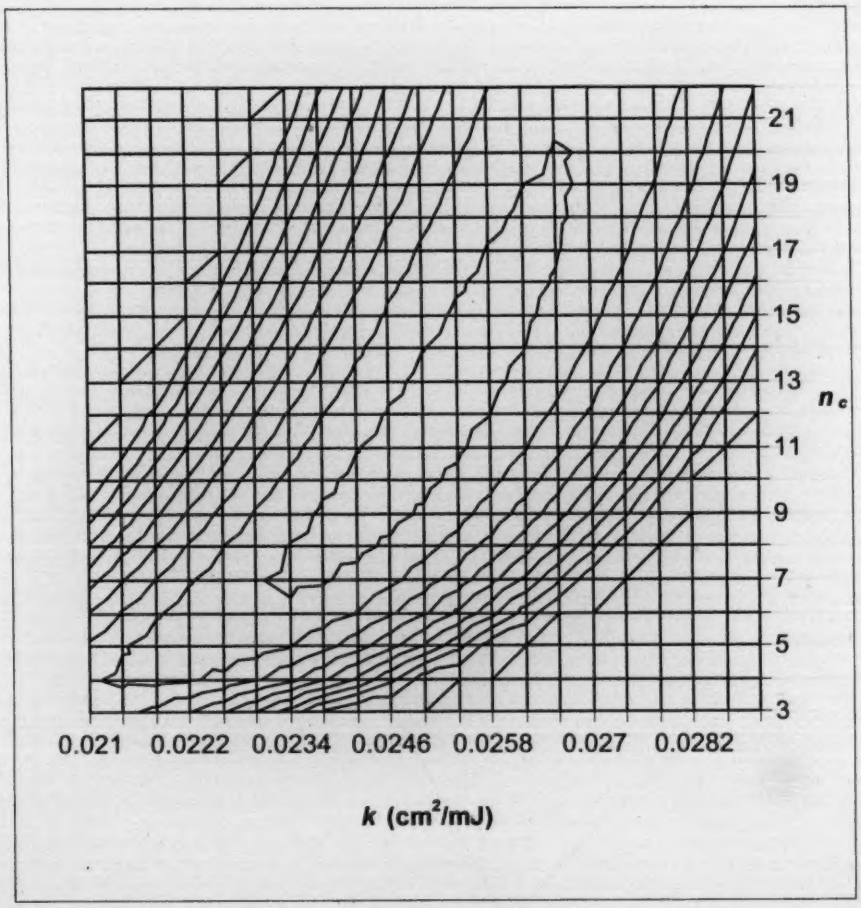

Figure B-10: 95% JCR of k and n_c of 291 nm band for *B. subtilis* spores (the inner region is 95% JCR)

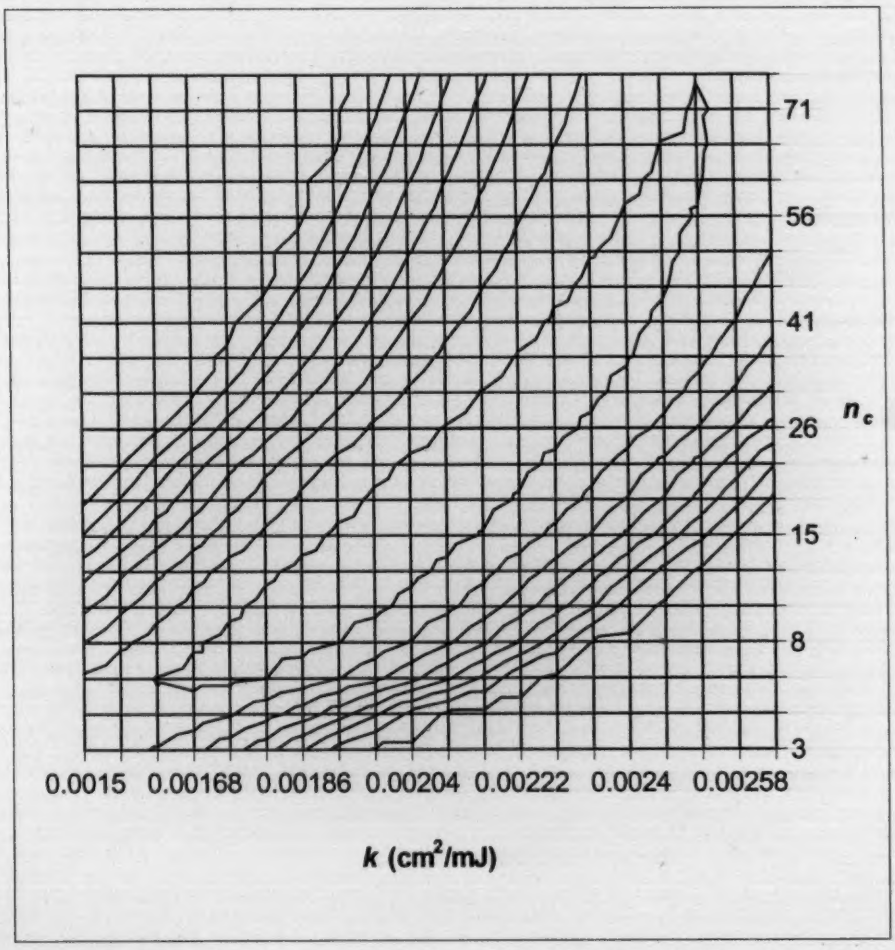

Figure B-11: 95% JCR of k and n_c of 302 nm band for *B. subtilis* spores (the inner region is 95% JCR)

Appendix B-3 CFU Enumeration of *Salmonella typhimurium* LT2

Table B-12 CFU enumeration of *S. typhimurium* LT2 for the the 222 nm band

Fluence (mJ/cm^2)	Dilution Factor	CFU Counts #1	#2	#3	Geometric Mean	N_o CFU/mL
0	1.00E+05	127	125	129	127.0	1.27E+07
0	1.00E+05	150	139	147	145.3	1.45E+07
0	1.00E+05	159	124	140	140.3	1.40E+07
2.50	1.00E+05	69	74	92	77.7	7.77E+06
2.50	1.00E+05	82	68	68	72.4	7.24E+06
2.50	1.00E+05	65	81	86	76.8	7.68E+06
5.00	1.00E+04	76	91	138	98.5	9.85E+05
5.00	1.00E+04	84	47	69	64.8	6.48E+05
5.00	1.00E+04	30	59	32	38.4	3.84E+05
7.51	1.00E+03	36	56	41	43.6	4.36E+04
7.51	1.00E+03	56	76	81	70.1	7.01E+04
7.51	1.00E+03	58	52	87	64.0	6.40E+04
10.01	1.00E+01	106	100	93	99.5	9.95E+02
10.01	1.00E+01	185	175	166	175.2	1.75E+03
10.01	1.00E+01	111	140	121	123.4	1.23E+03
12.51	1.00E+01	41	50	44	44.8	4.48E+02
12.51	1.00E+01	117	126	138	126.7	1.27E+03
12.51	1.00E+01	66	79	69	71.1	7.11E+02

Table B-13 CFU enumeration of *S. typhimurium* LT2 for the 225 nm band

Fluence (mJ/cm^2)	Dilution Factor	CFU Counts #1	#2	#3	Geometric Mean	N_o CFU/mL
0	1.00E+05	113	143	156	136.1	1.36E+07
0	1.00E+05	137	139	125	133.5	1.34E+07
0	1.00E+05	142	137	120	132.7	1.33E+07
3.46	1.00E+05	69	52	76	64.8	6.48E+06
3.46	1.00E+05	60	62	62	61.3	6.13E+06
3.46	1.00E+05	88	65	76	75.8	7.58E+06
6.93	1.00E+04	106	123	133	120.1	1.20E+06
6.93	1.00E+04	73	73	81	75.6	7.56E+05
6.93	1.00E+04	83	106	116	100.7	1.01E+06
10.39	1.00E+02	131	126	92	114.9	1.15E+04
10.39	1.00E+02	144	145	103	129.1	1.29E+04
10.39	1.00E+02	92	87	66	80.8	8.08E+03
13.85	1.00E+01	84	96	80	86.4	8.64E+02
13.85	1.00E+01	33	44	36	37.4	3.74E+02
13.85	1.00E+01	88	93	96	92.3	9.23E+02
17.31	1.00E+01	16	21	19	18.6	1.86E+02
17.31	1.00E+01	99	104	86	96.0	9.60E+02
17.31	1.00E+01	56	54	47	52.2	5.22E+02

Table B-14 CFU enumeration of *S. typhimurium* LT2 for the the 231 nm band

Fluence (mJ/cm^2)	Dilution Factor	CFU Counts #1	#2	#3	Geometric Mean	N_o CFU/mL
0	1.00E+05	126	127	131	128.0	1.28E+07
0	1.00E+05	121	128		124.5	1.24E+07
0	1.00E+05	116	131	148	131.0	1.31E+07
2.69	1.00E+05	98	86	76	86.2	8.62E+06
2.69	1.00E+05	80	93	118	95.8	9.58E+06
2.69	1.00E+05		95	94	94.5	9.45E+06
5.38	1.00E+05	31	59	28	37.1	3.71E+06
5.38	1.00E+05	43	48	36	42.0	4.20E+06
5.38	1.00E+05	41	49	53	47.4	4.74E+06
8.07	1.00E+04	190	169	176	178.1	1.78E+06
8.07	1.00E+04	162	141	124	141.5	1.41E+06
8.07	1.00E+04	189	138	152	158.3	1.58E+06
10.76	1.00E+03	225	231		228.0	2.28E+05
10.76	1.00E+03	217	223	266	234.4	2.34E+05
10.76	1.00E+03	265	289		276.7	2.77E+05
13.45	1.00E+02	318	249		281.4	2.81E+04
13.45	1.00E+02	203	225	216	214.5	2.14E+04
13.45	1.00E+02	195	208	182	194.7	1.95E+04

Table B-15 CFU enumeration of *S. typhimurium* LT2 for 243 nm band

Fluence (mJ/cm^2)	Dilution Factor	CFU Counts #1	#2	#3	Geometric Mean	N_o CFU/mL
0	1.00E+05	143	128	121	130.3	1.30E+07
0	1.00E+05	136	120	126	127.2	1.27E+07
0	1.00E+05	121	114	135	123.0	1.23E+07
3.63	1.00E+05	63		61	62.0	6.20E+06
3.63	1.00E+05	75	67		70.9	7.09E+06
3.63	1.00E+05	77	87	71	78.1	7.81E+06
7.26	1.00E+04	132	161	146	145.9	1.46E+06
7.26	1.00E+04	129	101	84	103.1	1.03E+06
7.26	1.00E+04	163	165	151	159.5	1.60E+06
10.89	1.00E+03	158	168	151	158.8	1.59E+05
10.89	1.00E+03	99	122	125	114.7	1.15E+05
10.89	1.00E+03	175	162	148	161.3	1.61E+05
14.52	1.00E+02	132	124	134	129.9	1.30E+04
14.52	1.00E+02	78	75	66	72.8	7.28E+03
14.52	1.00E+02	76	66	93	77.6	7.76E+03
18.15	1.00E+01	190	162	185	178.6	1.79E+03
18.15	1.00E+01	210	233	175	204.6	2.05E+03
18.15	1.00E+01	62	72	55	62.6	6.26E+02

Table B-16 CFU Enumeration of *S. typhimurium* LT2 for 251 nm band

Fluence (mJ/cm^2)	Dilution Factor	CFU Counts #1	#2	#3	Geometric Mean	N_o CFU/mL
0	1.00E+05	84	96	102	93.7	9.37E+06
0	1.00E+05	93	87	83	87.6	8.76E+06
0	1.00E+05	88	84		86.0	8.60E+06
2.83	1.00E+05	38	41	35	37.9	3.79E+06
2.83	1.00E+05	28	46	53	40.9	4.09E+06
2.83	1.00E+05	31	59	43	42.8	4.28E+06
5.65	1.00E+04	47	73	39	51.1	5.11E+05
5.65	1.00E+04	45	40	51	45.1	4.51E+05
5.65	1.00E+04	74	58	84	71.2	7.12E+05
8.48	1.00E+03	42	51	34	41.8	4.18E+04
8.48	1.00E+03	26	45	36	34.8	3.48E+04
8.48	1.00E+03	69	61	55	61.4	6.14E+04
11.30	1.00E+01	198	229	183	202.4	2.02E+03
11.30	1.00E+01	210	236	203	215.9	2.16E+03
11.30	1.00E+02	25	26	22	24.3	2.43E+03
14.13	1.00E+01	32	33	36	33.6	3.36E+02
14.13	1.00E+01	38	32	41	36.8	3.68E+02
14.13	1.00E+01	37	12	21	21.0	2.10E+02

Table B-17 CFU enumeration of *S. typhimurium* LT2 for LP lamp

Fluence (mJ/cm^2)	Dilution Factor	CFU Counts			Geometric Mean	N_o CFU/mL
		#1	#2	#3		
0	1.00E+05		127	145	135.7019	13570188
0	1.00E+05	117	125	131	124.2	1.24E+07
0	1.00E+05	118	116	128	120.6	1.21E+07
1.90	1.00E+05	60	64	70	64.5	6.45E+06
1.90	1.00E+05	63	85	100	81.2	8.12E+06
1.90	1.00E+05	78	112	82	89.5	8.95E+06
3.80	1.00E+04	192	181	156	175.7	1.76E+06
3.80	1.00E+04	177	199	235	202.3	2.02E+06
3.80	1.00E+04	193	189	168	183.0	1.83E+06
5.71	1.00E+03	237	230	224	230.3	2.30E+05
5.71	1.00E+03	139	134	133	135.3	1.35E+05
5.71	1.00E+03	189	163	148	165.8	1.66E+05
7.61	1.00E+02	183	196	150	175.2	1.75E+04
7.61	1.00E+02	162	182	109	147.6	1.48E+04
7.61	1.00E+03	43	37	57	44.9	4.49E+04
9.51	1.00E+01	135	139	137	137.0	1.37E+03
9.51	1.00E+01	165	175	153	164.1	1.64E+03
9.51	1.00E+01	168	166	163	165.7	1.66E+03

Table B-18 CFU enumeration of *S. typhimurium* LT2 for 262 nm band

Fluence (mJ/cm^2)	Dilution Factor	CFU Counts #1	#2	#3	Geometric Mean	N_o CFU/mL
0	1.00E+05	66	72	68	68.6	6.86E+06
0	1.00E+05	99	86	91	91.8	9.18E+06
0	1.00E+05	80	73	82	78.2	7.82E+06
1.87	1.00E+04	273	258	286	272.1	2.72E+06
1.87	1.00E+05	64	30	53	46.7	4.67E+06
1.87	1.00E+05	27	32	28	28.9	2.89E+06
3.75	1.00E+04	41	46	29	38.0	3.80E+05
3.75	1.00E+04	47	33	41	39.9	3.99E+05
3.75	1.00E+04	51	56	68	57.9	5.79E+05
5.62	1.00E+03	51	76	37	52.3	5.23E+04
5.62	1.00E+03	57	56	68	60.1	6.01E+04
5.62	1.00E+03	55	39	42	44.8	4.48E+04
7.50	1.00E+01	293	268		280.2	2.80E+03
7.50	1.00E+01	150	138	117	134.3	1.34E+03
7.50	1.00E+01	161	163	178	167.2	1.67E+03
9.37	1.00E+01	10	13	8	10.1	1.01E+02
9.37	1.00E+01	57	32	48	44.4	4.44E+02

Table B-19 CFU enumeration of *S. typhimurium* LT2 for 269 nm band

Fluence (mJ/cm^2)	Dilution Factor	CFU Counts			Geometric Mean	N_o CFU/mL
		#1	#2	#3		
0	1.00E+05	109	118	126	117.5	1.17E+07
0	1.00E+05	110	109	140	118.8	1.19E+07
0	1.00E+05	105	110	96	103.5	1.04E+07
1.69	1.00E+05	45	53	41	46.1	4.61E+06
1.69	1.00E+05	40	42	42	41.3	4.13E+06
1.69	1.00E+05	57	48	33	44.9	4.49E+06
3.39	1.00E+04	108	107	135	116.0	1.16E+06
3.39	1.00E+04	116	115	90	106.3	1.06E+06
3.39	1.00E+04	138	141	176	150.7	1.51E+06
5.08	1.00E+03	265	282	291	279.1	2.79E+05
5.08	1.00E+03	235	226	220	226.9	2.27E+05
5.08	1.00E+03	198	161	173	176.7	1.77E+05
6.77	1.00E+02	233	181	151	185.4	1.85E+04
6.77	1.00E+02	163	231	217	201.4	2.01E+04
6.77	1.00E+02	170	159	149	159.1	1.59E+04
8.46	1.00E+01	145	160	129	144.1	1.44E+03
8.46	1.00E+01	168	174	128	155.2	1.55E+03
8.46	1.00E+01	78	91	121	95.1	9.51E+02

Table B-20 CFU enumeration of *S. typhimurium* LT2 for 279 nm band

Fluence (mJ/cm^2)	Dilution Factor	CFU Counts #1	#2	#3	Geometric Mean	N_o CFU/mL
0	1.00E+05	136	135	142	137.6	1.38E+07
0	1.00E+05	139	118	117	124.3	1.24E+07
0	1.00E+05	108	110	139	118.2	1.18E+07
3.14	1.00E+05	28	54	46	41.1	4.11E+06
3.14	1.00E+05	34	52	39	41.0	4.10E+06
3.14	1.00E+05	39	39	39	39.0	3.90E+06
6.28	1.00E+04	69	77	28	53.0	5.30E+05
6.28	1.00E+04	57	76	53	61.2	6.12E+05
6.28	1.00E+04	71	80	40	61.0	6.10E+05
9.42	1.00E+02	164	163	143	156.4	1.56E+04
9.42	1.00E+02	195	147	267	197.1	1.97E+04
9.42	1.00E+02	168	183	82	136.1	1.36E+04
12.56	1.00E+01	52	40	29	39.2	3.92E+02
12.56	1.00E+01	29	35	53	37.7	3.77E+02
12.56	1.00E+01	83	82	78	81.0	8.10E+02
15.70	1.00E+01	55	64	63	60.5	6.05E+02
15.70	1.00E+01	28	26	23	25.6	2.56E+02
15.70	1.00E+01	41	55	60	51.3	5.13E+02

Table B-21 CFU enumeration of *S. typhimurium* LT2 for 291 nm band

Fluence (mJ/cm^2)	Dilution Factor	CFU Counts #1	#2	#3	Geometric Mean	N_o CFU/mL
0	1.00E+05	115	139	118	123.6	1.24E+07
0	1.00E+05	136	140	136	137.3	1.37E+07
0	1.00E+05	158	158	125	146.1	1.46E+07
9.49	1.00E+05	27	39	25	29.7	2.97E+06
9.49	1.00E+04	253	219	270	246.4	2.46E+06
9.49	1.00E+04	214	263	232	235.5	2.35E+06
18.98	1.00E+03	152	148	152	150.7	1.51E+05
18.98	1.00E+03	175	169	164	169.3	1.69E+05
18.98	1.00E+03	128	129	123	126.6	1.27E+05
28.47	1.00E+02	36	33	37	35.3	3.53E+03
28.47	1.00E+01	113	130	186	139.8	1.40E+03
28.47	1.00E+01	176	223	198	198.1	1.98E+03
37.96	1.00E+01	157	138	111	134.0	1.34E+03
37.96	1.00E+01	133	88	80	97.8	9.78E+02
37.96	1.00E+01	90	107	91	95.7	9.57E+02
47.45	1.00E+01	95	84	74	83.9	8.39E+02
47.45	1.00E+01	23	23	27	24.3	2.43E+02
47.45	1.00E+01	25	26	25	25.3	2.53E+02

Table B-22 CFU enumeration of *S. typhimurium* LT2 for 302 nm band

Fluence (mJ/cm^2)	Dilution Factor	CFU Counts #1	#2	#3	Geometric Mean	N_o CFU/mL
0	1.00E+05	161	138	137	144.925	1.45E+07
0	1.00E+05	136	149	124	136.0	1.36E+07
0	1.00E+05	169	150	138	151.8	1.52E+07
63.51	1.00E+05	47	66	53	54.8	5.48E+06
63.51	1.00E+05	36	43	31	36.3	3.63E+06
63.51	1.00E+05	45	59	55	52.7	5.27E+06
127.01	1.00E+04	31	35	23	29.2	2.92E+05
127.01	1.00E+03	263	237	219	239.0	2.39E+05
127.01	1.00E+04	32	49	54	43.9	4.39E+05
190.52	1.00E+02	86	60	73	72.2	7.22E+03
190.52	1.00E+02	163	125	141	142.2	1.42E+04
190.52	1.00E+02	93	88	121	99.7	9.97E+03
254.03	1.00E+01	81	78	73	77.3	7.73E+02
254.03	1.00E+01	31	34	49	37.2	3.72E+02
254.03	1.00E+01	51	69	76	64.4	6.44E+02
317.53	1.00E+01	28	20	23	23.4	2.34E+02
317.53	1.00E+01	15	20	16	16.9	1.69E+02
317.53	1.00E+01	7	13	17	11.6	1.16E+02

Appendix B-4: 95% JCR of Inactivation Rate Constant *k* and Number of Critical Targets n_c from the Multiple-target Model for *S. typhimurium* LT2

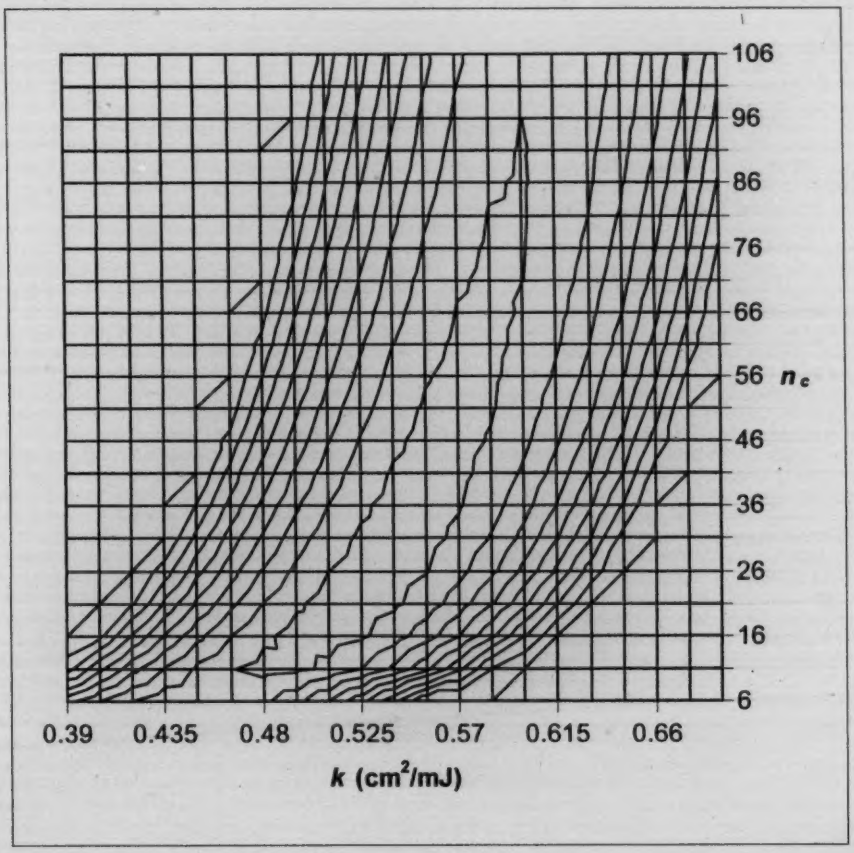

Figure B-12: 95% JCR of *k* and n_c of 222 nm band for *S. typhimurium* LT2 (the inner region is 95% JCR)

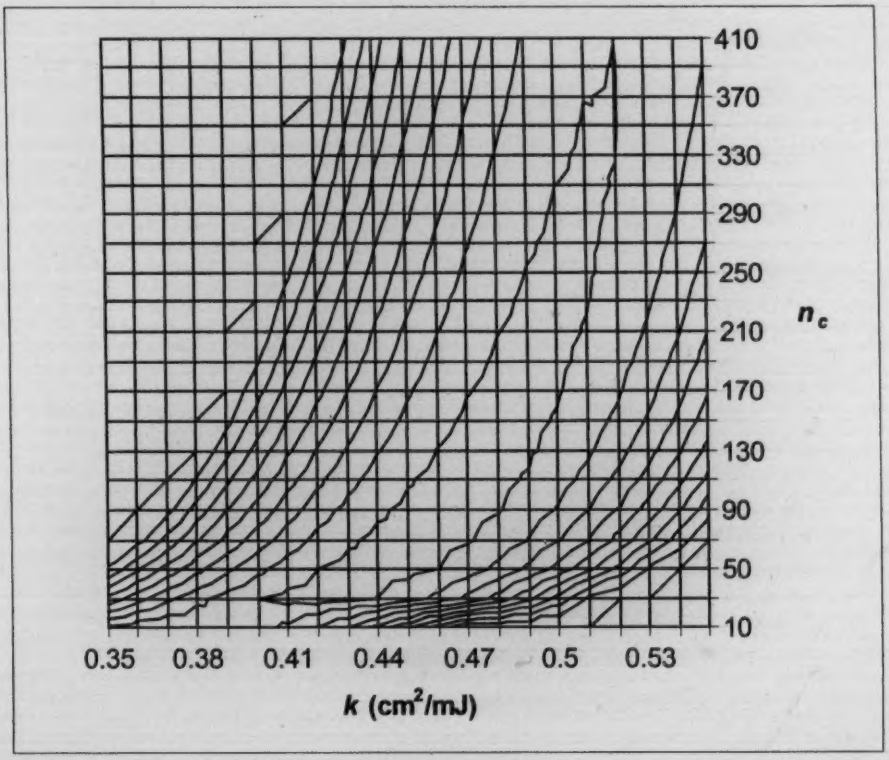

Figure B-13: 95% JCR of k and n_c of 225 nm band for *S. typhimurium* LT2 (the inner region is 95% JCR).

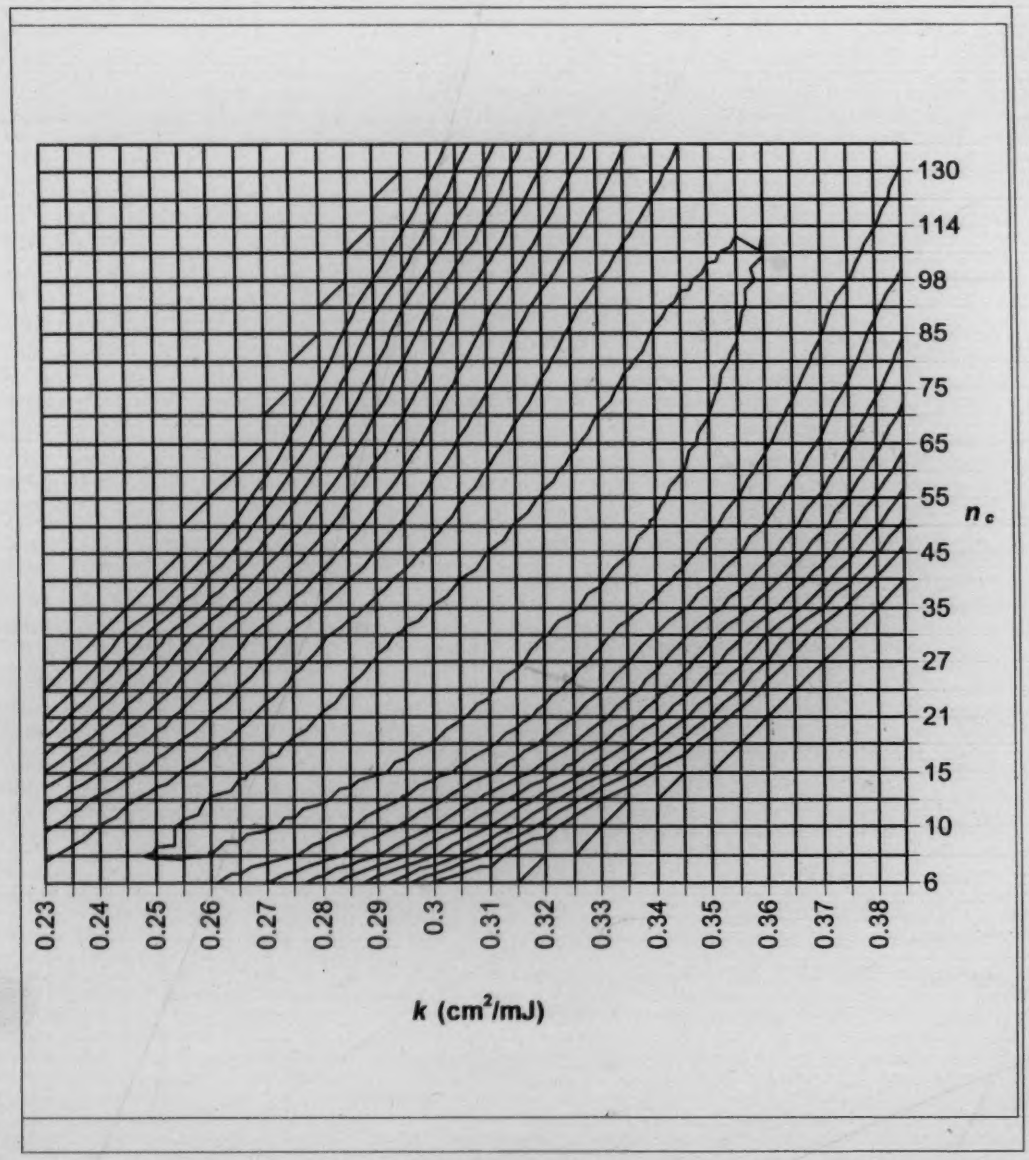

Figure B-14: 95% JCR of k and n_c of 231 nm band for *S. typhimurium* LT2 (the inner region is 95% JCR)

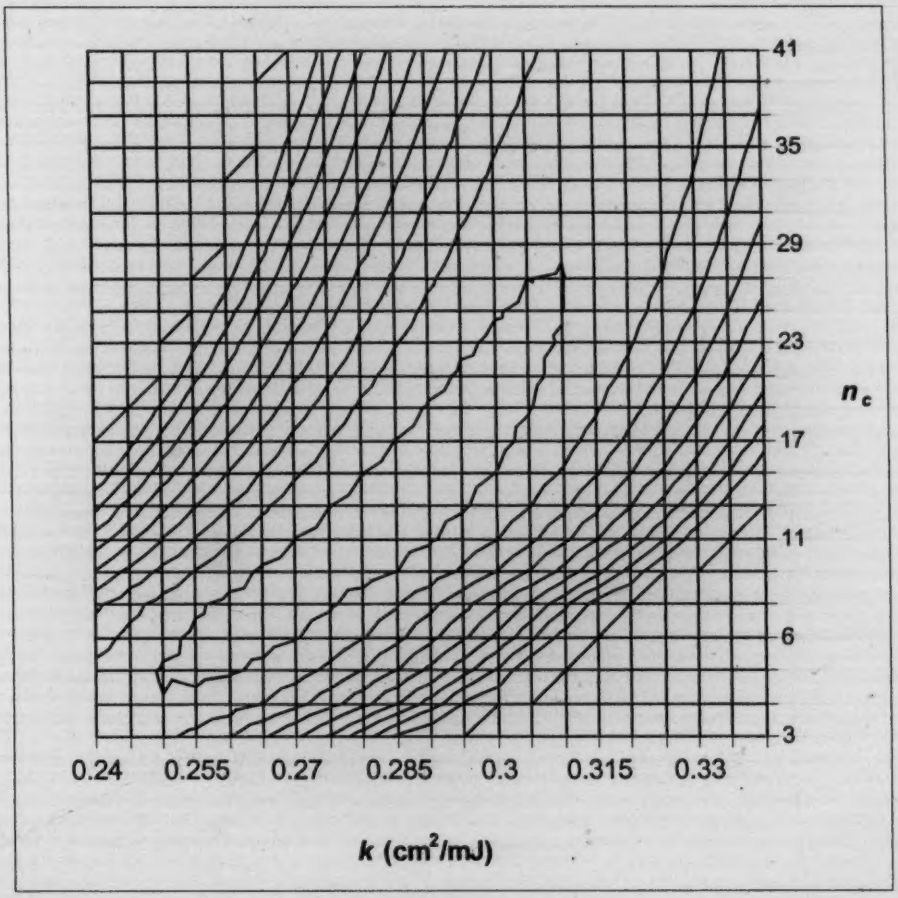

Figure B-15: 95% JCR of k and n_c of 243 nm band for *S. typhimurium* LT2 (the inner region is 95% JCR)

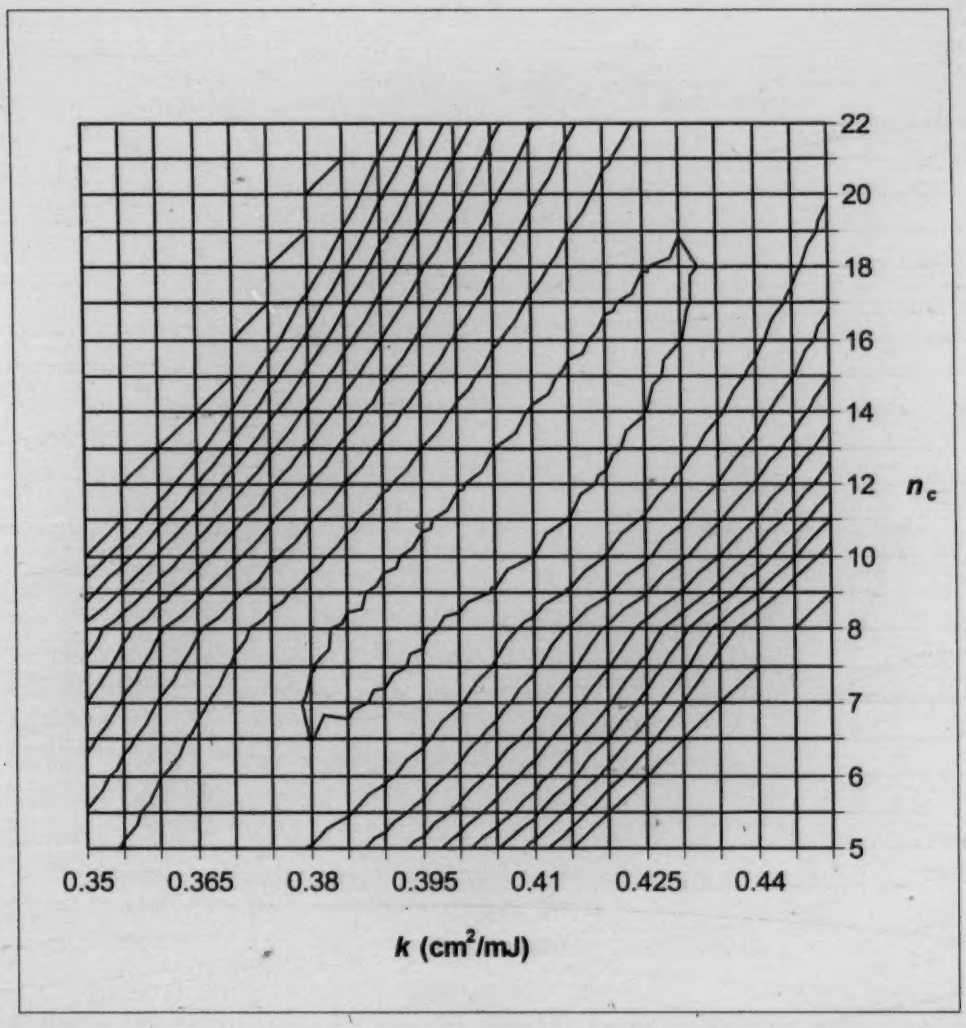

Figure B-16: 95% JCR of k and n_c of 251 nm band for *S. typhimurium* LT2 (the inner region is 95% JCR)

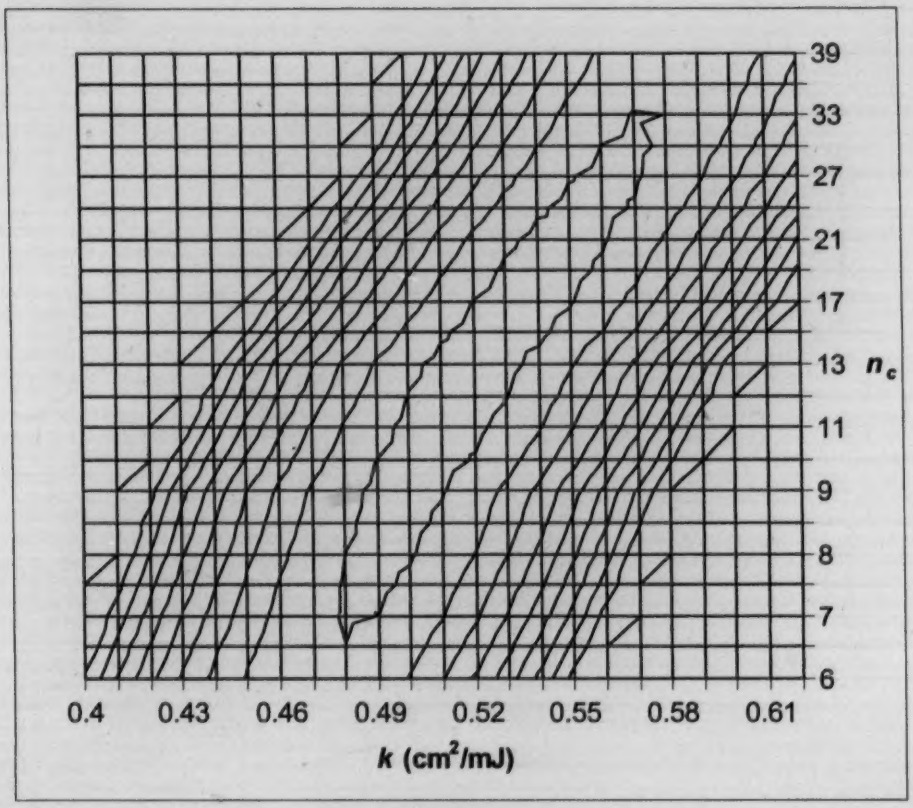

Figure B-17: 95% JCR of k and n_c of LP lamp 254 nm band for *S. typhimurium* LT2
(the inner region is 95% JCR)

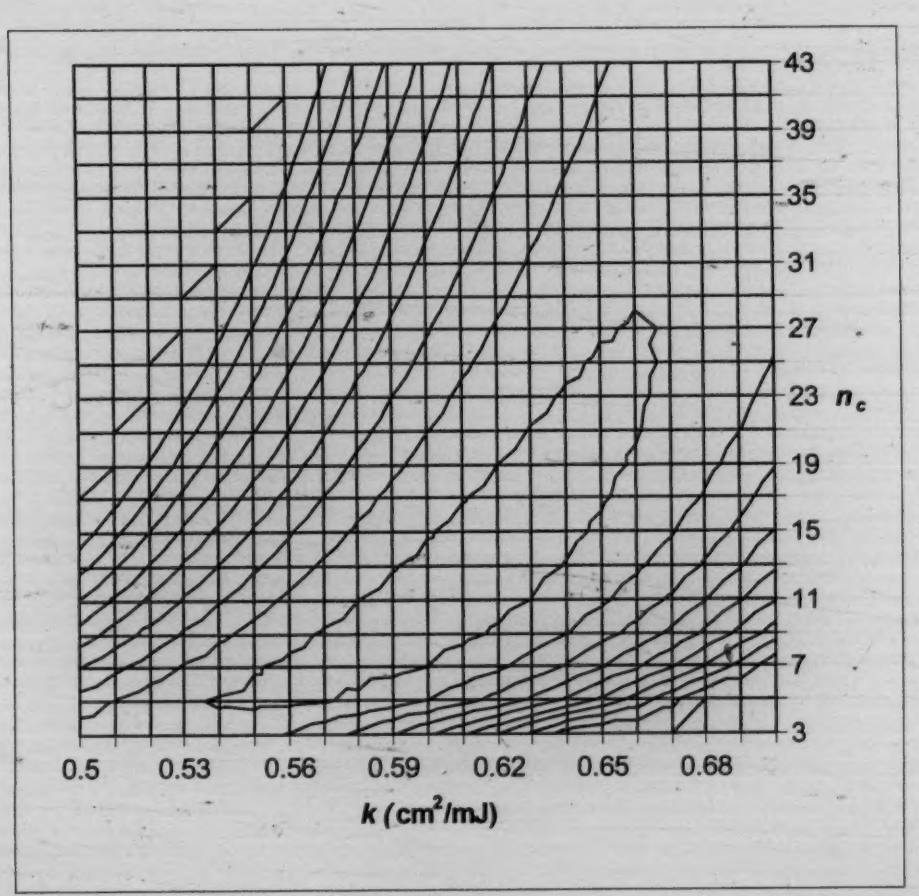

Figure B-18: 95% JCR of k and n_c of 262 nm band for *S. typhimurium* LT2 (the inner region is 95% JCR)

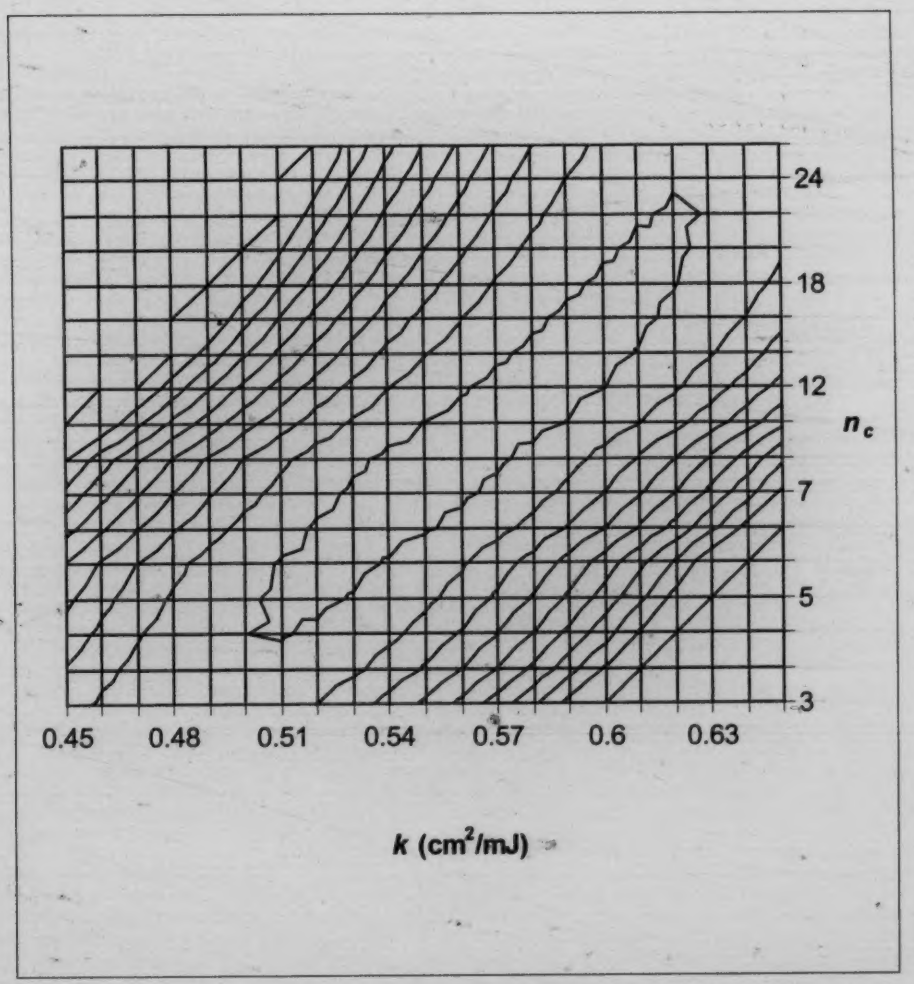

Figure B-19: 95% JCR of k and n_c of 269 nm band for *S. typhimurium* LT2

(the inner region is 95% JCR)

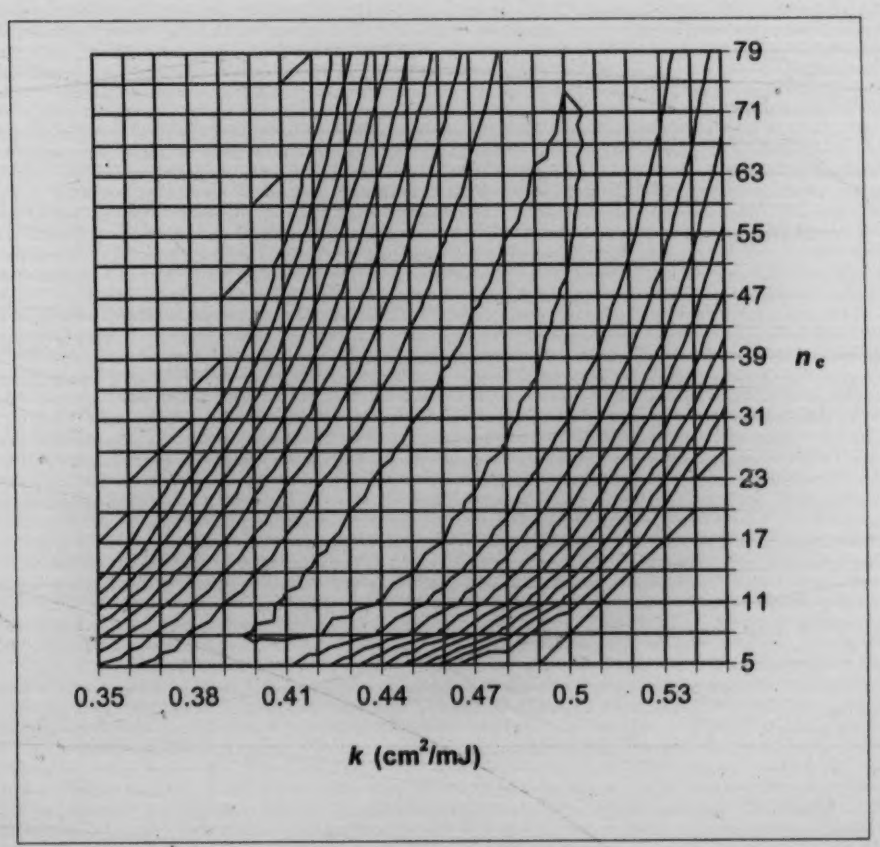

Figure B-20: 95% JCR of k and n_c of 279 nm band for *S. typhimurium* LT2 (the inner region is 95% JCR)

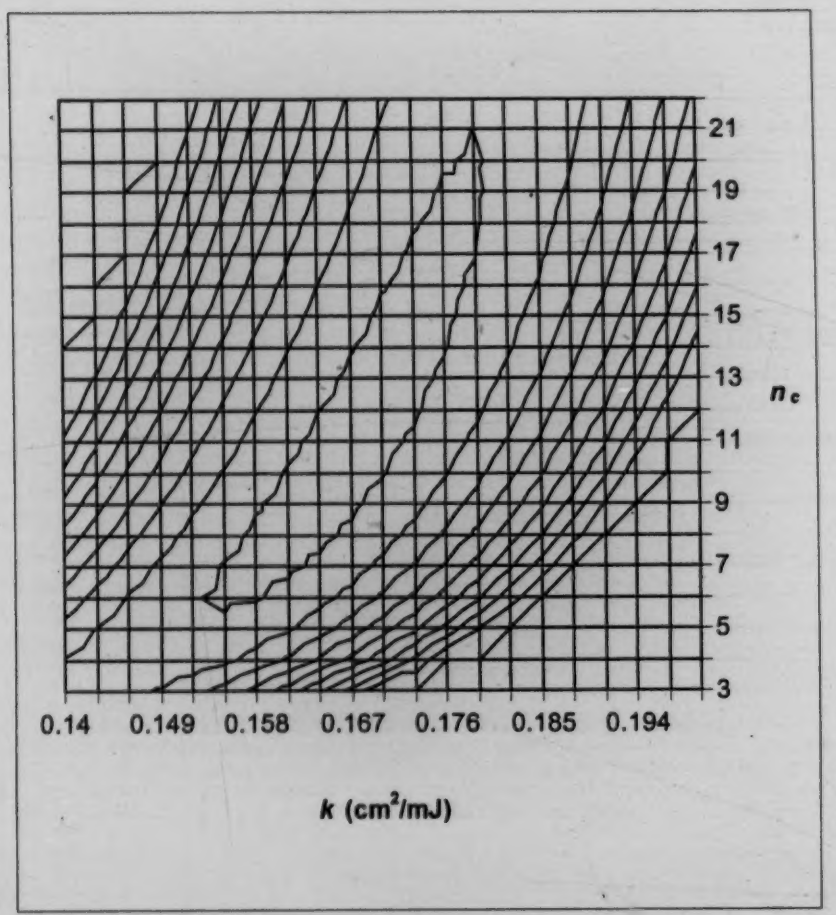

Figure B-21: 95% JCR of k and n_c of 291 nm band for *S. typhimurium* LT2 (the inner region is 95% JCR)

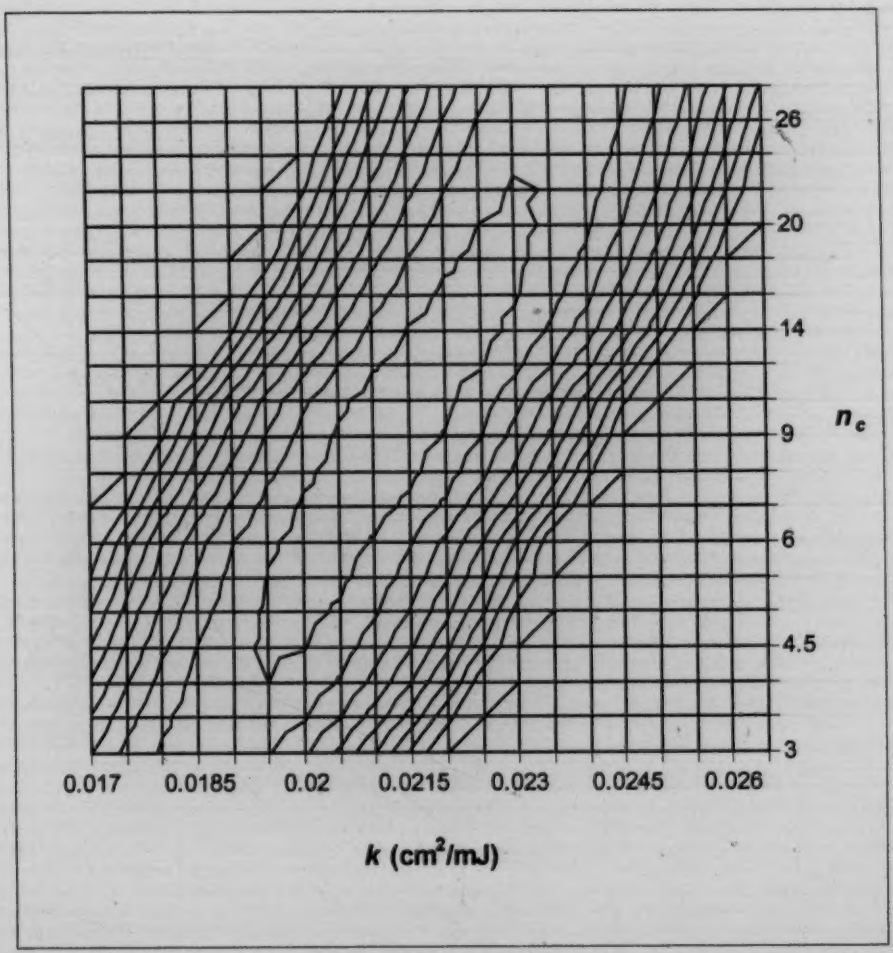

Figure B-22: 95% JCR of k and n_c of 302 nm band for *S. typhimurium* LT2 (the inner region is 95% JCR)

Appendix B-5: Original Results for Absorbance Measurement of DNA and decoated spores solution

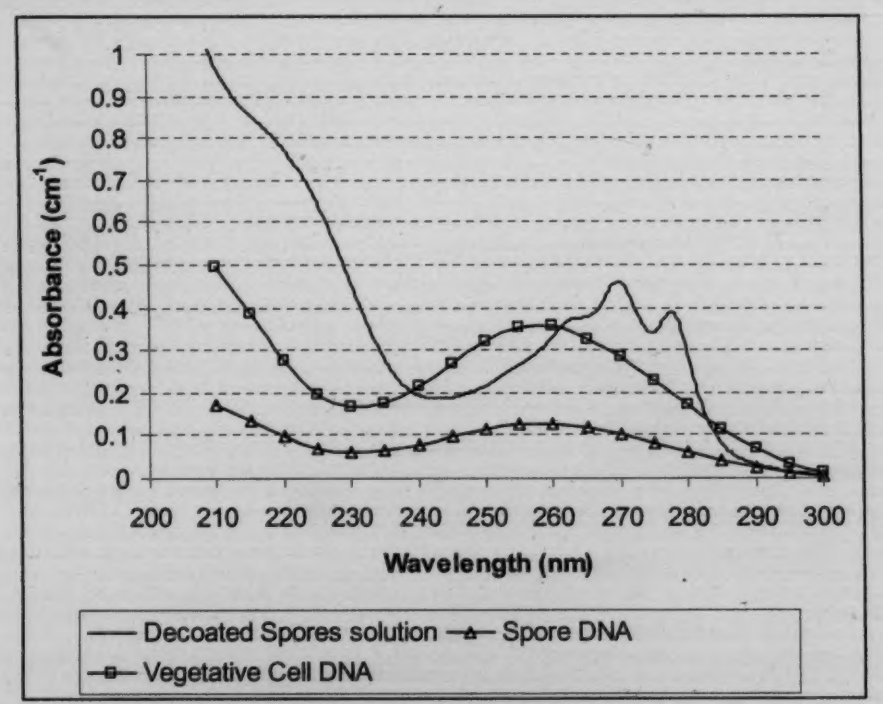

Figure B-23: Absorbance spectra of *Bacillus subtilis* measured using 1 cm-pathlength quartz cuvettes

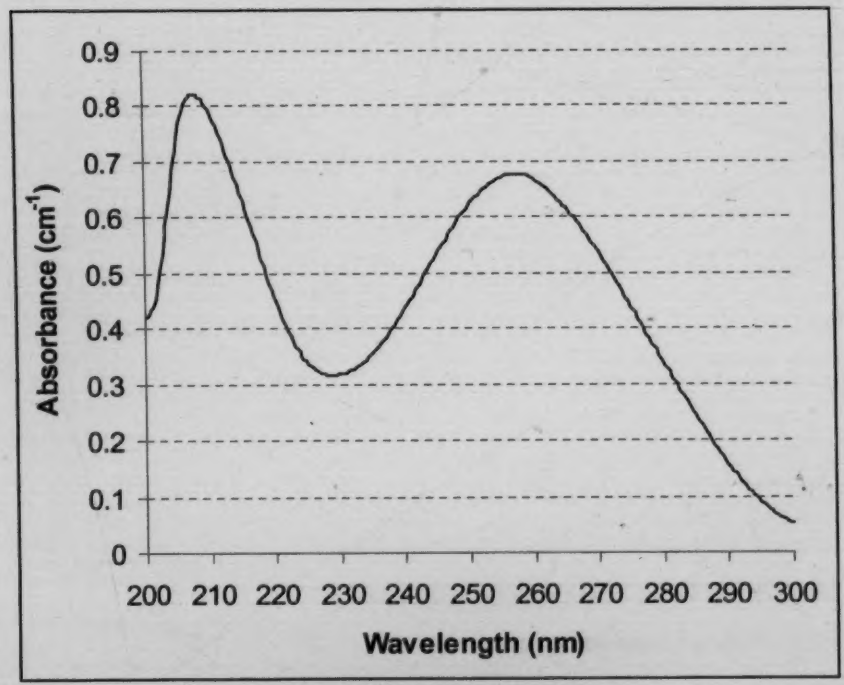

Figure B-24: DNA absorbance spectrum of *S. typhimurium* LT2 measured using 1 cm-pathlength quartz cuvettes

Appendix B-6: Paired t-Test for Comparison of the Difference of Action Spectra

Table B-23 Comparison of the difference of action spectra of *B. subtilis* spores using paired t-Test (95% confidence)

Wavelength (nm)	Relative *k* from this study	Mamane-Gravetz et al. (2005)		Cabaj et al. (2002)	
		Relative *k*	Difference	Relative *k*	Difference
220	2.200	1.410	0.790	0.930	1.270
225	1.650	1.050	0.600	0.830	0.820
230	1.400	0.980	0.420	0.750	0.650
235	1.220	0.780	0.440	0.700	0.520
240	1.050	0.660	0.390	0.650	0.400
245	0.900	0.830	0.070	0.830	0.070
250	0.790	0.930	-0.140	0.690	0.100
255	1.090	1.020	0.070	1.030	0.060
260	1.420	1.150	0.270	1.140	0.280
265	1.610	1.228	0.382	1.150	0.460
270	1.680	1.250	0.430	1.140	0.540
275	1.400	1.250	0.150	1.100	0.300
280	1.050	1.150	-0.100	1.050	0.000
285	0.720	0.880	-0.160	0.800	-0.080
290	0.350	0.350	0.000	0.036	0.314

Mean of Difference	0.241	0.380
Number of comparison	15	15
Degree of Freedom	14	14
Standard Deviation	0.284	0.355
T_o	3.286	4.149
T_c	2.510	2.510

Because both $T_0 > T_c$, it can be concluded that there are statistical difference with 95% confidence between the relative inactivation rate *k* values from the action spectrum of *B. subtilis* spores and those *k* values from the action spectra by Mamane-Gravetz et al. (2005) and Cabaj et al. (2002).

Table B-24 Comparison of the difference of action spectrum of *E. coli* and the action spectrum of *Salmonella* using paired t-Test (95% confidence)

Wavelength (nm)	*Salmonella* (This study)	*E. coli* (Gates 1930)	*Difference*
230	0.590	0.850	0.260
235	0.520	0.560	0.040
240	0.510	0.490	-0.020
245	0.550	0.620	0.070
250	0.720	0.760	0.040
255	1.040	1.020	-0.020
260	1.120	1.160	0.040
265	1.130	1.240	0.110
270	1.050	1.190	0.140
275	0.920	0.920	0.000
280	0.780	0.660	-0.120
285	0.550	0.490	-0.060
290	0.370	0.330	-0.040
295	0.210	0.160	-0.050
300	0.100	0.060	-0.040

Mean of Difference	0.023
Number of comparison	15
Degree of Freedom	14
Standard Deviation	0.095
T_o	0.955
T_c	2.510

Because $T_0 < T_c$, it can be concluded that there are no statistical difference with 95% confidence between the relative inactivation rate *k* values from the action spectrum of *Salmonella* and those from the action spectrum of *E. coli*.